

UCSF

UC San Francisco Electronic Theses and Dissertations

Title

Molecular Mechanisms Regulating Cell Intrinsic and Synaptic Homeostasis: Compensation in *Drosophila* shal Mutants

Permalink

<https://escholarship.org/uc/item/9h04t9c4>

Author

Bergquist, Sharon Brie

Publication Date

2011

Peer reviewed|Thesis/dissertation

Molecular Mechanisms that Regulate Cell Intrinsic and Synaptic Homeostasis:

Compensation in *Drosophila shal* Mutants

by

Sharon Brie Bergquist

DISSERTATION

Submitted in partial satisfaction of the requirements for the degree of

DOCTOR OF PHILOSOPHY

in

Neuroscience

in the

GRADUATE DIVISION

of the

Copyright 2011

by

Sharon Brie Bergquist

Acknowledgements

I am incredibly grateful for all of the people who have supported me through my time in graduate school. It is a testament to all of them that I have made it to this point.

I would first like to thank Grae Davis for being an exemplary mentor in every respect. His endless enthusiasm for science is contagious and I would not have made it through graduate school without this source of encouragement and excitement. He has also provided guidance and endless support at every step; I feel truly fortunate to have worked with Grae.

I would like to thank the wonderful people, past and present, in the Davis Lab. It has been a privilege to work with so many open-minded and intelligent individuals. The Davis lab is truly a team; we share our science, our struggles, and our successes. It is a pleasure to come to lab each day and I will miss it. A special thank you to Catherine O'Hare, Meg Younger, Ervin Johnson, Martin Mueller, Lani Keller, Mark Eddison and Ed Pym for their friendship in and out of the lab.

The neuroscience program at UCSF, students and faculty, have fostered an open and encouraging environment as well as an institution of academic excellence. I feel very fortunate to have been trained here and to have been exposed to so many incredible scientists. I would like to thank my thesis committee; they have all guided my research, provided helpful insights and positive encouragement. I would also especially like to thank Pat and Carrie for all of their work and support in getting all of us through graduate school.

I would like to thank my California family, my 'urban family' and my Colorado family, I am so very grateful for each and every one of the people I am lucky enough to

call friends. I am overwhelmed and humbled daily by my community, they are the people who make it all worth it.

Most importantly, I would like to thank Adam, Julie, Avery, Grandmother Cathe, Grandmother Jean and my parents for being my stable foundation and for teaching me the true meaning of love. I would like to thank my brother for sharing with me his joy for life and for his constant support, guidance and love. I would like to thank my mom for sharing with me her dedication and her laughter and for being my best friend. I would like to thank my dad for sharing with me his wisdom and his optimism and for teaching me to keep my eyes, my heart and my mind open in the pursuit of understanding.

PREFACE

Chapter 1 contains background information.

Chapter 2 has been published in *Neuron* (Bergquist et al., 2010). This paper was done in collaboration with Dion Dickman and Graeme Davis. Dion Dickman performed the original screen that identified the mutation that is the basis of my thesis work. Part of the data from the screen performed by Dion is presented in Table 2-1. I performed all other experiments and collected all other data presented in this chapter.

Chapter 3 presents currently unpublished data that has been collected in collaboration with Charlie Kim, Jay Parrish, Yuh Nung Jan, Joseph DeRisi, and Graeme Davis. Jay Parrish and Charlie Kim performed experiments that lead to the identification of Krüppel, which is the focus of this chapter. Part of their earlier work is the basis for the information presented in Figures 3-1 and 3-2 and Charlie Kim made both figures. To these figures I contributed only dissection and dissociation of Krüppel overexpressing motoneurons. In addition, Jay Parrish performed all experiments required for Figure 3-9 in addition to providing the figure. Finally, Graeme Davis contributed significantly to experiments required for Figure 3-6. I performed all other experiments and collected all other data presented in this chapter.

Chapter 5 also presents unpublished data collected in collaboration with Charlie Kim, Joseph DeRisi and Graeme Davis. Experiments were shared between Charlie Kim and I for all data presented. Charlie has provided guidance and support throughout the last year of my thesis.

For all work presented here and leading to my thesis, Graeme Davis has supervised my research and provided guidance and support.

**Molecular Mechanisms Regulating Cell Intrinsic and Synaptic
Homeostasis: Compensation in *Drosophila shal* Mutants**

by

Sharon B. Bergquist

Lily Jan

Chair, Thesis Committee

ABSTRACT

Homeostasis is the property of a system to precisely maintain constant function at a set point level of activity. Within the nervous system homeostatic mechanisms are thought to constrain neural plasticity to maintain stable activity over an animal's lifetime.

Homeostatic modulation of both synaptic efficacy and intrinsic neuronal excitability has been demonstrated in vertebrates and invertebrates (Davis & Goodman 1998a, Turrigiano & Nelson 2000, Marder & Prinz 2002, Perez-Otano & Ehlers 2005). Work in the laboratory of Graeme Davis has shown at the *Drosophila* neuromuscular junction (NMJ) that decreases in muscle sensitivity to neurotransmitter, through either genetic mutation of the Glutamate Receptor subunit IIA or pharmacological block of this same subunit, result in enhanced presynaptic neurotransmitter release. This increase in neurotransmitter release, or quantal content, precisely compensates for the block in postsynaptic sensitivity, restoring muscle excitation back to baseline. This process has been termed synaptic homeostasis. Work in many labs has demonstrated that the loss or mutation of a single ion channel results in the compensatory changes in abundance or function of other ion channels that often restore neuronal activity. These compensatory changes in ion channels are thought to be cell-intrinsic homeostasis.

There are many open questions regarding homeostatic compensation within the nervous system and the underlying molecular mechanisms. My thesis work focuses on the mechanisms underlying the involvement of voltage-gated potassium channels, Shal and Shaker (Sh), in both synaptic and cell-intrinsic homeostasis and concludes with a broader description of the modulation of ion channel expression in response to the loss of several independent ion channels in *Drosophila* motoneurons.

In Chapter 2, I demonstrate that a mutation in *shal* results in the loss of Shal expression and function and further, loss of Shal blocks synaptic homeostasis. In identifying the cause for blocked synaptic homeostasis I uncover a form of cell-intrinsic homeostasis within motoneurons; the reciprocal coupling of potassium channels Shal and Sh, where loss of either channel results in increased expression of the other. The increase in Sh at motoneuron terminals is ultimately responsible for occlusion of synaptic homeostasis, as blocking increased Sh either genetically or pharmacologically is sufficient to restore synaptic homeostasis. Importantly, acute inhibition of increased Sh function reveals synaptic homeostasis, demonstrating that Sh is not directly involved, but rather increased current is able to occlude the expression of homeostasis. Further, in demonstrating that the cell-intrinsic control of ion channel expression prevents the expression of synaptic homeostatic signaling, our data argue against coordinated control of independent homeostatic responses.

In Chapter 3, I demonstrate that *kr* and *sh* expression are developmentally linked in sensory neurons as well as motoneurons, *kr* is sufficient to increase *sh* expression in sensory and motoneurons and Kr expression is aberrantly increased in sensory neurons and throughout the CNS and ventral nerve cord of third instar *shal* mutants. Further, over-expression of Kr phenocopies *shal* mutant physiology. Finally I demonstrate that increased Kr can be induced in fewer than 24 hours following pharmacological block of Shal. Surprisingly however, increased Kr colocalized with sensory neuron markers, but

not motoneuron markers. Therefore, despite being sufficient for increasing Sh expression, Kr is not ultimately responsible for increased Sh in *shal* mutant motoneurons.

In Chapter 4, I present expression profiling DNA-microarray data performed on isolated motoneurons from six ion channel mutants. This project is on going and seeks to gain a complete picture of the changes in ion channel expression following loss of one ion channel. From this data I will be able to identify whether there is specific coupling between pairs or groups of ion channels and therefore rules governing ion channel compensation or whether each ion channel mutant drives a unique compensatory response. This data will also provide insight into the transcriptional regulation underlying changes in ion channel expression.

TABLE OF CONTENTS

ACKNOWLEDGEMENTS.....	iii
PREFACE.....	v
ABSTRACT.....	vi
TABLE OF CONTENTS.....	x
Chapter 1: General Background.....	1
<i>Synaptic Homeostasis at the NMJ.....</i>	<i>3</i>
<i>Homeostasis of Neuronal Activity: Synaptic Scaling.....</i>	<i>4</i>
<i>Homeostasis of Neuronal Activity: Ion Channel Homeostasis.....</i>	<i>5</i>
Chapter 2: A Hierarchy of Cell Intrinsic and Target-Derived Homeostatic	
Signaling.....	9
<i>Introduction.....</i>	<i>10</i>
<i>Results.....</i>	<i>13</i>
<i>Discussion.....</i>	<i>28</i>
<i>Figures.....</i>	<i>36</i>
Chapter 3: Transcription Factor Kruppel is sufficient to increase Shaker in	
Motoneurons.....	63
<i>Introduction.....</i>	<i>64</i>
<i>Results.....</i>	<i>66</i>
<i>Discussion.....</i>	<i>75</i>
<i>Figures.....</i>	<i>78</i>
Chapter 4: Description of Ion Channel Regulation in Drosophila Motoneurons.....	95

<i>Introduction</i>	96
<i>Results</i>	98
<i>Discussion</i>	101
<i>Figures</i>	103
Chapter 5: General Conclusions	107
EXPERIMENTAL PROCEDURES	110
REFERENCES	118
PUBLISHING AGREEMENT	128

Chapter One:
General Introduction

The brain is a complex system made up of billions of neurons and thousands of synaptic connections. Plasticity of synaptic connections and neuronal excitability underlie the brain's ability to respond to and store novel information. Hebbian correlation based forms of plasticity, such as long-term potentiation and depression, are now well-established models of how information is stored. However, it has also been recognized that this plasticity, when left unchecked, threatens the stability of the nervous system, leading to saturation of potentiation or quiescence. The brain must therefore maintain the ability to learn and adapt without compromising the essential structure and integrity of the circuits that allow for sensation and action. At the single cell level this stability problem becomes more daunting when we consider that neurons live (in the case of humans) for decades while the ion channels and receptors that determine their active properties turn over in minutes to hours (Marder and Prinz, 2002; Desai, 2003; Turrigiano, 2008). Homeostasis is a form of feedback regulation that maintains the function of a system at a set point level of activity. There have now been numerous studies demonstrating that within the nervous system homeostatic mechanisms act to constrain plasticity to promote stability. Homeostatic signaling systems also act through modulation of synaptic efficacy and membrane excitability and therefore must interface with mechanisms of plasticity to achieve stable, yet flexible neural circuitry (Marder and Prinz, 2002; Turrigiano and Nelson, 2004; Perez-Otano and Ehlers, 2005; Davis, 2006; Frank et al., 2009).

Synaptic Homeostasis and the NMJ

Homeostatic control of synaptic efficacy has been documented at the neuromuscular junction (NMJ) in both vertebrates and invertebrates (Davis and Bezprozvanny, 2001; Petersen et al., 1997; Plomp et al., 1994). In all cases impairment of postsynaptic neurotransmitter receptor sensitivity results in an increase in presynaptic release. This retrograde control of presynaptic release has been most well characterized in *Drosophila* (Petersen et al., 1997; Frank et al., 2006, 2009; Dickman and Davis, 2009; Bergquist et al. 2010; Mueller et al., 2011). Here genetic deletion of the postsynaptic glutamate receptor subunit, IIA (*GluRIIA*) leads to a decrease in quantal size of approximately 50%. Although muscle sensitivity to transmitter is impaired, muscle depolarization following nerve stimulation is normal. This is accomplished through an increase in presynaptic neurotransmitter release (Petersen et al. 1997). Increased release precisely offsets the decrease in receptor sensitivity to restore muscle excitation to baseline and is therefore referred to as synaptic homeostasis. Similarly, incubation of the NMJ with the glutamate receptor antagonist philanthotoxin-433 (PhTx) also leads to a decrease in quantal size of about 50%. Within 10 minutes this reduction in receptor sensitivity induces a rapid compensatory increase in presynaptic release, which again precisely restores muscle excitation.

The rapid induction enabled us to perform a large electrophysiology-based forward genetic screen to identify genes that, when mutated, block this compensatory process. As a result the molecular mechanisms underlying synaptic homeostasis are beginning to emerge. Mutations in *cacophony* (*cac*), the gene that encodes the presynaptic Cav2.1 calcium channel subunit, cause a decrease in calcium influx through the channel and block synaptic homeostasis. In addition, *GluRIIA* mutants are

significantly more sensitive to calcium channel antagonists nickel and cadmium. Both support the conclusion that synaptic homeostasis requires increased calcium influx that is achieved through increased presynaptic calcium channel number or activity. In further support of this conclusion it was also recently demonstrated that the presynaptic signaling system including the Eph receptor, Ephexin, and Cdc42, which converge on Cac, are all also required for synaptic homeostasis. These data further suggest the Eph receptor may function to receive the homeostatic, retrograde signal derived from muscle (Frank et al. 2006 and 2009). In a parallel pathway, there is growing evidence to suggest modulation of vesicle trafficking and/or localization within the presynaptic terminal is also required for synaptic homeostasis (Dickman and Davis, 2009; Mueller et al., 2010).

Homeostasis of Neuronal Activity: Synaptic Scaling

Homeostatic control of neuronal activity was first demonstrated in cultured neocortical neurons. Blocking network activity for prolonged periods of time results in hyperactivity when antagonists are removed. The reciprocal is also true; elevation of network activity by reducing inhibition initially raises firing rates, but over many hours firing rates return to baseline (Turrigiano et al., 1998). Further work demonstrated that this homeostatic mechanism globally changes synaptic strengths equally (or is multiplicative), measured as the scaling of the total distribution of quantal amplitudes, across the neuron. This multiplicative scaling preserves the relative weights of each synaptic contact to the neuron while simultaneously maintains the overall activity of the neuron at a set point level (Turrigiano et al., 1998; Desai 2003; Turrigiano and Nelson, 2004). A similar scaling has been shown *in vivo* in rat visual cortex. Here monocular deprivation prevents

the normal developmental decrease in mEPSC amplitude. This suggests there is global hypersensitivity in response to decreased input activity (Desai et al., 2002). In these examples, synaptic scaling is accomplished through the regulation of postsynaptic receptor density.

In order to accomplish synaptic scaling, neurons must somehow sense their activity level. Scaling could require widespread changes in network activity where many neurons and glia are affected simultaneously. In support of this model, glial derived TNF- α signaling is required for scaling following TTX inhibited neuronal cultures (Stellwagen and Malenka, 2006). Alternatively, neurons could sense their own firing rates to scale their own synapses cell intrinsically. Buffering somatic calcium has been shown to induce synaptic scaling, suggesting that drops in neuronal firing, which lead to a drop in calcium, could result in synaptic scaling in each neuron individually. These data also provide evidence that global changes in calcium levels are monitored by the homeostat as the readout of neuronal activity (Ibata et al., 2008; Turrigiano 2008). These models are not mutually exclusive, but it remains to be determined whether they function in the same pathway or are independent mechanisms of homeostasis.

Homeostasis of Neuronal Activity: Ion Channel Homeostasis

In addition to regulating postsynaptic receptor density, there is also evidence for homeostatic control of neuronal activity through modulation of ion channel abundance. Long-term perturbation of activity in cultured neurons also results in compensatory changes in ion channel abundance. Incubation with TTX for several days to silence cultured neurons leads to increased sodium current densities and decreased potassium

current densities acting to counteract inhibition by increasing excitability (Desai et. al., 1999). Further evidence for homeostatic control of neuronal activity through ion channel modulation comes from primary cultures of dissociated lobster stomatogastric ganglion (STG) neurons. *In vivo* these neurons show bursting activity due to descending neuromodulatory input. Initially in culture, removed from their synaptic input, these neurons are silent, but following a few days they will resume burst firing. This return to baseline is the result of increasing inward currents and decreasing outward currents (Turrigiano et. al. 1995; Marder and Prinz, 2002).

In addition to these experiments, evidence for modulation of ion channel abundance to homeostatically control neuronal activity comes from knockout mutants. Often ion channel knockouts show physiological phenotypes that are much less severe than pharmacological blockade of the same channel would predict. Many recent studies have shown that this is a result of compensatory changes in the function or abundance of other ion channels. Deletion of the voltage gated potassium channel $K_v4.2$ causes compensatory increases in the similar potassium channel, $K_v1.4$ currents in hippocampal neurons (Chen et al., 2006). Similarly, in pyramidal neurons there is an increase in potassium currents I_k and I_{ss} in $K_v4.2$ knockouts (Nerbonne et al., 2008). Deletion of the voltage gated sodium channel, $Na_v1.6$ leads to compensatory increases in $Na_v1.1$ and 1.2 in retinal ganglion cells (Van Wart and Matthews, 2006). In Purkinje cells, $Na_v1.6$ knockout results in increased T- and P-type calcium channels along with $Na_v1.1$ (Swensen and Bean, 2005; Van Wart and Matthews, 2006). In all cases, neuronal activity recorded at the soma was similar to wild-type recordings indicating that these changes in ion channel function and/or abundance are homeostatic.

The molecular mechanisms leading from changes in activity to homeostatic alterations in ion channel abundance are completely unknown. As with the other forms of homeostasis, how and where changes in activity are sensed are also uncertain. This is especially relevant to ion channel compensation as localization of channels is highly regulated within neurons. In the $K_v4.2$ knockouts compensatory increases in the other potassium currents restores somatic firing properties, however, there was no compensation for potassium channel currents in the dendrites where $K_v4.2$ is localized. As a result dendrites in these mutants were hyperexcitable. These data argue that neuronal excitability or output might be of greater importance for neurons to monitor and maintain, or more simply that homeostatic sensors are localized to the soma.

Modeling work suggests that the same neuronal activity patterns can be generated from numerous, plausible combinations of ion channels (Prinz et al., 2004). Further, huge variation in absolute channel abundance has been demonstrated in identified neurons from different animals despite these neurons sharing identical firing properties (Schulz et al., 2006). These data support a model where neurons set their level of activity and ion channels are free variables at the neuron's disposal to maintain activity. This would allow knockout animals to simply readjust the balance of all ion channels expressed to retarget proper activity of the neuron. However, it appears from studies of ion channel mutants so far, that rather than readjustment of all ion channels in response to the loss of any one, there are specific changes in a relatively small number of other ion channels. This suggests that there may pairs or groups of coupled ion channels and therefore identifiable rules governing which ion channels will be altered in response to the loss of any one.

The physiology of *Drosophila* motoneurons and the NMJ have been well characterized. This in combination with the ability to combine genetic, electrophysiology and molecular techniques make *Drosophila* an ideal experimental system for studying the homeostatic regulation of ion channels, membrane excitability, and synaptic efficacy. Chapter 2 provides a detailed account of how mutations in *shal*, which encodes an A-type voltage-gated potassium channel, block synaptic homeostasis and how this mechanism uncovers the homeostatic coupling of A-type potassium currents in motoneurons. Chapter 3 identifies the transcription factor, *kruppel* as a possible mediator of A-type potassium channel coupling. Chapter 4 shows the changes in expression in five ion channel mutants.

Chapter 2:
A Hierarchy of Cell Intrinsic and Target-Derived Homeostatic
Signaling

Introduction

Homeostatic signaling systems are believed to interface with the mechanisms of neural plasticity to achieve stable, yet flexible, neural circuitry (Davis, 2006; Marder and Goaillard, 2006; Turrigiano, 2008). In each example, a perturbation such as activity blockade or neurotransmitter receptor inhibition causes a transient change in neural function. Then, over some period of time, baseline neural function is restored in the continued presence of the perturbation. The means by which homeostatic signaling systems respond to a perturbation and restore neural function are diverse. They include the modulation of ion channel expression, postsynaptic neurotransmitter receptor abundance, and synaptic vesicle release (Davis, 2006; Marder and Goaillard, 2006; Turrigiano, 2008).

Compensatory changes in the abundance of depolarizing or hyperpolarizing ion channels are generally believed to reflect the action of cell-intrinsic, homeostatic mechanisms that control neuronal firing (Marder et al., 1996; Marder and Prinz, 2002). For example, lobster stomatogastric ganglion neurons, when placed in isolated cell culture, will recalibrate the abundance of inward and outward channel densities to reestablish normal neural activity in the absence of synaptic drive (Turrigiano et al., 1995). Since this compensatory reaction restores neural activity, it is considered homeostatic. In addition, this form of compensation occurs in an isolated cell and therefore must reflect cell-intrinsic signaling. More recently, there have been numerous studies demonstrating that the loss or mutation of a single ion channel gene causes a compensatory change in the abundance of other similar ion channels, often restoring neuronal firing properties (Chen et al., 2006; MacLean et al., 2003; Marder et al., 1996;

Marder and Goaillard, 2006; Muraro et al., 2008; Nerbonne et al., 2008; Swensen, 2005; Van Wart and Matthews, 2006). Although the initial loss of an ion channel will alter circuit-level neuronal function, the compensatory changes made are generally thought to be the result of cell-autonomous, homeostatic signaling, much like that observed in isolated lobster central neurons (but see; Desai et al., 1999).

There are also several examples where inter-cellular signaling is an essential component underlying the homeostatic control of neuronal function. For example, the homeostatic control of glutamate receptor abundance in response to activity blockade is influenced by intercellular BDNF signaling (Rutherford et al., 1998) and requires glia-derived secretion of TNF-alpha (Kaneko et al., 2008; Stellwagen and Malenka, 2006). At the *Drosophila* neuromuscular junction (NMJ), inhibition of postsynaptic glutamate receptors induces a compensatory, homeostatic increase in presynaptic neurotransmitter release. This trans-synaptic signaling system includes the Eph receptor, Ephexin and Cdc42 and ultimately converges upon the Ca_v2.1 calcium channel (Frank et al., 2009). In addition, this form of homeostatic modulation is gated by the presence of low, persistent levels of BMPs in a non-cell autonomous manner (Goold and Davis, 2007).

To date, homeostatic processes that control neural function have been studied, primarily, in isolation. The ability of homeostatic signaling systems to function at the level of an individual cell and at the level of two or more cells within a neural circuit raises a number of interesting questions. For example, what happens when two independent perturbations occur, one inducing cell-intrinsic forms of compensation and another acting to induce inter-cellular or circuit level forms of compensation? Do the compensatory mechanisms function independently or are they coordinated through some

master-sensor of neural function? One way to probe this question is to provide sequential, conflicting perturbations to a neural system. If the system achieves an adaptive response that is different from either perturbation alone, restoring normal neural function, this would be consistent with integrated mechanisms of homeostatic compensation. An alternative possibility is that one form of compensation would predominate or occlude the other. This result could define whether homeostatic compensation is favored at the level of the individual cell compared to the surrounding neural circuit, or vice versa.

Beginning with gene identification through a large-scale genetic screen (Dickman and Davis, 2009), we now reveal how two independent and opposing homeostatic signaling systems interact in the *Drosophila* neuromuscular system. We report the isolation of a subset of potassium channel mutations that block synaptic homeostasis at the NMJ. In defining how these potassium channel mutations block synaptic homeostasis we uncover a second homeostatic signaling system, one that homeostatically and reciprocally couples the expression of A-type potassium channels in *Drosophila* motoneurons. We then demonstrate that the cell-intrinsic control of ion channel expression prevents the expression of trans-synaptic homeostatic signaling at the NMJ. Taken together, our data argue against coordinated control of independent homeostatic responses. If generalized, these data could influence our view of neurological disease if an initial stress initiates a primary homeostatic response that is restorative, but with consequences for the future capacity of that cell to adapt or respond to additional perturbations (Bernard et al., 2004; Bernard and Johnston, 2003; Bernard et al., 2001; Cossart et al., 2001; El-Hassar et al., 2007; Frohlich et al., 2008; Glykys and Mody, 2006; Mody, 2005).

Results

We recently performed a large-scale, electrophysiology-based forward genetic screen to identify genes that, when mutated, disrupt the homeostatic modulation of presynaptic neurotransmitter release (Dickman and Davis, 2009). This screen was based on the observation that incubation of the *Drosophila* NMJ with the glutamate receptor antagonist philanthotoxin-433 (PhTx; 4-10 μ M) for 10min is sufficient to decrease postsynaptic glutamate receptor sensitivity and induce a rapid, compensatory increase in presynaptic neurotransmitter release (Frank et al., 2006; Frank et al., 2009). The increase in presynaptic neurotransmitter release precisely offsets the decrease in postsynaptic receptor function and restores muscle excitation to baseline ‘set-point’ levels, a process referred to as synaptic homeostasis (Frank et al., 2006; Frank et al., 2009; Dickman and Davis, 2009). In this screen, PhTx was applied to the NMJ of individual mutant *Drosophila* larvae. For each mutant line, we recorded from 3-10 NMJ and calculated the average mEPSP amplitude, EPSP amplitude and quantal content (Dickman and Davis, 2009). This allowed us to quantify the effect of PhTx on postsynaptic receptor sensitivity and to quantify the homeostatic modulation of presynaptic neurotransmitter release for each mutant line.

This screen identified fourteen mutations that appear to block synaptic homeostasis. Remarkably, only three of these mutations fit into a common category, which turned out to be *Drosophila* potassium channels. In total, mutations that potentially disrupt twenty-three known or predicted potassium channel genes were screened including mutations in *shaker*, *shal*, *shab*, *shaw*, *orc1*, *KCNC2*, *eag*, *slo*, and *KCNQ* (Atkinson et al., 1991, Ganetzky, 1983; Kaplan and Trout, 1969; Koh et al., 2008).

The nature of each potassium channel mutation that we screened and data for the average mEPSP and EPSP amplitudes for each of these mutations are presented in Table 1. One potassium channel mutation, *shaker*¹⁴, was found to have an unusually large EPSP amplitude, even in the presence of PhTx, as might be expected for a mutation that broadens the presynaptic action potential (Dickman and Davis, 2009). However, three potassium channel mutants (*shal*, *shab*, *CG34366*) had unusually small EPSP amplitudes in the presence of PhTx (being more than two standard deviations smaller than the distribution mean for all mutations screened; Dickman and Davis, 2009), identifying them as mutations that potentially block synaptic homeostasis.

To investigate why three independent potassium channel mutations emerged from our genetic screen, we first determined whether the observed defects in synaptic homeostasis could be a secondary consequence of altered baseline transmission or impaired synapse morphology. First, we find that NMJ morphology is normal in all three mutants and, therefore, cannot account for impaired synaptic homeostasis (Fig. 1). Second, we find that baseline synaptic transmission in the absence of PhTx is not severely perturbed in these three mutants, indicating that a large disruption of baseline transmission cannot account for impaired synaptic homeostasis. It appears, therefore, that three independent potassium channel mutants disrupt either the induction or expression of synaptic homeostasis at the *Drosophila* NMJ.

The demonstration that potassium channel mutations block synaptic homeostasis was a surprise since an increase in neuromuscular excitability is the predicted phenotype of these channel mutations. To define why these potassium channel mutants might disrupt synaptic homeostasis we first focused our attention on a single gene, *shal*. We

chose to focus on *shal* because it is known to be expressed in *Drosophila* neurons but not muscle, and it is known to mediate a rapidly activating and inactivating A-current in *Drosophila* motoneurons (Baker and Salkoff, 1990; Baro et al., 1996; Birnbaum et al., 2004; Jan et al., 1977; Solc and Aldrich, 1988; Tsunoda and Salkoff, 1995). In addition, *shal* is highly conserved throughout evolution and mutations in *shal* have been linked to altered neural plasticity and neurological disease including chronic pain, epilepsy and heart arrhythmia (Birnbaum et al., 2004; Castro et al., 2001). Thus, defining how *shal* mutations disrupt synaptic homeostasis may have widespread implications.

Shal localizes to the motoneuron axon initial segment and is absent from the NMJ

We identified two transposon insertions in the *shal* gene as well as a deficiency chromosome that uncovers the *shal* locus (Fig. 2A). To identify whether these mutations are protein null and to explore where the Shal channel resides within *Drosophila* motoneurons, we took advantage of a previously developed Shal antibody (Baro et al., 2000). In wild-type animals Shal protein is highly expressed in central neuropil (possibly dendritic arborizations) and within the initial portion of the motor nerve as it exits the ventral nerve cord (VNC) (Fig. 2B). The presence of immuno-staining in the initial portion of the motor nerve strongly suggests that Shal protein is present in *Drosophila* motoneurons, consistent with prior physiological analyses (Tsunoda and Salkoff, 1995). Protein localization within the motoneurons tapers dramatically over the first 120 μ m of axon (measured from the origin of the motor nerve at a site adjacent to the neuropil within the central nervous system). Ultimately, after ~120 μ m Shal expression decreases to background levels (Fig. 2B and D). No detectable staining is observed at the

neuromuscular junction (data not shown) indicating that Shal is restricted to the dendrites and axon initial segment of motoneurons. Consistent with this conclusion, we find no effect of the Shal-specific toxin, phrixotoxin, on neuromuscular synaptic transmission in wild-type animals (Fig. 3) (Gasque et al., 2005). Finally, the specificity of the antibody staining data is confirmed by staining the *shal*⁴⁹⁵ mutant animal with anti-Shal. Anti-Shal staining is absent in this homozygous mutant and when this mutation is placed in trans to a deficiency that uncovers the *shal* locus (Fig. 2C-D). These results also indicate that the *shal*⁴⁹⁵ mutation is a protein null. Consistent with this conclusion, we assayed *shal* expression by quantitative real time polymerase chain reaction (qPCR) comparing wild type and *shal*⁴⁹⁵ (see methods). We find that *shal* expression is decreased by 97.7% (\pm 0.86, compared to wild type) in the *shal*⁴⁹⁵ homozygous mutant background (see also below for additional quantification). The localization of *shal* to the axon initial segment, at or near the site of action potential initiation in motoneurons, is consistent with *shal* being important for the control of motoneuron excitability.

Absence of an A-current in the motoneuron soma of *shal* mutants

We next examined the presence of the A-type current in *Drosophila* motoneuron soma comparing wild type and *shal* mutant animals to determine if loss of Shal protein eliminates the somatic A-type current in our *shal* mutant animals. Compared to wild type, there is a dramatic reduction in the A-current in *shal* mutant animals (Fig. 2E). At a holding potential of -10mV we observe a 100pA A-type current in wild type and the complete absence of an A-type current in the *shal* mutant. However, at higher holding potentials, we observe the emergence of a rapidly inactivating current in the *shal* mutant

animals that reaches approximately 50% wild type levels at the highest holding potentials tested. One possibility is that this represents residual Shal protein not detected by the antibody. We consider this unlikely because *shal* expression is effectively eliminated in the *shal* mutant (assayed by qPCR, see above). An alternative explanation is that the residual A-current in *shal* mutants is due to the activity of a different channel that is not localized to the soma but which could be activated at an electrotonically distant site (dendrite or axon) when high voltage steps are applied to the soma. Finally, this current could reflect the activity of KCNC2-type channels that are characterized by high voltage activation (Rudy and McBain, 2001) and are encoded in the *Drosophila* genome (see below). Regardless, our data indicate that there has not been a dramatic, compensatory replacement of an A-current at or near the motoneuron soma.

***shal* mutants have a mild deficit in baseline transmission**

Having identified a protein null mutation in *shal* we performed a detailed characterization of baseline synaptic transmission in this mutant (Fig. 4 and Table 2). There is no significant change in mEPSP amplitude comparing wild type (w^{1118}) with *shal*⁴⁹⁵/+ or *shal*⁴⁹⁵ homozygous mutants or *shal*⁴⁹⁵/*Df* (Fig. 4A and C). There is a small, statistically significant, deficit in EPSP amplitude observed in the *shal*⁴⁹⁵ mutant and *shal*⁴⁹⁵/*Df* when compared to wild type. We observe corresponding changes in quantal content (Fig. 4 D, E) (see methods). This mild effect on synaptic electrophysiology is also observed across a range of external calcium concentrations (Fig. 4B). The mild decrease in baseline synaptic transmission is unexpected for several reasons. First, loss of an A-type potassium channel would be expected to broaden the action potential and potentiate

release. Second, we cut the nerve and stimulate below the level where Shal protein is no longer present in the axon. Thus, it is unclear why loss of Shal would have any effect on synaptic transmission at the NMJ. Below we identify compensatory changes at the nerve terminal that could reasonably explain this result.

The rapid induction and sustained expression of synaptic homeostasis are blocked in *shal* mutants

We next analyzed synaptic homeostasis in greater detail in the *shal* mutants. First, we repeated the application of PhTx to wild type and *shal* mutant animals. In *shal* mutant animals, mEPSP amplitudes are similarly suppressed by application of PhTx, but EPSP amplitudes fail to recover to wild-type levels (Fig. 5A and Table 2). Calculation of quantal content demonstrates that the normal, homeostatic enhancement of presynaptic release is completely blocked in the *shal*⁴⁹⁵ mutant. Statistically identical defects in synaptic homeostasis were observed in four different *shal* mutant combinations (Fig. 5B-C). Together, these data demonstrate that the rapid induction of synaptic homeostasis is blocked by mutations that eliminate Shal.

In order to determine whether *shal* mutations also block the persistent expression of synaptic homeostasis we placed the *shal*⁴⁹⁵ mutation in the *GluRIIA*^{SP16} (*GluRIIA*) mutant background. It has been previously demonstrated that mEPSP amplitudes are decreased in the *GluRIIA* mutant throughout larval development and that there is a robust homeostatic increase in presynaptic release (Frank et al., 2006; Petersen et al., 1997). Here we demonstrate that the expression of synaptic homeostasis in the *GluRIIA* mutant is blocked in the *shal* mutant (Fig. 6 and Table 2). This result was confirmed by

demonstrating a block of synaptic homeostasis when the *shal*⁴⁹⁵/*Df* allelic combination is placed in the *GluRIIA* mutant background. Thus, *shal* is required for both the rapid induction and persistent expression of synaptic homeostasis. The rapid induction of synaptic homeostasis is a local phenomenon that can occur at the isolated NMJ (Frank et al., 2006) raising the question why loss of Shal, which is not present at the NMJ, blocks this process.

Homeostatic Coupling of I_A Channel Expression in Drosophila

In systems as diverse as the lobster stomatogastric ganglion and the mouse hippocampus, loss or over-expression of an individual ion channel has been observed to drive compensatory changes in the expression of other ion channels (Chen et al., 2006; MacLean et al., 2003; Nerbonne et al., 2008; Swensen, 2005). This has been referred to as a form of cell-intrinsic homeostatic compensation that stabilizes neural activity (Marder et al., 1996; Marder and Prinz, 2002). *Drosophila* motoneurons express two channels encoding A-type currents, Shal and Shaker (Wei et al., 1990). In vertebrates, loss of K_v4.2 (Shal) initiates a compensatory increase in the K_v1 (Shaker) current, though ion channel expression was not determined in this study (Chen et al., 2006). Here we test whether there is homeostatic coupling between I_A currents in *Drosophila* motoneurons.

First, we tested *shaker* RNA expression comparing wild type and *shal* mutant animals. Currently, antibodies are not available to Shaker in *Drosophila*. Therefore, we tested mRNA expression using qPCR. We find an increase in *shaker* expression in the *shal* mutant (252% ± 30.7 compared to wild type) assaying mRNA derived from dissected central nervous systems (Fig. 7). As a control, we document a statistically

significant decrease in *shaker* expression when we drive expression of a UAS-*shaker*-RNAi (*shakerRNAi*) in the nervous system confirming that *shaker* is expressed presynaptically and that we can accurately measure both an increase and decrease in *shaker* expression via qPCR (Fig. 7). Thus, in the *shal* mutants, there is an up-regulation of neuronal *shaker* expression that could alter channel abundance in the motor axon and presynaptic nerve terminal where Shaker normally resides (Gho and Ganetzky, 1992; Martinez-Padron and Ferrus, 1997; Sheng et al., 1993).

Next we tested whether I_A channel expression is reciprocally coupled, something that is unknown in any system. We show that neuronal expression of *shakerRNAi* knocks down *shaker* expression and that this causes an increase in *shal* mRNA ($223\% \pm 22.4$ increase compared to wild type) (Fig. 7). We recognize that the knockdown of *shaker* expression is incomplete and sought to repeat this experiment in a *shaker* mutation. Unfortunately, molecular null mutations in *shaker* are no longer commonly available. Therefore, we repeated our experiment and assayed *shal* expression in a *shaker*¹⁴ mutation, which is a functional null (Lichtinghagen et al., 1990). Consistent with the results of *shaker* knockdown, we find that *shal* expression is dramatically increased in the *shaker*¹⁴ mutant (Fig. 7). This result confirms a reciprocal regulation of I_A channel expression in *Drosophila* motoneurons.

Finally, as a control, we asked whether the increase in Shaker transcription occurs in the *GluRIIA; shal* double mutant, just as it does in the *shal* mutant. We find a robust, statistically significant increase in *shaker* ($189 \pm 12.5\%$ increase compared to wild type; $p < 0.05$) in the *GluRIIA; shal* double mutant that is not statistically different from that observed in *shal* alone. In the double mutant animals, EPSP amplitudes are significantly

smaller than that observed in the *shal* mutant alone. Thus, the magnitude of the postsynaptic EPSP amplitude does not strongly influence the compensatory change in *shaker* transcription, consistent with the hypothesis that the compensatory regulation ion channel expression is cell intrinsic.

A compensatory increase in presynaptic Shaker blocks synaptic homeostasis in the *shal* mutant background.

Shaker is expressed at the presynaptic nerve terminal of Drosophila motoneurons (Ganetzky and Wu, 1982; Jan et al., 1977; Wu et al., 1983). One possibility, therefore, is that loss of Shal initiates an increase in presynaptic Shaker and this is the cause of impaired synaptic homeostasis. Such an effect could also explain reduced baseline transmission in the *shal* mutant. If this is the case, then a *shaker* mutation might restore synaptic homeostasis when placed in the background of the *shal* mutant. To test this hypothesis, we generated double mutant animals harboring mutations in both *shal* and *shaker*.

As shown previously, *shaker* mutant NMJs have normal mEPSP amplitudes ($p > 0.3$ compared to wild type) and a dramatic increase in the average EPSP amplitude (Fig. 8A and Table 2). At the extracellular calcium concentration used (0.3mM Ca^{2+}), the increase in EPSP amplitude can be primarily accounted for by an increase in presynaptic release due, most likely, to broadening of the presynaptic action potential. When PhTx is applied for 10min under these conditions, wild-type animals show a decrease in mEPSP amplitude and a robust homeostatic increase in presynaptic release (Fig. 8). The *shaker* mutant animals also show a decrease in mEPSP amplitude and a robust homeostatic

increase in presynaptic release. Only *shal* mutant animals fail to show homeostatic compensation (Fig. 8).

We next assayed baseline transmission and homeostatic compensation in two mutant combinations, the *shaker-shal* double mutant and *shal* animals that harbor a heterozygous mutation in *shaker* (*sh/+*). We observe robust homeostatic compensation in the *shaker-shal* double mutant in contrast to *shal* mutants alone (Fig. 8). A quantitatively identical result is observed when only a single copy of *shaker* is removed, indicating that the restoration of synaptic homeostasis is sensitive to the dosage of *shaker* (Fig. 8). These data support the hypothesis that the compensatory increase in *shaker* transcription observed in *shal* mutants could be responsible for blocking synaptic homeostasis. It should be noted, however, that there is an increase in baseline transmission caused by the *shaker* mutation, both in the heterozygous and homozygous condition (Fig 8A and Table 2).

To further investigate whether increased presynaptic Shaker is responsible for the block of synaptic homeostasis in *shal* mutants, we used RNAi to knock down *shaker* specifically in presynaptic neurons. We expressed *shakerRNAi* in presynaptic neurons in *shal* mutant animals, achieving significant *shaker* knockdown by qPCR ($69.19 \pm 6.11\%$; see methods) and hypothesized that synaptic homeostasis would again be restored. This is precisely what we observed (Fig. 9). This experiment is important for two additional reasons. First, this demonstrates that neuronal Shaker knockdown rescues synaptic homeostasis in *shal*. Second, there is no statistically significant change in baseline synaptic transmission caused by neuronal Shaker knockdown ($p > 0.1$; Table 2). Since presynaptic *shaker* knockdown restores synaptic homeostasis in *shal* without a change in

baseline transmission, we can conclude that the restoration of synaptic homeostasis is caused by preventing an increase in *shaker* expression, and is not secondary to a large increase in baseline transmission. These data strongly support the hypothesis that increased levels of presynaptic Shaker are responsible for the block of synaptic homeostasis observed in *shal* mutant animals.

Transgenic overexpression of *shaker* blocks synaptic homeostasis

To this point we have provided molecular and genetic evidence that increased levels of presynaptic Shaker in the *shal* mutant cause a block of synaptic homeostasis. To further test this model we asked whether transgenic overexpression of *shaker* is sufficient to block synaptic homeostasis in an otherwise wild type background. We used the motoneuron-specific driver *Ok6-gal4* to express a previously published, modified Shaker potassium channel termed **E**lectrical **K**nock**O**ut-222 (EKO) (White et al., 2001).

Presynaptic expression of EKO does not alter the PhTx-dependent decrease in mEPSP amplitude, but completely blocks the homeostatic increase in presynaptic release normally observed in wild type (Fig. 10). Thus, increased Shaker is sufficient to block the acute expression of synaptic homeostasis. It should be noted that expression of EKO decreases evoked release by ~55% compared to wild type (Table 2). However, we have previously identified other mutations in synaptic genes that disrupt synaptic transmission to an equal or greater extent compared to EKO expression but do not block synaptic homeostasis (Goold and Davis, 2007). Furthermore, a 10-fold decrease in extracellular calcium concentration, reducing transmission below that observed in EKO, also does not block synaptic homeostasis (Frank et al., 2006). Thus, a decrease in baseline

transmission is not correlated with impaired synaptic homeostasis. Together, our data further support the model that a compensatory increase in synaptic Shaker is responsible for the defect in synaptic homeostasis observed in the *shal* mutant background.

Increased Shaker blocks the expression versus the induction of synaptic homeostasis

Shaker function is accessible to pharmacological inhibition, allowing us to test whether elevated Shaker blocks the induction versus the expression of synaptic homeostasis. To do so, we asked whether acute pharmacological inhibition of Shaker can restore synaptic homeostasis in the *shal* mutant. We tested a range of 4-AP concentrations in wild type and selected a concentration ($25\mu\text{M}$) that produces only a modest change in EPSP amplitude in wild type (27%). When $25\mu\text{M}$ 4-AP is applied following application of PhTx to the *shal* mutant NMJ, a robust homeostatic increase in presynaptic release is observed (Fig. 11). This homeostatic increase in presynaptic release is significantly greater than the increase in baseline transmission observed when 4-AP is applied to *shal* mutants alone (Table 2). In addition, we show that application of PhTx to wild type causes a homeostatic increase in quantal content and there is no further increase in quantal content when 4-AP is co-applied with PhTx (Figure 11 D-F). When taken together with the genetic experiments described above, we conclude that elevated levels of synaptic Shaker impair synaptic homeostasis in the *shal* mutant background. Furthermore, since acute application of 4-AP restores homeostatic compensation when applied after PhTx it demonstrates that increased Shaker can mask the expression of previously induced synaptic homeostasis (Fig. 11). This implies that the homeostatic

control ion channel abundance in individual cells can supercede or prevent expression of additional forms of homeostatic compensation.

Impaired synaptic homeostasis in an additional, novel potassium channel mutant.

Finally, we sought to address two additional questions. First, is altered Shaker expression a common form of compensation that would adjust for loss of any neuronal potassium current? Second, we sought to control for the possibility that shaker knockdown might non-specifically restore homeostatic compensation to any given mutant background. We are able to address both of these issues by analysis of an additional potassium channel mutation isolated in our genetic screen. In our genetic screen, we identified a transposon insertion within the coding region of *CG34366* (*CG34366*⁴³⁷⁷) that decreases gene expression, assayed by qPCR, by 38.01% (± 6.85) compared to wild type. The *CG34366* gene encodes the *Drosophila* homolog of the human *KCNC2* (*K_v3.2*) potassium channel (Fig. 12A). This channel is expressed in the embryonic *Drosophila* central nervous system but no genetic or functional analyses have yet been performed (Hodge et al., 2005). The *K_v3* potassium channels are widely expressed in the mammalian nervous system (Rudy and McBain, 2001) and can be localized to both the cell soma and synaptic terminals (Goldberg et al., 2005; Itri et al., 2005; Rudy and McBain, 2001). These channels have positively shifted voltage dependencies and very fast deactivation kinetics. The *K_v3* channels facilitate action potential repolarization, sometimes being referred to as the fast delayed rectifier, and are necessary for the fast repetitive firing observed in numerous neuronal types including purkinje cells and neurons with the globus pallidus and superchiasmatic nucleus (Goldberg et al., 2005; Hernandez-Pineda et al., 1999; Itri et

al., 2005; Rudy and McBain, 2001). The $K_v3.1/K_v3.2$ double knockout mice show broadened action potentials, increased synaptic transmission and associated decrease in paired-pulse ratios (Goldberg et al., 2005). This is consistent with the required function of these channels in action potential repolarization and subsequent synaptic transmission.

We first analyzed baseline synaptic transmission in the $K_v3.2$ mutant (Fig. 12C-D). The $K_v3.2$ mutants show modest changes in baseline synaptic transmission (Fig. 12C; Table 2). The average amplitude of spontaneous miniature release events is slightly decreased compared to wild type ($p < 0.05$) and there is an associated, statistically significant decrease in EPSP amplitude ($p < 0.01$). However, there is no deficit in quantal content compared to wild type, underscoring the mild nature of these effects (Fig. 12C-D and Table 2). There is also no change in muscle resting membrane potential (-69 ± 0.4 mV in wild type versus -70.1 ± 1.3 mV in the $K_v3.2$ mutant) and only a slight change in muscle input resistance (10.5 ± 0.7 M Ω in wild type versus 8.5 ± 0.7 M Ω in the $K_v3.2$ mutant, $p = 0.05$) that is within normal genotypic variation (see Table 2). We next confirmed that there is a block of synaptic homeostasis following application of PhTx to the $K_v3.2$ mutant animals. Application of PhTx causes a significant decrease in mEPSP amplitude, similar to that observed in wild type. However, there is no compensatory increase in presynaptic transmitter release, confirming a block of synaptic homeostasis identical to that observed in *shal* mutants (Fig. 12C-D and Table 2).

Next, we performed a series of experiments to determine if loss of $K_v3.2$ causes an increase in synaptic shaker, as observed in the *shal* mutant. First, we tested for a change in *shaker* expression via qPCR. However, there is no significant change in *shaker* transcript (Fig. 12B). We also performed a genetic test of altered Shaker abundance in

K_v3.2 mutants. We knocked down *shaker* expression presynaptically in the *K_v3.2* mutant and asked whether this would restore synaptic homeostasis, as it did in the *shal* mutant background. However, *shaker* knockdown (via RNAi expression) did not restore synaptic homeostasis in *K_v3.2* animals (Fig. 12E and Table 2). From these data we are able to draw two conclusions. First, these data demonstrate that the rescue of synaptic homeostasis in *shal* mutants by neuronal expression of *shaker* RNAi is specific and not a consequence of increased transmission. Second, altered *shaker* expression is not a generalized compensatory response. This result emphasizes that *shaker* and *shal* expression seem to be specifically coupled in a homeostatic manner. It remains to be determined whether loss of *K_v3.2* directly prevents synaptic homeostasis, or whether there is a unique compensatory response in *K_v3.2* mutant animals that also blocks expression of synaptic homeostasis. An answer to this question will be the subject of future studies.

DISCUSSION

An electrophysiology-based forward genetic screen identified three potassium channel mutations, including mutations in *shal* and *Drosophila Kv3.2*, that block the expression of synaptic homeostasis following inhibition of postsynaptic glutamate receptor function.

We have focused on how mutations in a single potassium channel, *shal*, lead to a blockade of synaptic homeostasis. We demonstrate that loss of *shal* induces a compensatory increase in *shaker* expression, and vice versa, suggesting homeostatic maintenance of A-type channel abundance in *Drosophila* motoneurons. The compensatory increase in *shaker* expression is remarkable, however, because it does not replace the A-type current recorded at the motoneuron soma (Fig. 2). Rather, increased Shaker functions to restrict neurotransmitter release from the motoneuron terminal, decreasing baseline release and blocking any further homeostatic enhancement of presynaptic release. There are several implications. First, our data demonstrate that the unique subcellular localization of each ion channel will determine how any compensatory change in ion channel abundance affects neural activity and synaptic transmission. Second, it appears that cell-autonomous control of intrinsic excitability can occlude the expression of subsequent inter-cellular homeostatic signaling. This suggests a hierarchical control of cell-intrinsic excitability compared to circuit level homeostatic regulation. This also calls into question the concept of a master, homeostatic sensor of neuronal activity. Finally, we define a form of compensation that may largely preserve neuronal output properties without restoring cellular excitation at the level of the cell soma.

Blocking the expression of synaptic homeostasis by increased Shaker.

Here we demonstrate that a compensatory increase in Shaker expression is necessary and sufficient to block the subsequent expression of synaptic homeostasis following postsynaptic GluR inhibition. In a *shal* mutant we observe a ~250% increase in *shaker* expression (Fig. 7). If we prevent this increase in Shaker expression in any of three different ways, 1) genetically by introducing *shaker* mutations (Fig. 8), 2) transgenically through neuron-specific dsRNA knockdown of *shaker* (Fig. 9), or 3) pharmacologically (Fig. 11), then we restore synaptic homeostasis in the *shal* mutant. Furthermore, acute block of Shaker by 4-AP following PhTx provides evidence that increased Shaker levels block the expression of synaptic homeostasis, not the induction of this form of homeostatic plasticity (Fig. 11). Finally, we demonstrate that exogenous overexpression of a Shaker transgene (EKO) is sufficient to block synaptic homeostasis in an otherwise wild type background (Fig. 10). Thus, the compensatory increase in Shaker expression in the *shal* mutant blocks subsequent expression of synaptic homeostasis.

We also provide numerous experiments that argue against the possibility that loss of Shaker rescues synaptic homeostasis through a non-specific potentiation of synaptic transmission. First, neuronal expression of *shaker* RNAi in the *shal* mutant background reduces *shaker* transcript (~70% reduction) and restores synaptic homeostasis without potentiating baseline transmission. Second, pharmacological inhibition of Shaker was performed using 4-AP concentrations that have a minimal effect on baseline synaptic transmission (~27% change), yet synaptic homeostasis is restored. Finally, synaptic homeostasis is also blocked in the $K_v3.2$ mutant, but there is no change in *shaker* expression nor does presynaptic knockdown of *shaker* in the $K_v3.2$ mutant rescue

synaptic homeostasis (Fig. 12). We conclude that the increased *shaker* expression is specific to the *shal* mutant and that reducing *shaker* expression or function in the *shal* mutant is sufficient to reveal the expression of synaptic homeostasis in the *shal* mutant.

Why does increased expression of Shaker, at or near the synaptic terminal block the expression of synaptic homeostasis? We presume that increased expression of Shaker in the *shal* mutant causes a decrease in action potential width. Unfortunately, it is not possible to record the presynaptic action potential from the synaptic terminal because the terminal is embedded within the muscle and is otherwise surrounded by the muscle basal lamina. There are several possible ways that a narrower action potential could block expression of synaptic homeostasis. One possibility is that synaptic homeostasis requires an increase in action potential duration and this is prevented by increased Shaker expression. If so, it is unlikely that Shaker is the direct target of this homeostatic signaling system because homeostatic compensation is observed in the *shaker* mutant background (Fig. 8). Alternatively, a narrower action potential could prevent recruitment of newly inserted presynaptic calcium channels. Genetic data indicate that synaptic homeostasis involves a change in calcium influx at a fixed number of active zones and this could be achieved by an increase in the number of presynaptic calcium channels (Frank et al., 2006; Frank et al., 2009).

Homeostatic control of ion channel expression: Restoring neural activity versus constraining neuronal output.

The transcriptional coupling of *shaker* and *shal* would seem to be a homeostatic mechanism since both channels encode A-type potassium currents. However, these

channels localize to different subcellular compartments. Thus, increased Shaker expression should not homeostatically restore wild-type motoneuron excitability since the somatic A-current remains absent. Rather, increased Shaker seems to inhibit presynaptic neurotransmitter release and may thereby guard against inappropriately enhanced glutamatergic transmission. This effect differs from current homeostatic hypotheses because baseline neural activity is not re-established, but neural output is constrained within reasonable limits.

The importance of channel localization during homeostatic compensation is also highlighted by recent studies in vertebrate central neurons. It was recently demonstrated that $K_{v4.2}$ knockout animals lack dendritically recorded A-type currents in hippocampal neurons (Chen et al., 2006). The absence of a dendritic A-type current potentiates back propagating action potentials and enhances LTP (Chen et al., 2006). Thus, at the level of the neuronal dendrite, this is an example of failed homeostatic compensation. However, this study also documents a compensatory increase in somatically recorded K_{v1} -type currents (Chen et al., 2006). It seems plausible that the observed compensatory increase in somatic K_{v1} -type currents could counteract increased dendritic excitability and, thereby, homeostatically restrain neural output. This possibility is supported by data from additional studies examining $K_{v4.2}$ knockouts in other neuronal cell types (Nerbonne et al., 2008). In these studies, neuronal firing properties measured at the soma are largely normal in the $K_{v4.2}$ knockout despite the absence of the dendritic A-type current.

Homeostatic coupling of specific ion channel pairs.

Here we demonstrate that *shal* and *shaker*, which encode A-type potassium channels, are reciprocally, homeostatically coupled. What drives the compensatory change in ion channel expression following loss of a given ion channel? One possibility, suggested by prior research in other systems (see below) is that the neuron senses a persistent change in cellular activity and initiates a homeostatic response that modulates the expression of other ion channels. Our data are consistent with an activity-dependent model. Knockdown of *shaker* expression (65% of the wild type level) leads to a 223% increase in *shal* expression. Remarkably, we observe a 1300% increase in *shal* expression in the *shaker*^{I4} mutant, which is a point mutation resulting in a non-functional channel (Lichtinghagen et al., 1990). In the *shaker*^{I4} experiment, the mutant *shaker* transcript continues to be expressed at 80% wild type levels (Fig. 7). Thus, the degree to which *shal* expression is increased correlates with the severity of altered channel function rather than the loss of *shaker* message. This suggests that altered channel function or altered neural activity could be the trigger for the compensatory response. These data also raise an interesting question. If the expression of one ion channel, such as *shal*, is specifically coupled to the expression of another channel, such as *shaker*, how could this be achieved by a general monitor of neural activity?

Several studies have now documented that prolonged inhibition of an ion channel, or genetic ablation of an ion channel, can lead to increased expression of a different ion channel with overlapping function, again suggesting coupling between specific pairs of ion channels. For example, loss of Na_v1.6 causes increased expression of Na_v1.1 in purkinje cells (Burgess et al., 1995) and increased expression of Na_v1.2 in retinal ganglion cells (Van Wart and Matthews, 2006). Similarly, loss of A-type potassium

currents in *Kv4.2* (the vertebrate *shal* homolog) knockout animals causes a compensatory increase in both I_K and I_{SS} that preserves action potential shape and neuronal firing properties (Nerbonne et al., 2008). In these examples, the compensatory changes in sodium or potassium channel expression seem to homeostatically maintain appropriate neuronal firing properties. These studies support the hypothesis that ion channels are free variables that can be adjusted by a homeostatic monitor of neural activity and that specific pairs of ion channels may be homeostatically coupled (Marder and Bucher, 2007; Marder and Goaillard, 2006; Schulz et al., 2006).

An alternate form of regulation has been suggested by work in lobster stomatogastric neurons where there is evidence for an activity-independent mechanism that couples *shal* and I_h expression (MacLean et al., 2003). In this system, overexpression of *shal* leads to increased I_h current (channel expression was not tested). However, overexpression of a pore-blocked *shal* also leads to increased I_h current. Thus, altered neural function does not appear to be the trigger for a compensatory change in I_h current. Rather, the cell could monitor the level *shal* message or protein and regulate I_h current accordingly. This mechanism would allow for specific coupling of ion channel pairs, but appears to be different from the phenomenon identified in *Drosophila* motoneurons.

One interesting possibility is that the developmental programs that initially specify the active properties of a given neuron could, later, control ion channel expression in a homeostatic manner. Modeling studies suggest that there are large numbers of physiologically plausible combinations of ion channels that could give rise to a cell with a specific firing property (Prinz et al., 2004). However, if the expression of

pairs or combinations of ion channels are somehow coupled, then the parameter space for defining the firing properties of a given cell type would be dramatically simplified (Schulz et al., 2007). It is interesting, therefore, to speculate that the apparent homeostatic compensation for loss of a given ion channel could represent the re-use of an earlier developmental program that initially served to balance the expression of specific pairs or combinations of ion channels during cell fate specification (Borodinsky et al., 2004; Marder and Bucher, 2007; Marder and Goaillard, 2006; Muraro et al., 2008; Schulz et al., 2006; Schulz et al., 2007). It will be important to determine whether there are any general rules by which one might predict how a cell will respond to the altered expression of a specific ion channel or whether all such relationships will be defined in a cell-type specific manner.

Control of intrinsic excitability at the expense of network modulation

The regulation of A-type currents in *Drosophila* motoneurons occludes trans-synaptic, homeostatic modulation of neurotransmitter release. The consequence is that the postsynaptic muscle target is unable to restore normal synaptic drive from the motoneuron terminal and remains hypo-excitabile. Specifically, EPSP amplitudes are significantly smaller in the *shal; GluRIIA* double mutant animals compared to either *shal* or *GluRIIA* alone (Fig. 6). Thus, at the neuromuscular junction, the regulation of motoneuron intrinsic excitability supercedes the homeostatic control of motor unit function.

The homeostatic modulation of synaptic transmission can be induced in seconds to minutes. By contrast, the compensatory control of ion channel expression clearly

involves gene transcription and is likely to be induced more slowly. One question is whether, given enough time, the mechanisms of synaptic homeostasis can adjust to the change in ion channel expression observed in the *shal* mutant background. This does not appear to be the case. The *GluRIIA* mutation causes a persistent change in postsynaptic receptor function leading to a persistent homeostatic increase in presynaptic release that is present throughout the four days of larval development. Synaptic homeostasis is still blocked in the *GluRIIA; shal* double mutant and we observe a statistically similar increase *shaker* transcription.

It is worth emphasizing that the homeostatic modulation of presynaptic release appears to have been executed, unaltered in the *shal* mutant background because acute application of 4-AP reveals normal homeostatic compensation in the *shal* mutant. These data argue against the possibility that independent homeostatic signaling systems are somehow coordinated at the level of the motor unit, or perhaps neural circuit. Thus, even though an initial homeostatic action is restorative, any change in the balance of ion conductances that control the action potential could dramatically alter how a cell responds to a future perturbation. It has been speculated in systems ranging from crustacean central neurons to the vertebrate cortex, that normal cell-to-cell differences in ionic conductances recorded from an identified cell type might reflect the activity of homeostatic signaling systems (Marder and Prinz, 2002, Davis, 2006). The question remains, will these different cells respond similarly to future homeostatic pressures?

Table 1. Potassium Channel Mutations Tested in a PhTx-Dependent Electrophysiology Screen

Gene (Predicted Function)	Mutant Allele	Mutation Type	Insertion		mEPSP + PhTx ^b	EPSP + PhTx ^b	References ^a
			Location				
<i>wild type</i>	N/A	N/A	N/A		0.51 (0.03)	32.0 (2.8) n = 10	N/A
<i>shaw</i>	<i>UAS-trunc-shaw</i>	antimorph	N/A		0.40 (0.15)	30.4 (5.6) n = 4	Hodge et al. (2005)
<i>ether-a-go-go</i>	<i>eag1</i>	LOF	N/A		0.56 (0.14)	29.8 (4.3) n = 5	Ganetzky and Wu (1983)
<i>slowpoke</i>	<i>slo1</i>	functional null	N/A		0.49 (0.10)	26.3 (4.3) n = 7	Atkinson et al. (1991)
<i>hyperkinetic</i>	<i>hk1</i>	LOF	N/A		0.51 (0.11)	20.2 (4.5) n = 6	Kaplan and Trout (1969)
<i>easily shocked</i>	<i>P(EP1319)</i>	transposon	NC-exon		0.50 (0.26)	35.3 (6.6) n = 3	Flybase
CG10864 (K channel)	<i>P(EY12625)</i>	transposon	upstream		0.46 (0.34)	35.8 (5.7) n = 4	Flybase
CG1090 (potassium antiporter)	<i>P(EP3028)</i>	transposon	intron		0.59 (0.21)	41.4 (6.6) n = 4	Flybase
CG3536 (CNG channel)	<i>Pbac(f00046)</i>	transposon	exon		0.38 (0.12)	35.4 (4.5) n = 4	Flybase
CG8713 (potassium channel)	<i>Pbac(e00867)</i>	transposon	NC-intron		0.42 (0.27)	32.9 (3.2) n = 3	Flybase
<i>I_h</i>	<i>Pbac(e01599)</i>	transposon	intron		0.43 (0.13)	34.5 (4.7) n = 5	Flybase
<i>KCNQ-channel</i>	<i>P(EY08364)</i>	transposon	exon		0.43 (0.09)	35.4 (2.8) n = 4	Flybase
<i>Mrityu</i> (potassium channel)	<i>P(EY01340)</i>	transposon	NC-exon		0.48 (0.17)	27.9 (4.6) n = 5	Flybase
<i>SK</i> (potassium channel)	<i>P(SK-BG01378)</i>	transposon	intron		0.50 (0.10)	32.4 (3.6) n = 4	Flybase
CG30078 (potassium channel)	<i>P(EY01618)</i>	transposon	intron		0.46 (0.11)	40.2 (3.4) n = 5	Flybase
CG12904 (slo-type channel)	<i>Pbac(f03574)</i>	transposon	intron		0.45 (0.07)	30.3 (5.6) n = 4	Flybase
<i>quiver or sleepless</i>	<i>P(EY04063)</i>	LOF	exon		0.41 (0.09)	37.2 (6.1) n = 5	Koh et al. (2008)
CG11984 (potassium regulator)	<i>P(d08881)</i>	transposon	NC-intron		0.47 (0.14)	31.9 (4.1) n = 4	Flybase
<i>eag-like (K⁺ channel)</i>	<i>Pbac(f00820)</i>	transposon	NC-intron		0.45 (0.08)	27.9 (2.9) n = 6	Flybase
<i>Ork1</i>	<i>P(d09258)</i>	transposon	NC-intron		0.38 (0.20)	28.1 (6.7) n = 3	Flybase
<i>shaker</i>	<i>sh¹⁴</i>	functional null	N/A		0.45 (0.18)	48.4 (7.9) n = 5	Jan et al. (1977)
CG34366	<i>Pbac(f04377)</i>	LOF	intron		0.37 (0.02)	14.0 (1.8) n = 14	Flybase
<i>shal</i>	<i>Pbac(f00495)</i>	LOF	intron		0.6 (0.02)	12.2 (1.0) n = 20	Flybase
<i>shab</i>	<i>Pbac(f05893)</i>	transposon	NC-intron		0.49 (0.04)	17.7 (2.3) n = 8	Flybase

The *shaker* mutation has EPSP amplitudes, recorded in the presence of PhTx, that are more than two standard deviations larger than the distribution mean. Mutations in bold have amplitudes that are two standard deviations smaller than the distribution mean. Sample size for mEPSP and EPSP amplitudes are the same for a given genotype. LOF, loss of function; NC, non-coding; CNG, cyclic nucleotide; slo, slowpoke; trunc, truncated.

^a References are given for previously published genetic lesions. Transposon insertion sites are based upon Flybase annotation as indicated.

^b Data are in mV (\pm SEM). Wild type mEPSP and EPSP amplitudes without PhTx are 1.05 (0.03) and 32.4 (2.35) mV n = 16.

Table 2. Quantification of Synaptic Transmission

Condition	Genotype	PhTox	mEPSP	EPSP	QC	V _m	R _{in}	N
0.4mM Ca ⁺⁺	wt	-	1.11 (0.05)	34.31 (1.19)	32.7 (1.79)	-69.4 (0.9)	10.5 (0.7)	31
	wt	+	0.53 (0.02)	31.35 (1.37)	62.42 (4.41)	-66.6 (1.4)	11.1 (1.0)	20
	<i>sha</i> ^{#95} /+	-	1.13 (0.08)	31.64 (1.69)	28.82 (1.47)	-68.9 (1.8)	5.7 (0.2)	13
	<i>sha</i> ^{#95} /+	+	0.52 (0.06)	24.72 (1.72)	51.11 (6.76)	-65.6 (1.9)	5.1 (0.1)	8
	<i>sha</i> ^{#95}	-	1.06 (0.05)	28.87 (1.05)	28.49 (1.59)	-72.4 (1.0)	10.4 (0.8)	27
	<i>sha</i> ^{#95}	+	0.6 (0.02)	12.21 (1.01)	21.18 (2.09)	-74.7 (1.3)	7.2 (0.9)	20
	<i>sha</i> ^{#95} /DF	-	1.11 (0.11)	29.96 (1.36)	29.00 (3.28)	-68.8 (1.6)	8.8 (1.0)	8
	<i>sha</i> ^{#95} /DF	+	0.51 (0.03)	17.81 (1.38)	37.18 (4.14)	-67.9 (1.7)	6.9 (0.9)	11
	<i>sha</i> ^{#95} / <i>sha</i> ^{#00}	-	0.82 (0.06)	22.25 (1.77)	28.58 (3.12)	-70.5 (1.8)	5.3 (0.3)	10
	<i>sha</i> ^{#95} / <i>sha</i> ^{#00}	+	0.33 (0.02)	9.82 (1.35)	30.49 (3.35)	-69.6 (1.5)	5 (0.3)	10
	<i>sha</i> ^{#00}	-	0.72 (0.05)	25.51 (1.47)	37.56 (3.83)	-73.2 (2.4)	5 (0.2)	9
	<i>sha</i> ^{#00}	+	0.41 (0.03)	9.30 (0.77)	24.39 (3.14)	-69.3 (0.8)	4.9 (0.1)	7
	<i>shRNAi</i> ⁺ ; <i>sha</i> ^{#95}	-	1.07 (0.06)	29.93 (2.4)	28.69 (2.42)	-77.9 (2.2)	5.8 (0.6)	13
	<i>shRNAi</i> ⁺ ; <i>sha</i> ^{#95}	+	0.61 (0.04)	11.28 (2.33)	18.79 (3.56)	-74.7 (1.7)	7.2 (1.1)	8
	C155/+; <i>shRNAi</i> ⁺ ; <i>sha</i> ^{#95}	-	1.31 (0.06)	33.77 (3.04)	26.02 (2.33)	-75.6 (2.3)	7.4 (0.4)	14
	C155/+; <i>shRNAi</i> ⁺ ; <i>sha</i> ^{#95}	+	0.64 (0.02)	34.77 (4.77)	54.87 (7.05)	-77.8 (2.7)	9.8 (0.8)	8
	Ok6/EKO-222	-	0.96 (0.08)	14.38 (2.05)	15.08 (1.9)	-78.1 (2.6)	7.3 (0.4)	10
	Ok6/EKO-222	+	0.39 (0.03)	7.56 (1.86)	20.14 (5.35)	-71.2 (1.5)	7.9 (0.5)	9
	CG34366 ⁴³⁷⁷ (K _v 3.2)	-	0.76 (0.05)	29.18 (1.52)	39.51 (2.26)	-71.1 (1.6)	8.5 (0.7)	17
K _v 3.2	+	0.37 (0.02)	14.03 (1.77)	40.52 (5.42)	-70.1 (1.3)	6.6 (0.8)	14	
K _v 3.2; <i>shRNAi</i> ⁺	-	1.11 (0.10)	21.68 (2.94)	20.69 (3.29)	-74.0 (2.0)	6.3 (0.6)	9	
K _v 3.2; <i>shRNAi</i> ⁺	+	0.49 (0.03)	13.14 (2.03)	26.54 (3.39)	-75.4 (1.3)	6.1 (0.5)	10	
C155/+;K _v 3.2; <i>shRNAi</i> ⁺	-	0.90 (0.05)	32.37 (3.36)	36.00 (3.14)	-78.1 (1.1)	4.7 (0.2)	9	
C155/+;K _v 3.2; <i>shRNAi</i> ⁺	+	0.49 (0.02)	17.15 (1.85)	35.14 (3.83)	-66.1 (1.9)	5.7 (0.6)	11	
4-AP (25μM)	wt	-	1.03 (0.06)	47.23 (2.16)	47.07 (2.47)	-69.6 (1.7)	7.1 (0.6)	12
0.4mM Ca ⁺⁺	wt	+	0.54 (0.03)	39.62 (3.97)	76.32 (9.92)	-69.0 (2.5)	11 (0.6)	8
	<i>sha</i> ^{#95}	-	0.96 (0.05)	30.56 (2.04)	34.21 (2.80)	-72.4 (1.5)	5.0 (0.2)	22
	<i>sha</i> ^{#95}	+	0.55 (0.02)	28.49 (2.30)	52.81 (5.12)	-76.9 (1.7)	5.7 (0.3)	13

Table 2. Quantification of Synaptic Transmission

Condition	Genotype	PhTox	mEPSP	EPSP	QC	V _m	R _{in}	N
0.3mM Ca ⁺⁺	wt	-	1.07 (0.03)	23.76 (1.57)	22.54 (1.66)	-68.2 (1.0)	7.0 (0.2)	21
	wt	+	0.54 (0.03)	18.25 (2.90)	35.72 (6.71)	-65.4 (1.0)	7.2 (0.4)	14
	<i>shal</i> ^{#95}	-	0.76 (0.05)	12.59 (1.65)	17.90 (3.22)	-71.8 (1.1)	5.0 (0.4)	8
	<i>shal</i> ^{#95}	+	0.55 (0.01)	5.73 (0.95)	10.45 (1.81)	-74.5 (0.6)	5.0 (0.3)	8
	<i>sh</i> ¹⁴	-	1.05 (0.07)	43.36 (3.26)	42.60 (4.02)	-77.8 (1.1)	5.3 (0.3)	10
	<i>sh</i> ¹⁴	+	0.55 (0.02)	48.23 (0.91)	88.43 (4.33)	-69.0 (1.8)	7.1 (0.2)	8
	<i>sh</i> ¹⁴ ; <i>shal</i> ^{#95}	-	1.12 (0.05)	44.21 (2.5)	39.97 (2.72)	-74.7 (1.7)	6 (0.4)	10
	<i>sh</i> ¹⁴ ; <i>shal</i> ^{#95}	+	0.69 (0.01)	54.83 (2.96)	79.44 (3.02)	-72.3 (1.6)	8.4 (0.7)	8
	<i>sh</i> ¹⁴ /+	-	0.97 (0.04)	42.45 (2.02)	43.99 (1.33)	-72.9 (1.7)	5.1 (0.4)	8
	<i>sh</i> ¹⁴ /+	+	0.51 (0.02)	35.29 (5.0)	69.06 (9.36)	-66.1 (6.9)	7.0 (0.4)	7
	<i>sh</i> ¹⁴ /+; <i>shal</i> ^{#95}	-	1.13 (0.07)	39.68 (2.70)	36.38 (3.16)	-72.6 (1.9)	7.6 (1.0)	12
	<i>sh</i> ¹⁴ /+; <i>shal</i> ^{#95}	+	0.62 (0.03)	41.0 (2.18)	66.7 (2.24)	-77.3 (1.4)	5.1 (0.4)	13
	0.4mM Ca ⁺⁺	<i>GluRIIA</i>	-	0.39 (0.01)	28.34 (1.21)	75.91 (5.06)	-71.3 (1.1)	9.9 (0.8)
<i>GluRIIA;shal</i> ^{#95}		-	0.51 (0.03)	16.84 (1.19)	36.16 (3.95)	-73.7 (1.4)	5.8 (0.2)	19
<i>GluRIIA;shal</i> ^{#95} /Df		-	0.38 (0.04)	10.30 (1.15)	30.37 (5.30)	-68.4 (1.4)	6.1 (0.4)	10

1. Genotypes to be compared, with and without PhTx, are presented sequentially and are shaded similarly.
2. Values are presented as mean (±standard error).
3. QC refers to quantal content (see Methods)
4. N refers to the number of neuromuscular recordings

Figure 1. *shal*⁴⁹⁵ and *CG34366*⁴³⁷⁷ mutants have normal NMJ morphology. Synapse morphology is normal in *shal*⁴⁹⁵ and *CG34366*⁴³⁷⁷ compared to wt animals. Synapses were co-stained with anti-nc82 to visualize presynaptic active zones and anti-dlg to visualize postsynaptic synaptic membrane. The number of boutons per segment A3 muscle 6/7 NMJ were counted and averages are graphed (N= 6-8 animals, 12-14 NMJ). There is no significant difference between wt and mutant NMJ.

A

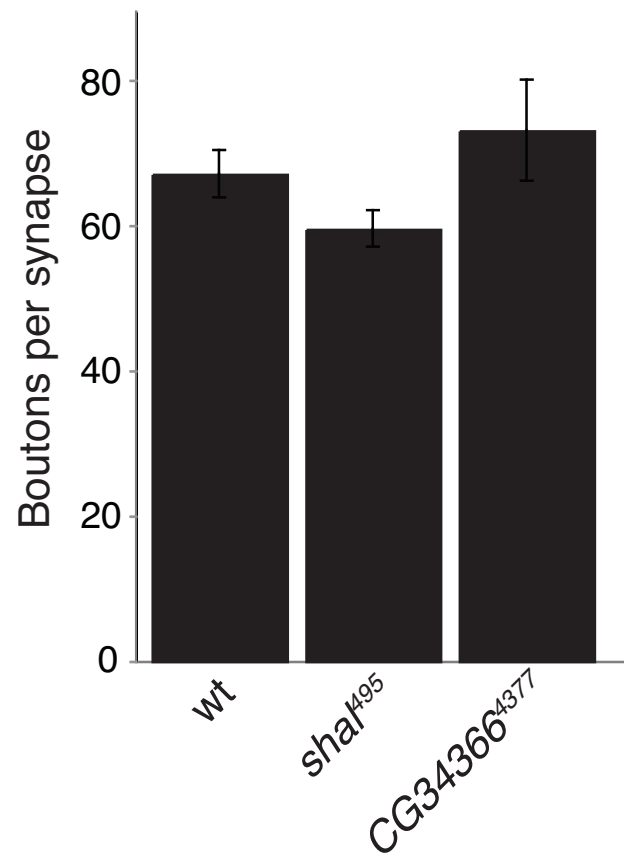


Figure 2. Analysis of Shal localization and current in wild type and *shal* mutants

(A) Diagram of the *Drosophila shal* gene locus (black bars are coding sequence, grey boxes mRNA), indicating the sites of transposon insertion and a deficiency chromosome (red line). (B-C) Representative images of Shal protein (green) within the ventral nerve cord and peripheral axons in wt (B) and *shal*⁴⁹⁵ (C). HRP (red) labels the neuronal membrane (scale bar = 40 microns). Side panels show the axon initial segment at higher magnification for each color channel (scale bar = 64 microns). Shal is highly expressed in the neuropil and in peripheral axons as they exit the ventral nerve cord. Anti-Shal staining is absent in *shal*⁴⁹⁵ mutants. (D) Quantification of Shal staining intensity in the axon initial segment as a function of distance from the ventral nerve cord in wt (black), *shal*⁴⁹⁵ (red), and *shal*⁴⁹⁵/*Df* (grey). Shal is reduced to background in the first ~120 μ m of axon. (E) Average I_A recorded at the motoneuron soma as a function of voltage step for wt (blue) and *shal*⁴⁹⁵ (red). Inset shows representative subtracted I_A traces from wt and *shal*⁴⁹⁵. Mutations in *shal* result in a reduced I_A compared to wt.

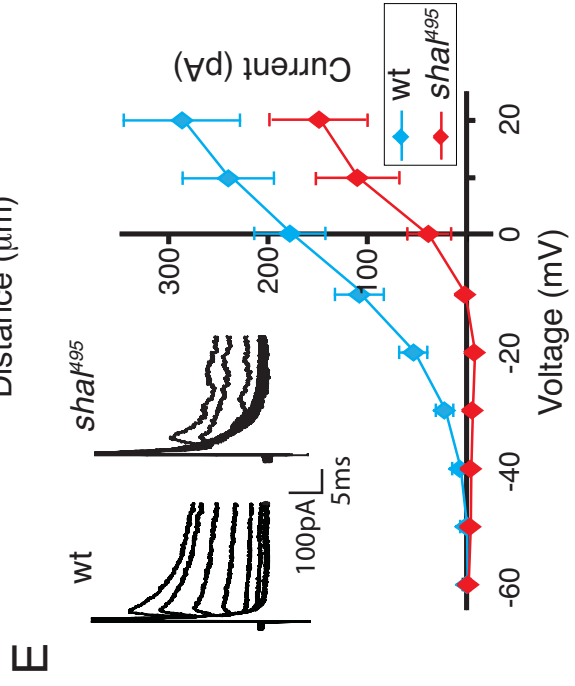
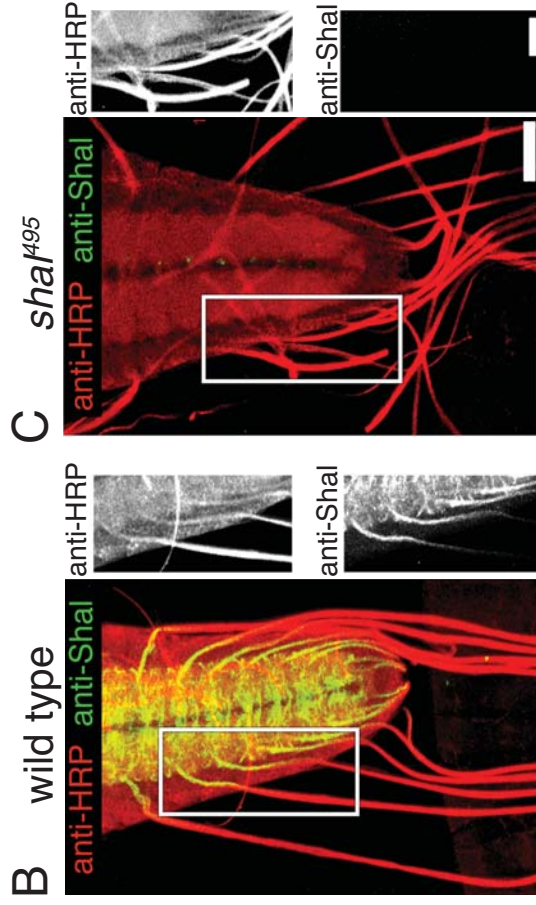
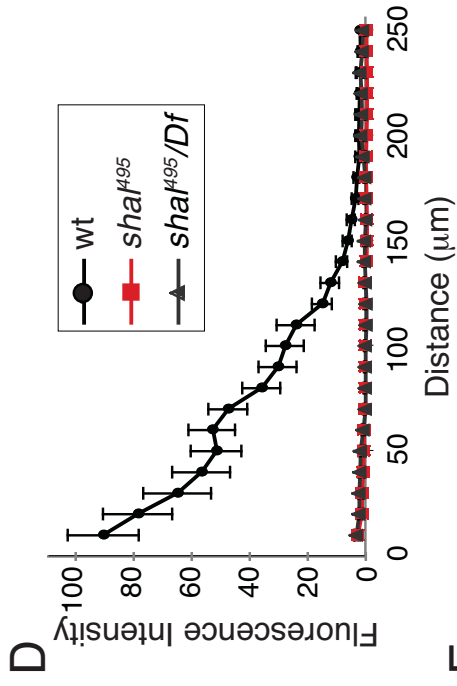
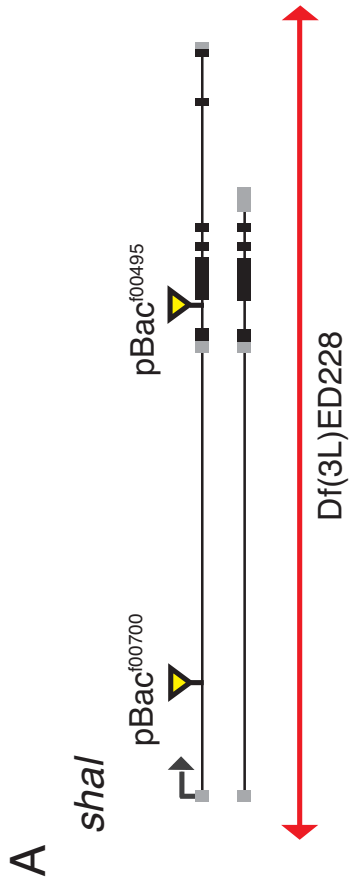


Figure 3. Wild-type NMJs are insensitive to the Shal specific toxin, Phrixotoxin.

EPSP amplitude before (black) and after (red) incubation with $1\mu\text{M}$ Phrixotoxin (PaTx).

Amplitudes are not significantly different following toxin application suggesting Shal protein does not localize to the NMJ.

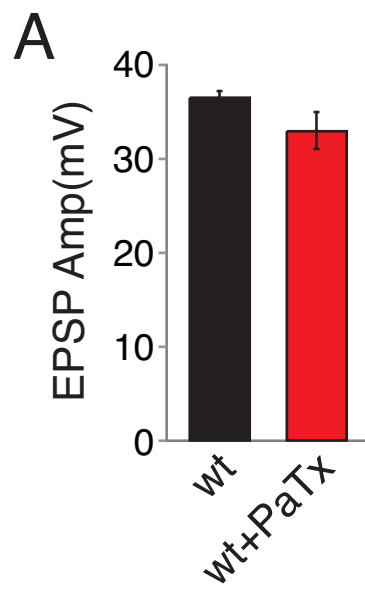


Figure 4. *shal* mutants exhibit mild deficits in baseline transmission. (A)

Representative EPSP and mEPSP traces for wt, *shal*⁴⁹⁵, and *shal*⁴⁹⁵/*Df*. (B) Extracellular calcium concentration is plotted against quantal content on a logarithmic scale. Quantal content values were corrected for nonlinear summation as done previously (Frank et al., 2006, 2009). (C-E) Average mEPSP (C), EPSP (D), and quantal content (corrected for non-linear summation) (E) are shown for wt, *shal*⁴⁹⁵/+, *shal*⁴⁹⁵, and *shal*⁴⁹⁵/*Df*. EPSP amplitudes in *shal*⁴⁹⁵ and *shal*⁴⁹⁵/*Df* are significantly reduced compared to wt ($p < 0.05$ for *shal*⁴⁹⁵/*Df* compared to wild type and $p < 0.01$ for *shal*⁴⁹⁵ compared to wild type, Student's t-test). Corresponding reductions in quantal content were observed. * $p < 0.05$; ** $p < 0.01$. All values are listed in Table 2.

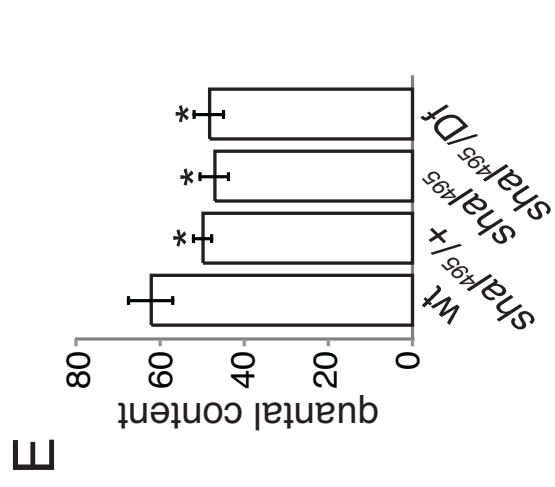
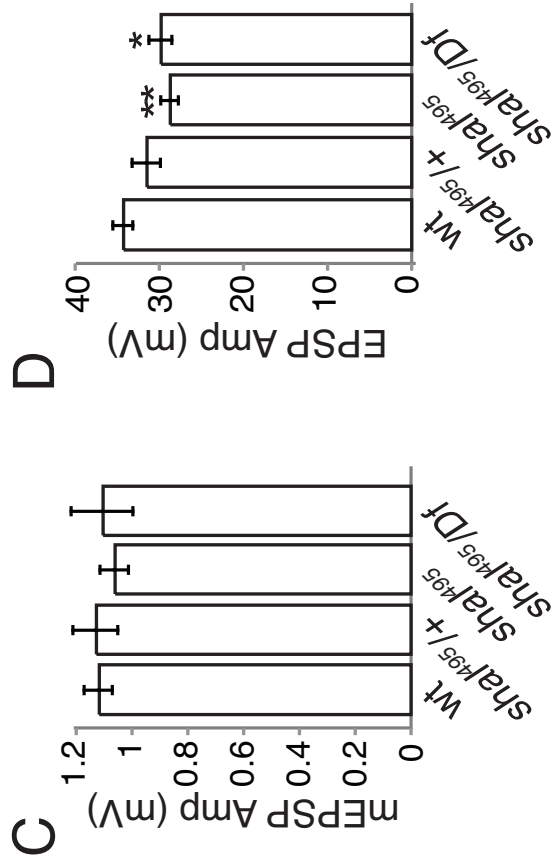
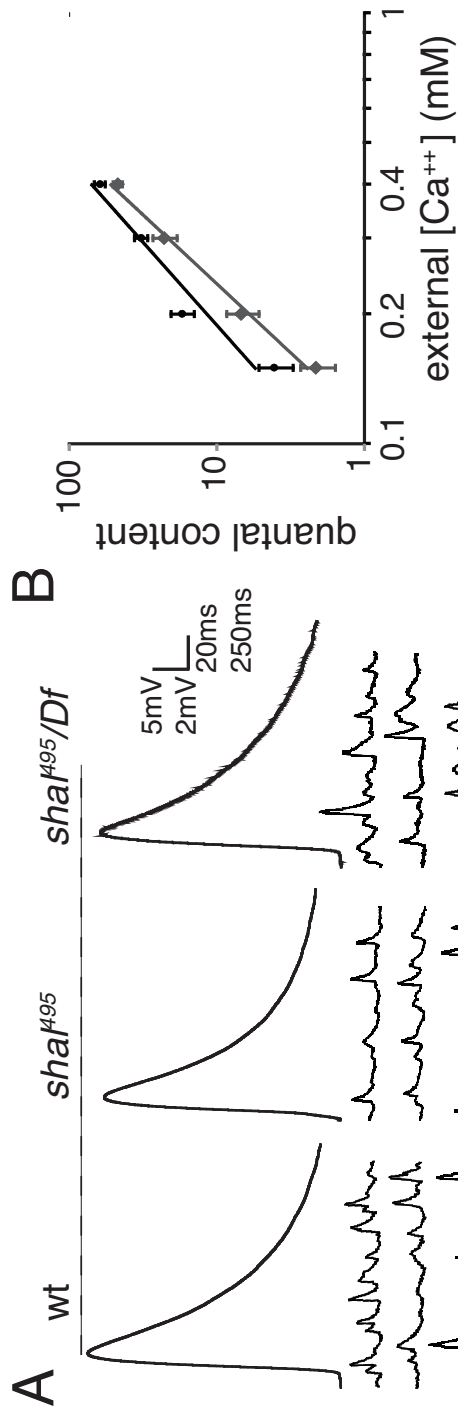


Figure 5. *shal* mutants block the acute induction of synaptic homeostasis.

(A) Representative EPSP and mEPSP traces for wt and *shal*⁴⁹⁵ in saline and following a 10 min PhTx incubation. Wild type EPSPs return to baseline following PhTx incubation, *shal*⁴⁹⁵ EPSPs do not. (B) Average mEPSP values, normalized to their own baseline for the indicated genotypes, in the absence of PhTx (white bars) and following PhTx incubation (black bars). (C) Average quantal content normalized to baseline as in (B). All statistical comparisons are made within single genotypes. Mutations in *shal* prevent a homeostatic increase in quantal content following PhTx incubation. *** indicates $p < 0.001$ (Student's t-test). Absolute values are listed in Table 2.

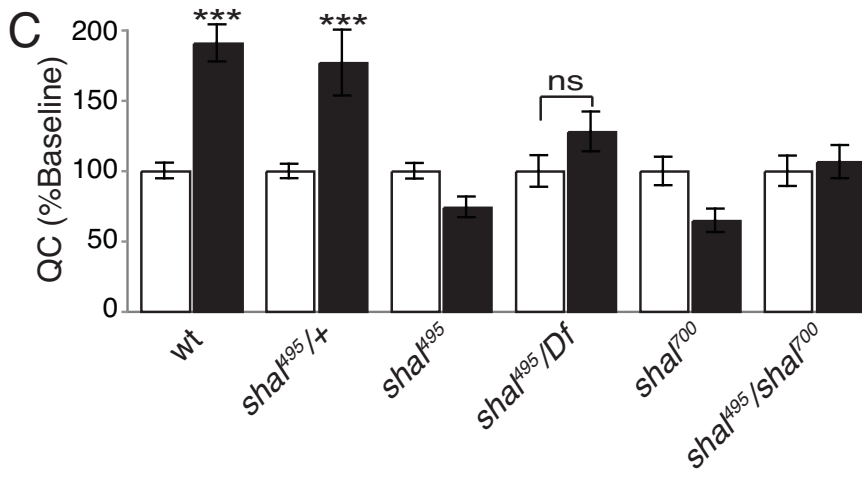
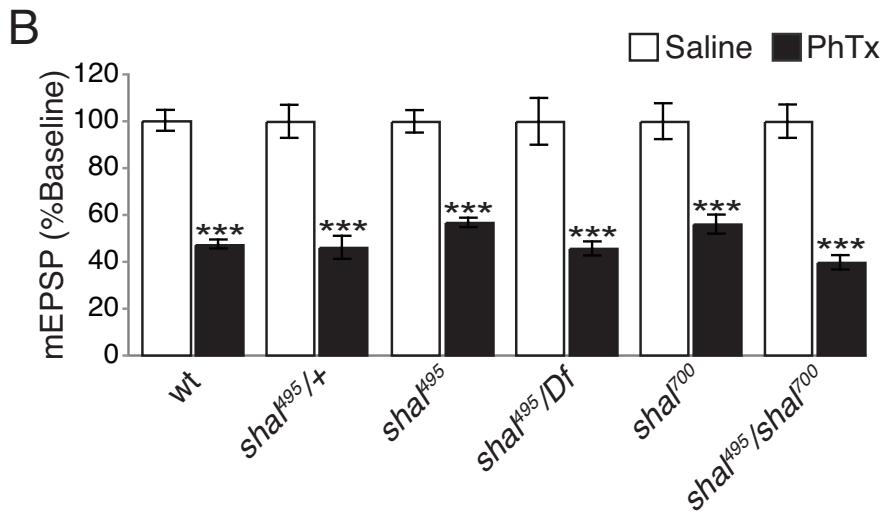
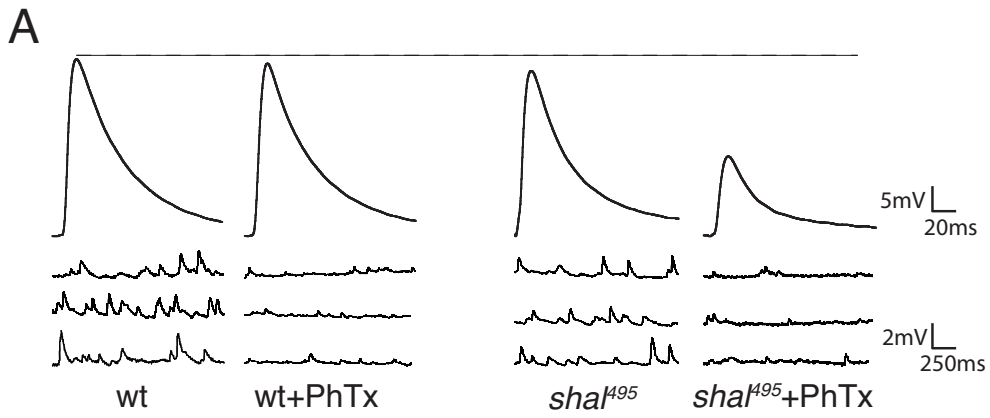


Figure 6. *shal* mutants block sustained expression of synaptic homeostasis.

(A) Representative traces for the indicated genotypes. The *GluRIIA* mutants have reduced mEPSP amplitudes while EPSP amplitudes remain equivalent to wild type due to a presynaptic increase in quantal content. Mutations in *shal* block the homeostatic increase in quantal content when placed in the *GluRIIA* mutant background, resulting in a smaller EPSP. (B-C) Quantification of average mEPSP amplitude (B) and quantal content (C) for wild type and *shal* mutations alone (white bars) and when placed in the *GluRIIA* mutant background (grey bars). Values are normalized to the genotypic baseline in the absence of *GluRIIA*. All statistical comparisons are made within a given genetic background, with or without the presence of the *GluRIIA* mutation. *** indicates $p < 0.001$ (Student's t-test). Absolute values are listed in Table 2.

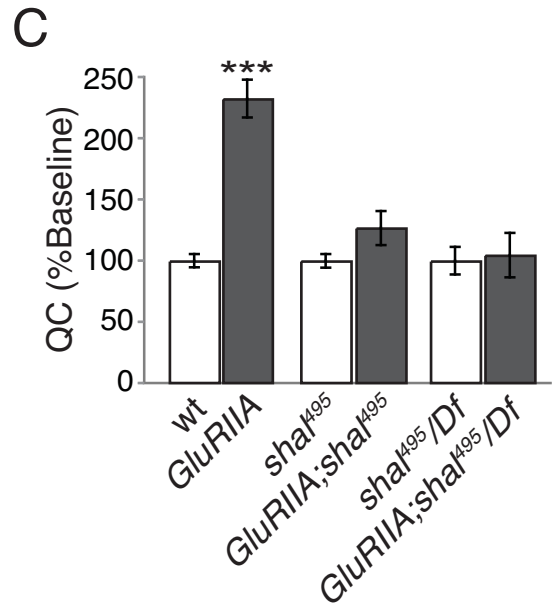
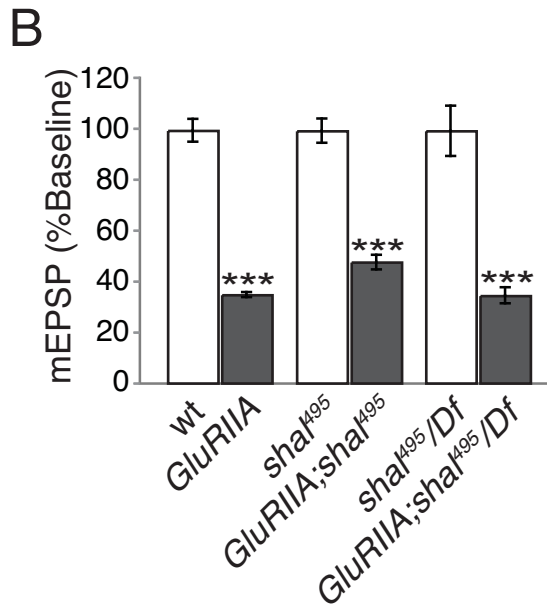
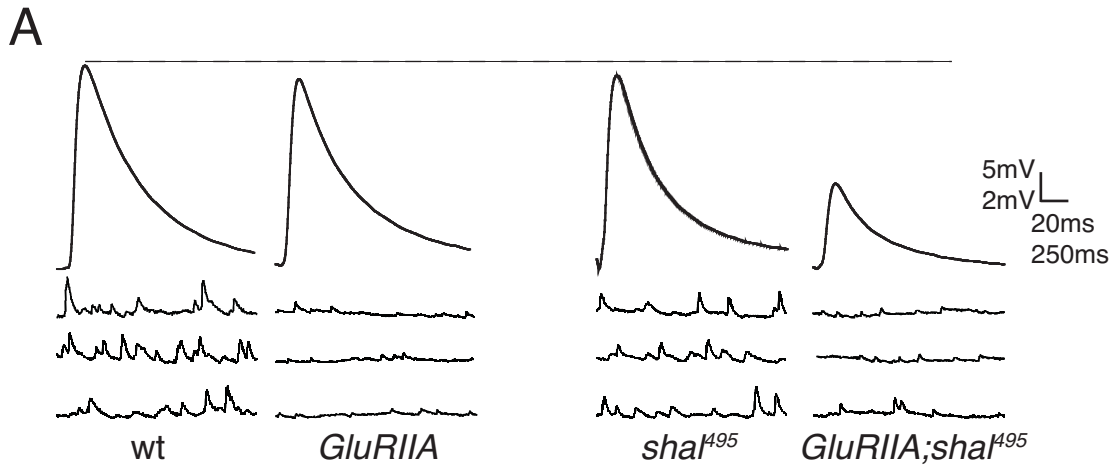


Figure 7. *shaker* and *shal* expression are transcriptionally linked. *shal* RNA expression (black bars) and *shaker* RNA expression (red bars) were measured in the following genotypes: *shal*⁴⁹⁵, neuronal expression of *shakerRNAi* (*c155-gal4/+; shakerRNAi/+*), as well as *shaker*¹⁴ (*sh*¹⁴) mutants. *shakerRNAi* is shortened to *shRNAi* for display. All bars are represented as percent of wild type animals. Mutations in *shal* lead to an increase in *shaker* RNA expression. Neuronal RNAi knockdown of *shaker* results in an increase in *shal* RNA expression. *shal* expression is dramatically increased in *sh*¹⁴ mutants.

A

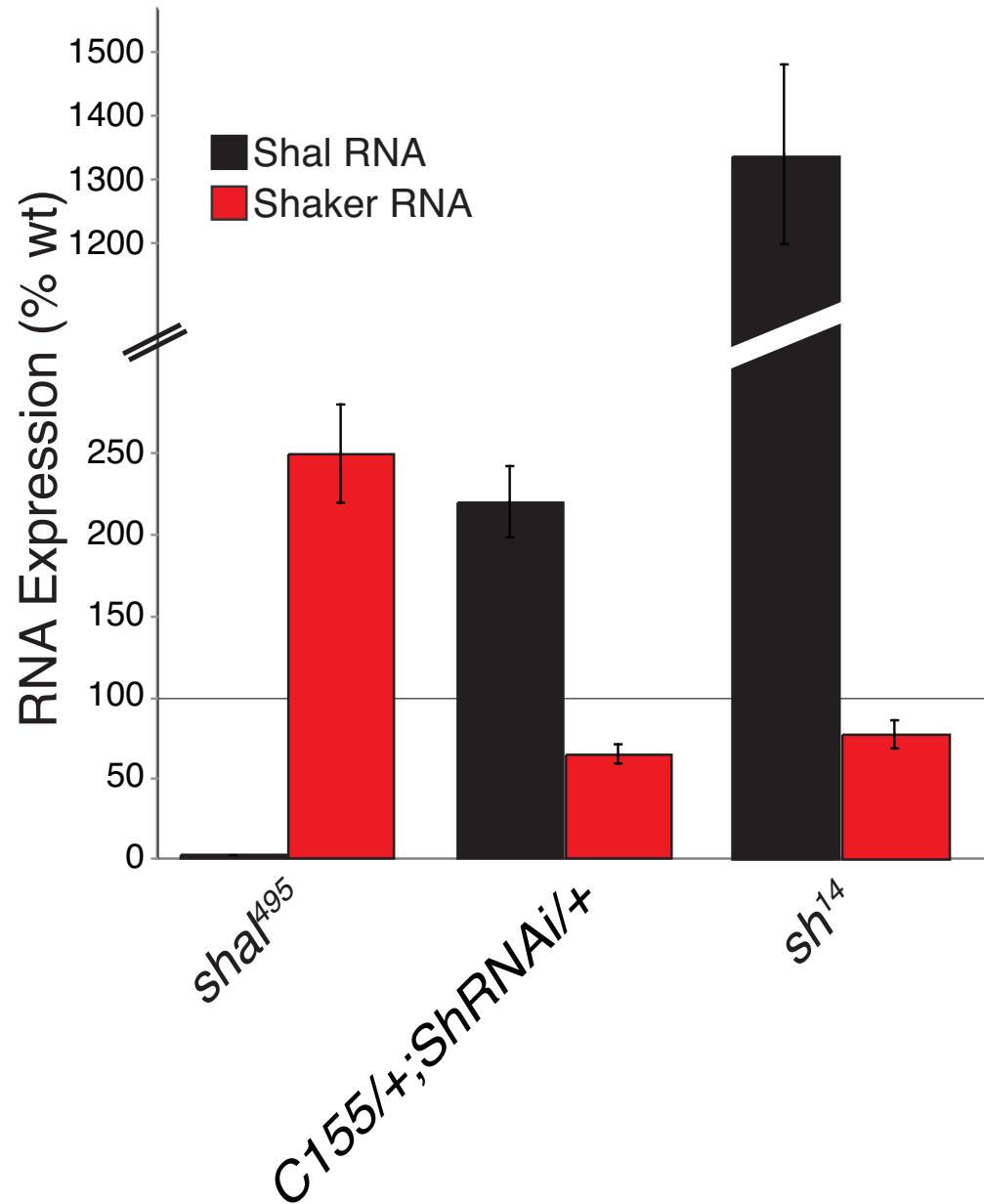


Figure 8. Synaptic homeostasis is restored by loss of Shaker. (A) Representative mEPSP and EPSP traces, with and without PhTx, recorded in 0.3mM calcium for the indicated genotypes. (B-C) Average mEPSP amplitudes (B) and quantal content (C) with (black) and without (white) PhTx incubation for each genotype. Values are normalized to each genotypic baseline. Comparisons are made within a single genotype. ** indicates $p < 0.01$; *** indicates $p < 0.001$ (Student's t-test). The compensatory increase in quantal content is restored with the removal of one or both copies of *shaker*. Absolute values are listed in Table 2.

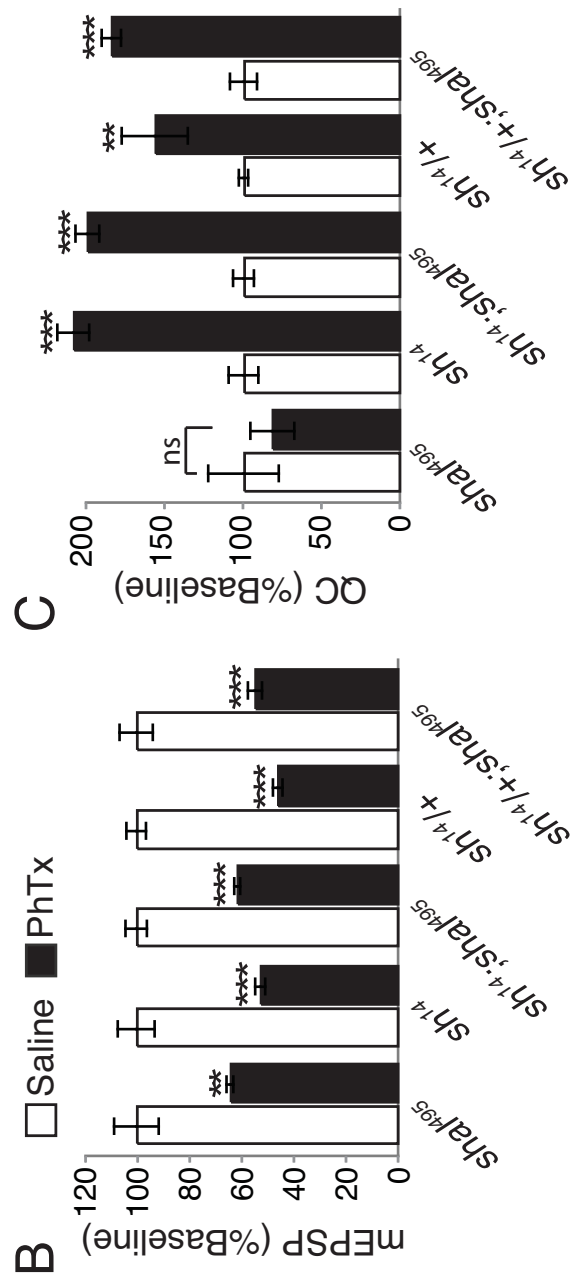
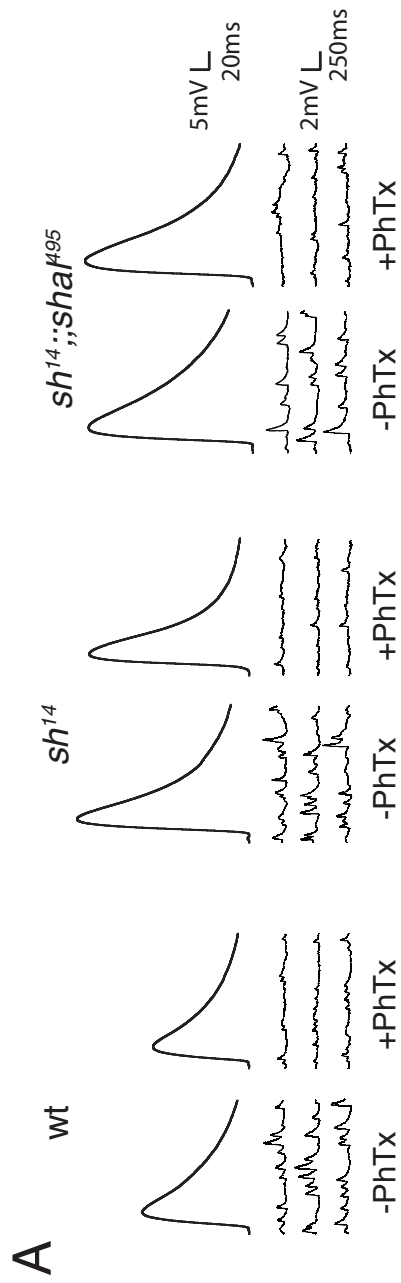


Figure 9. Presynaptic knockdown of Shaker is sufficient to restore homeostatic compensation. (A-C) Average mEPSP amplitude (A), EPSP amplitude (B), and quantal content (C) in the presence (black) or without (white) PhTx incubation for each of the indicated genotypes including neuronal expression of *shakerRNAi* in the *shal* mutant background (*c155-gal4/+; UAS-shakerRNAi/+; shal⁴⁹⁵*). Note that *shakerRNAi* is shortened to *shRNAi* for display. Values are normalized to each genotypic baseline. When *shakerRNAi* was driven with the neuronal driver *c155-gal4* in the *shal* mutant background, a homeostatic increase in quantal content was restored. Statistical comparisons were made within single genotypes, comparing the presence or absence of PhTx. *** indicate $p < 0.001$ (Student's t-test). Absolute values are listed in Table 2.

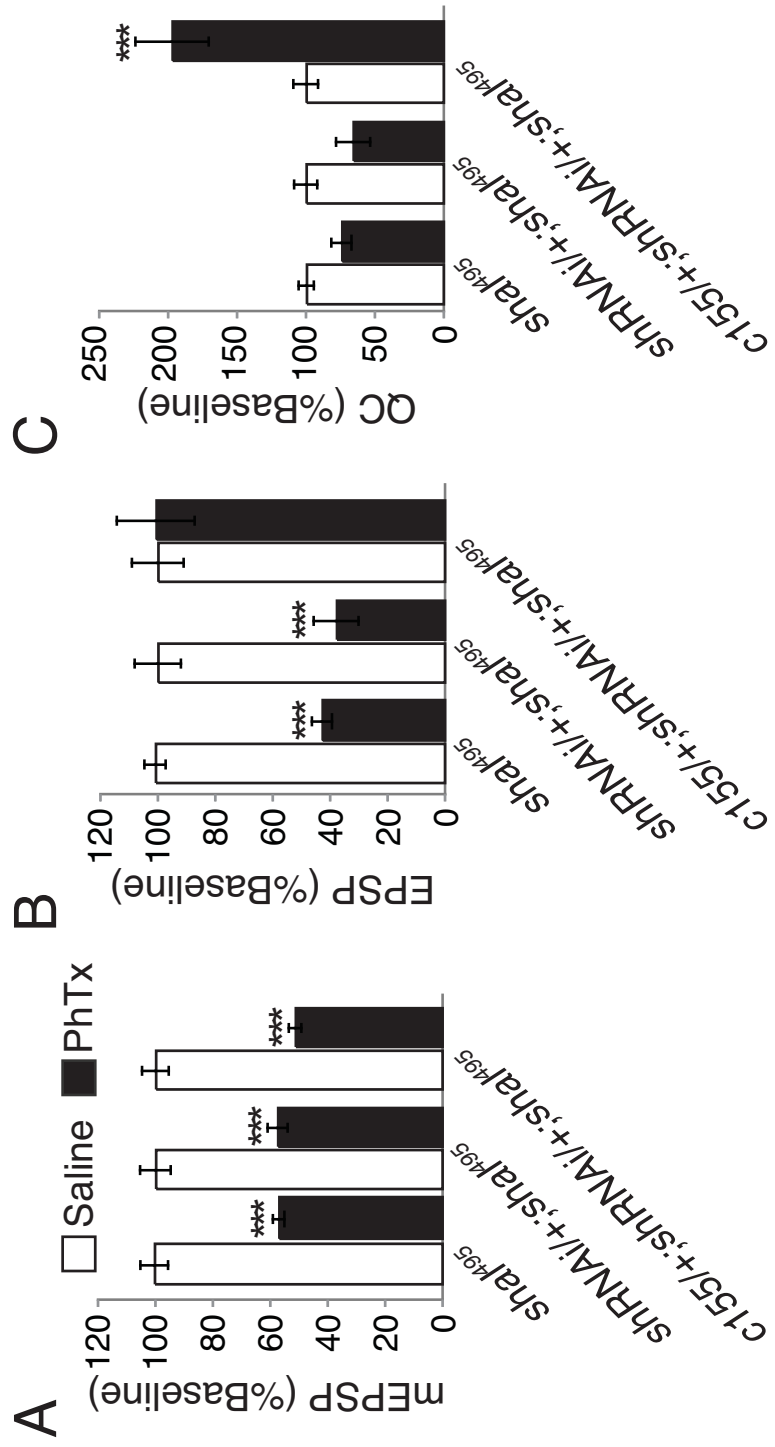


Figure 10. Overexpression of Shaker presynaptically blocks homeostatic compensation. (A-C) Average mEPSP amplitude (A), EPSP amplitude (B), and quantal content (C) in the presence (black) and without (white) PhTx incubation for wild type (wt) and when the modified *Shaker* transgene (EKO) is overexpressed in motoneurons (*Ok6-gal4/+; EKO/+*). Values are normalized to each genotypic baseline. No homeostatic increase in quantal content is observed in animals overexpressing the modified Shaker channel, EKO in motoneurons. All statistical comparisons are made within single genotypes, in the presence or absence of PhTx. *** indicates $p < 0.001$, * indicates $p < 0.05$ (Student's t-test). Absolute values are listed in Table 2.

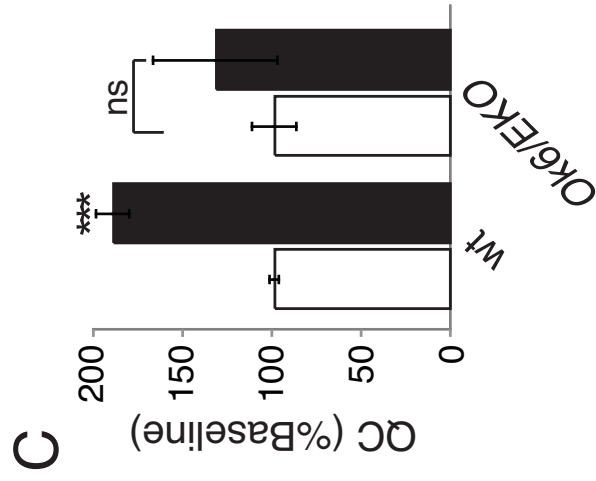
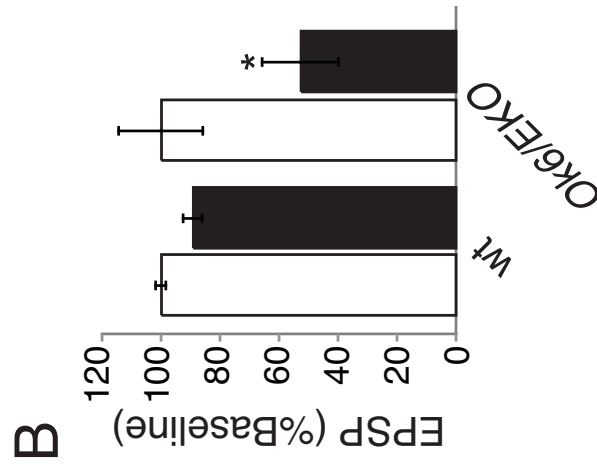
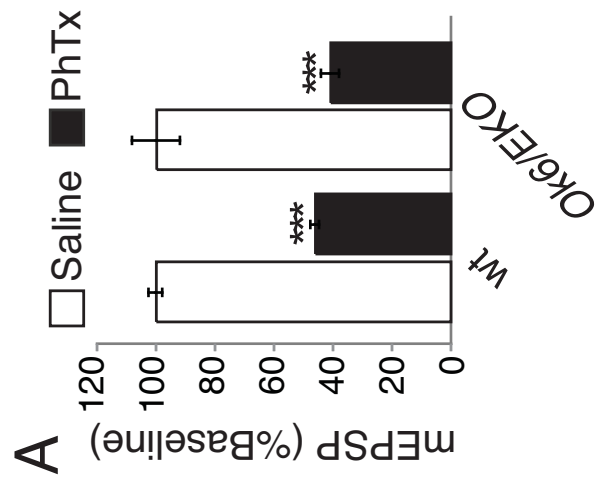


Figure 11. Acute pharmacological inhibition of Shaker restores synaptic

homeostasis. (A-C) Average mEPSP amplitude (A), EPSP amplitude (B), and quantal content (C) for *shal*⁴⁹⁵ in the presence of PhTx (black), without PhTx incubation (white), in the presence of 4-AP alone (gray) and in the presence of both 4-AP and PhTx (red).

Addition of 4-AP following PhTx incubation reveals a robust, homeostatic increase in quantal content in *shal*⁴⁹⁵ (C). **(D-F)** Same as above, but for recordings made in wild-type controls. Wild-type animals show robust homeostatic compensation following PhTx incubation. There is no further increase in quantal content with co-application of PhTx and 4-AP. Values are normalized to baseline (*shal* + *PhTx* is normalized to *shal*, while *shal* + both 4-AP and PhTx is normalized to *shal* + 4-AP alone). *** indicate $p < 0.001$, ** indicates $p < 0.01$ (One-Way ANOVA with Bonferroni post test). Absolute values are listed in Table 2.

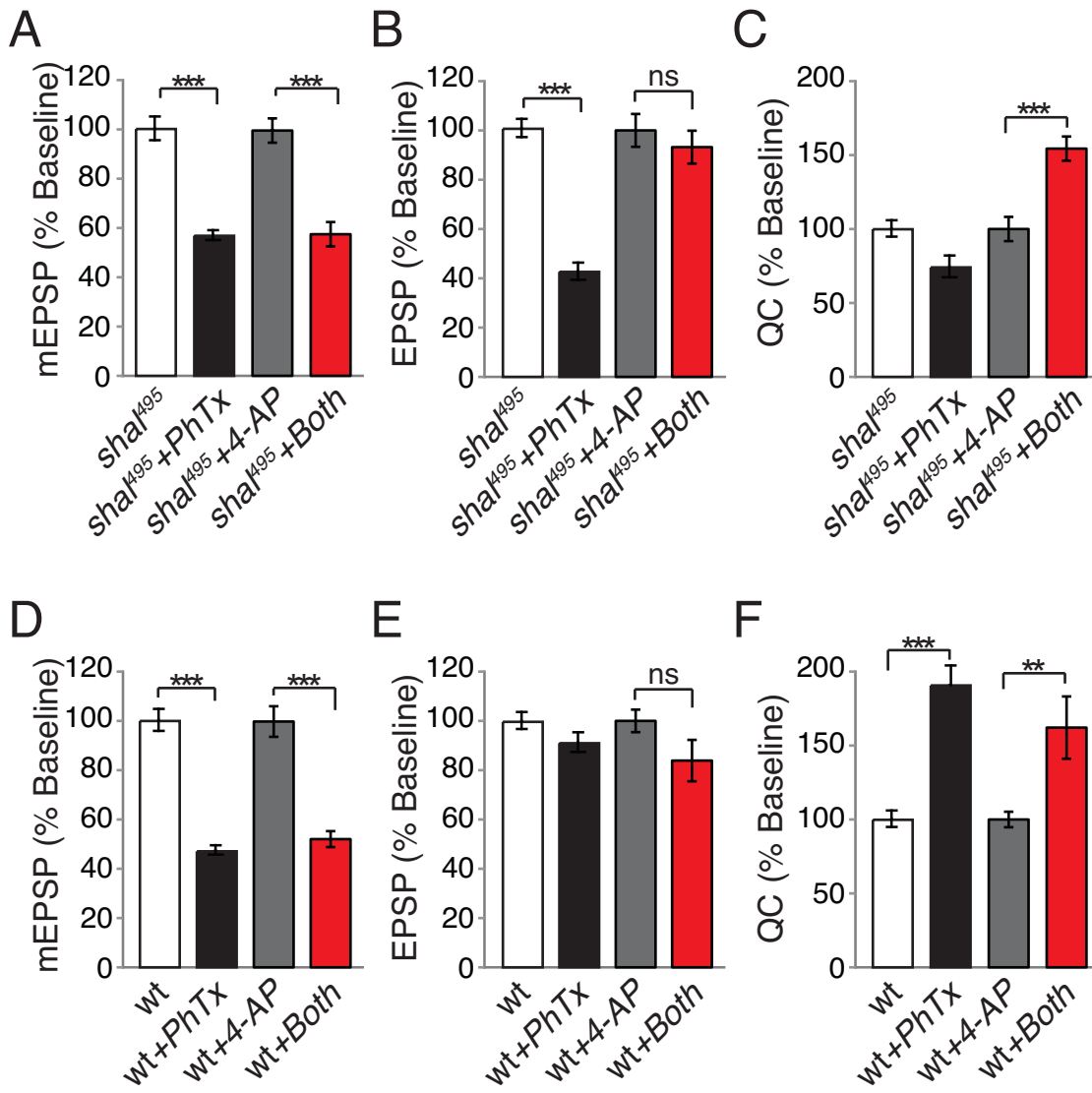
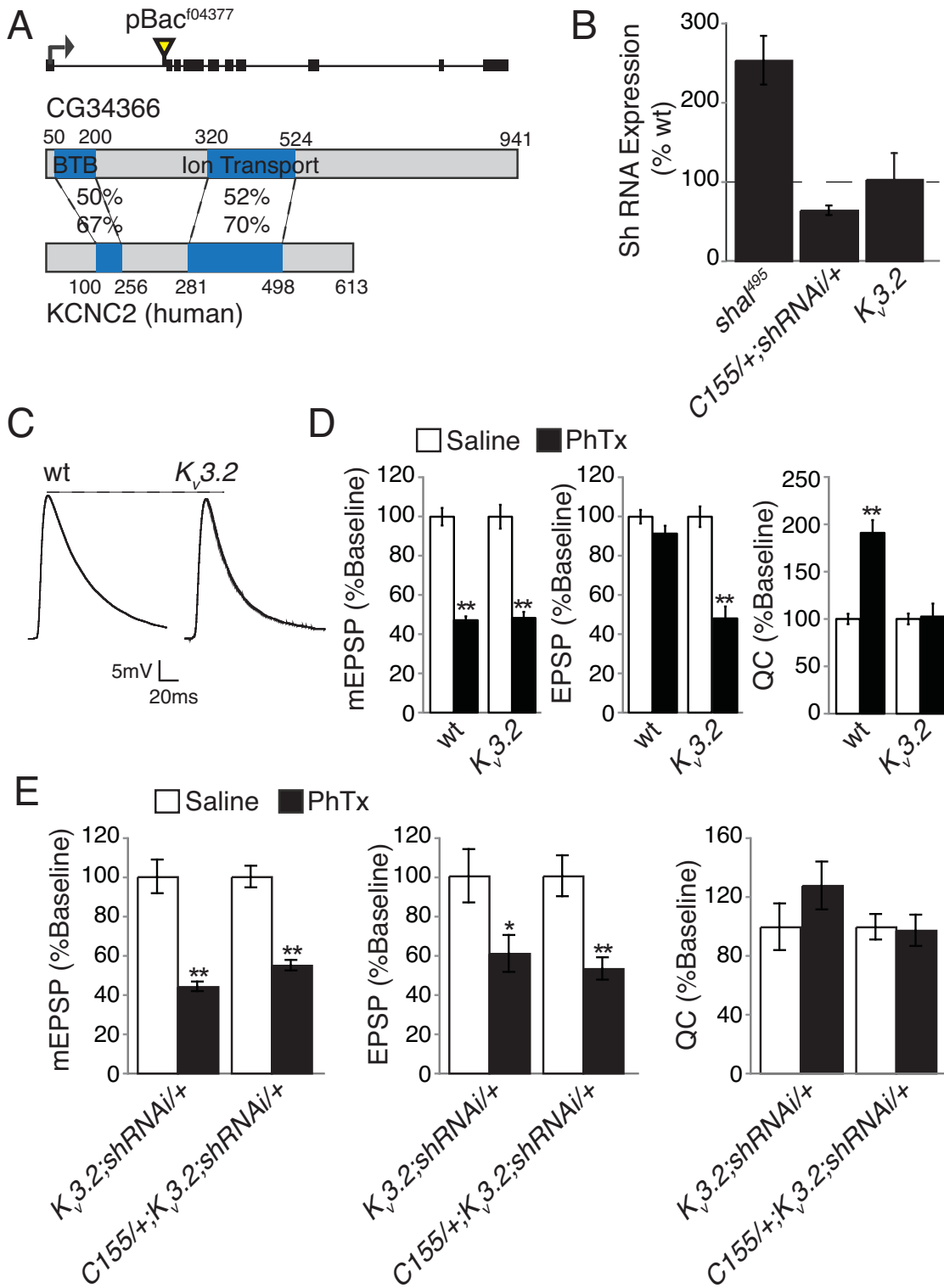


Figure 12. Impaired synaptic homeostasis in a Drosophila K_v3.2-like potassium channel mutation is not rescued by neuronal expression of *shakerRNAi*. (A)

Diagram of the Drosophila *CG34366* gene locus indicating the site of transposon insertion. Black boxes indicate coding sequence. *CG34366* shows homology to human K_v3.2. Blue regions indicate known domains. Sequence identity (top) and similarity (bottom) are given. (B) Shaker RNA expression as a percent of wild type is given for *shal⁴⁹⁵* and animals with neuronal Shaker knockdown (*c155-gal4/+ ;shakerRNAi/+*) and in the *CG34366⁴³⁷⁷* mutant as indicated (note *CG34366⁴³⁷⁷* is indicated as K_v3.2 for purposes of display). *Shaker* expression is unchanged in the *CG34366⁴³⁷⁷* mutant. (C) Representative EPSP traces for wt and *CG34366⁴³⁷⁷*. The *CG34366⁴³⁷⁷* EPSP amplitude is slightly reduced compared to wild type (p < 0.01 Student's t-test – see Table 2 for average values). (D) Average mEPSP, EPSP, and quantal content without (white bars) and with (black bars) 10 min PhTx incubation for wild type and *CG34366⁴³⁷⁷*. The *CG34366⁴³⁷⁷* mutation shows no homeostatic increase in quantal content. All values are also listed in Table 2. (E) Average mEPSP amplitude, EPSP amplitude, and quantal content in the presence (black) and without (white) PhTx incubation for the indicated genotypes including *CG34366⁴³⁷⁷* mutant with presynaptic Shaker knockdown (*c155-gal4/+ ; CG34366⁴³⁷⁷ ; UAS-shakerRNAi/+*) and control (*CG34366⁴³⁷⁷ ; UAS-shakerRNAi/+*). Values are normalized to the appropriate genotypic baseline. All statistical comparisons are made within single genotypes. Presynaptic knockdown of *shaker* does not rescue synaptic homeostasis in *CG34366* mutants. *** indicate p < 0.001, * indicates p < 0.05 (Student's t-test). Absolute values are listed in Table 2.



Chapter 3:
**Transcription Factor, *krüppel* is Activate by Loss or Inhibition
of Shal to Mediate Ion Channel Abundance**

Introduction

The activity of a neuron is determined by the number and combination of ion channels it expresses. In order to maintain stable neuronal activity over time, homeostatic signaling systems, operating at the level of individual cells, have been proposed to constrain mechanisms of plasticity (Davis and Bezprozvanny, 2001; Frank et al., 2006; Marder and Goaillard, 2006; Marder and Prinz, 2002; Perez-Otano and Ehlers, 2005; Turrigiano and Nelson, 2004). One mechanism by which homeostatic regulatory systems are thought to control neuronal excitability is through the regulation of depolarizing and hyperpolarizing ion channel abundance (Desai, 2003; Davis, 2006; Marder and Prinz, 2002; Turrigiano and Nelson, 2004). This has been demonstrated in cultured neurons, where chronic perturbation of activity leads to compensatory changes in ion channel expression (Desai et al., 1999). This has also been observed in lobster stomatogastric ganglion neurons which, when removed from their synaptic inputs and isolated in cell culture, are initially silent, but return to their baseline *in vivo* activity levels by altering their ion channel composition (Turrigiano et al., 1995).

Further evidence that the homeostatic regulation of ion channels can restore set point activity levels comes from knockout mutations. Loss of an ion channel does not result in the altered activity predicted from pharmacological block of the same channel. Once again, this is often due to compensatory changes in other ion channels, which work to restore neuronal firing properties (Chen et al., 2006; MacLean et al., 2003; Marder et al., 1996; Marder and Goaillard, 2006; Nerbonne et al., 2008; Swensen and Bean, 2005; Van Wart and Matthews, 2006).

Currently very little is known about the transcriptional regulation of ion channel abundance. While much work has been done to elucidate the transcription factors required for differentiation and the establishment of neuronal identity (Thomas, 2002; Spitzer et al., 2002; Thaler et al., 2002; Isshiki et al., 2001), the transcription factors and molecular mechanisms required to maintain identity (and the complement of ion channels that determine a neuron's identity) are entirely unknown. Also unknown is how mechanisms of ion channel maintenance are altered when the neuron is presented with a homeostatic challenge, such as loss of an ion channel or chronic perturbations in activity and what additional transcription factors might be required to compensate for these severe insults.

We previously demonstrated A-type potassium channels, Shal and Shaker (Sh), are homeostatically, reciprocally coupled in *Drosophila* motoneurons where loss of either channel leads to increased expression of the other. This provided us with an opportunity to identify transcription factors underlying homeostatic changes in ion channel abundance. Here we identify the motoneuron cell fate transcription factor, *kruppel* (*kr*), as a regulator of Sh expression in early larval development with the ability to increase Sh expression in sensory and motoneurons. We further show that Kr is aberrantly upregulated in *shal* mutants and, remarkably, can be turned on in response to pharmacological block of A-type potassium channels. Finally we provide evidence that Kr is required for the upregulation of Sh in *shal* mutants in sensory neurons, but not motoneurons, indicating that individual classes of neurons may have unique mechanisms of compensation.

Results

We recently demonstrated that loss of the voltage gated A-type potassium channel, *shal*, induces a compensatory increase in the expression of a second A-type potassium channel, *shaker* (*sh*) and vice versa, suggesting homeostatic maintenance of A-type channel abundance in *Drosophila* motoneurons. To define how neurons achieve this cell intrinsic coupling of A-type potassium channels, we focus on the up-regulation of *sh* in *shal* mutants. We chose this focus because, as we describe below, we identify the transcription factor, *kriippel* (*kr*), to be linked to *sh* expression during early larval development. We hypothesized that *kr* might also be responsible for increasing *shaker* expression in *shal* mutants.

***kriippel* is Linked to *shaker* Expression in Neuronal Development**

Recently a large study to gain insight into the molecular underpinnings of developmental progression of post-mitotic neurons was performed by following gene expression patterns of dissociated, FACS-sorted GFP-labeled cells in developing *Drosophila* embryos and larvae using microarray-based expression profiling. Multi-dendritic sensory neuron specific driver, UAS-21-7, motoneuron specific driver, UAS-Ok371 and the pan-neural driver, UAS-*elav* were used to drive GFP in specific populations of neurons in order to isolate them for expression profiling. Multiple independently isolated samples were then profiled at 24 hr intervals starting from the end of embryogenesis and spanning larval development, at 20-24, 48, 72, 96 and 120 hrs after egg laying (AEL). To increase the likelihood of capturing expression signatures of most genes, custom microarrays

designed to include multiple probes for virtually all *Drosophila* genes, including more than 16,000 alternatively spliced mRNAs.

From this dataset we were able to predict the transcription factor that regulates *sh* expression through development, hypothesizing that the same transcription factor might also be responsible for increasing *sh* expression in *shal* mutants. We used an information theoretic approach to model the regulatory network of developing larval neurons and identified *kr* as a putative central regulator. Moreover, *kr* was directly connected to *sh*, suggesting a direct regulatory link. The web in figure 1 shows the only genes, of all genes expressed in the genome, found to be directly linked to either *kr* or *sh* in development using this statistical method.

Overexpression of *krüppel* is Sufficient to Increase *shaker* Expression

To investigate whether Kr is sufficient to drive expression of Sh, we asked whether transgenic overexpression of *kr* leads to increased *sh* expression in both sensory and motoneurons in 3rd instar larvae. We independently used the sensory neuron-specific driver *21-7-gal4* and the motoneuron-specific driver *Ok371-gal4* to overexpress UAS-*kr* in each neuronal class and find, in animals with *kr* overexpression (OE), *sh* is significantly increased compared with wild-type controls in both populations assayed by microarray (Figure 2). These data show that Kr is sufficient to drive expression of Sh in neurons and make Kr a strong candidate for regulating the increase in Sh seen in *shal* mutants.

Krüppel is Aberrantly Expressed Specifically in 3rd Instar *shal* Mutants

If Kr is responsible for increasing Sh in *shal* mutants, the model would imply that Kr should also be increased in the *shal* mutant background. We were able to take advantage of a previously developed Kr antibody to assay Kr expression in *shal* mutants. Consistent with the gene expression data acquired by microarray, Kr protein is absent from neurons by 3rd instar in wild-type animals (Figure 3A and C). In contrast, there is clear up-regulation of Kr positive cells throughout the CNS and ventral nerve cord (VNC) (where motoneurons are located) in *shal* mutant animals (Figure 3B and C). This result strongly supports the hypothesis that increased Kr drives increased Sh in *shal* mutants.

As Shaker and Shal are reciprocally, transcriptionally coupled and *shal* is increased in *sh* mutants, we wondered whether Kr might also be aberrantly expressed in *sh* mutants. However, we see no increase in Kr staining in *sh* mutants (Figure 4). We further assayed Kr expression in an additional five voltage gated ion channel mutants. We see no increase in Kr in *eag*, *slo*, *hk* nor *cac* mutants. There is a small but significant increase in Kr positive cells in *para* mutants, but this increase is an order of magnitude less than the increase seen in *shal* mutants, underscoring the specificity of increased Kr within the *shal* mutant background (Figure 4).

Overexpression of *krüppel* Phenocopies *shal* Mutant NMJ Physiology

The above results demonstrate that Kr and Sh are linked developmentally, that increasing *kr* expression is sufficient to increase *sh* and that Kr is aberrantly increased in *shal* mutants. These data support a model in which Kr expression is increased due to loss of Shal and this increased expression of Kr drives the compensatory increase in Shaker. We next sought to determine whether the increase in *sh* expression seen at the transcript level

by array translates into increased Sh protein. Although specific tools to visualize Sh specifically in motoneurons are currently unavailable, the electrophysiological function of Sh is well characterized, permitting functional determination of Sh activity. Incubation of the *Drosophila* NMJ with philanthotoxin-433 (PhTx), a glutamate receptor antagonist, for 10 min decreases postsynaptic receptor sensitivity and induces compensatory increase in presynaptic neurotransmitter release. This increase in release precisely compensates for the decrease in postsynaptic receptor sensitivity to restore muscle excitation to baseline levels, a process termed synaptic homeostasis. We have shown previously that increased Sh at the NMJ of *shal* mutants blocks the expression of synaptic homeostasis at the NMJ. It follows that if increased Kr causes increased Sh protein, then Kr overexpression should also block synaptic homeostasis. To test this hypothesis we used the *Ok371-gal4* driver to overexpress UAS-*kr* specifically in motoneurons.

We assayed baseline transmission and homeostatic compensation in animals overexpressing Kr. There is no significant change in mEPSP amplitude comparing *Ok371-gal4/+; Uas-kr/+* (Kr OE) with wild-type control *Ok371-gal4/+*. There is a statistically significant deficit in EPSP amplitude in Kr OE (Figure 5A) and a corresponding decrease in quantal content when compared to wild-type controls. We also observe a small but significant decrease in EPSP amplitude in *shal* mutants. These results phenocopy the increase in Sh observed following loss of *shal* (Bergquist et al., 2010).

We next analyzed synaptic homeostasis in Kr OE animals. Following the application of PhTx, mEPSP amplitudes are similarly suppressed in Kr OE and control

animals. However, EPSP amplitudes fail to recover to baseline and calculation of quantal content demonstrates that the normal, homeostatic enhancement of presynaptic release is blocked. Therefore, Kr OE is sufficient to block the acute expression of synaptic homeostasis (Figure 5B-C).

To further test whether increased presynaptic Sh is responsible for the block of synaptic homeostasis in Kr OE animals, we used RNAi to knock down *sh* specifically in motoneurons. We have previously demonstrated that driving this construct presynaptically effectively knocks down *sh* expression to $69.19 \pm 6.11\%$, and that this knockdown in *shal* mutants rescues synaptic homeostasis. We therefore hypothesized that homeostasis would similarly be restored by expression of this *sh RNAi* in the Kr OE background. This is what we observe (Figure 5B-C). In addition, baseline transmission is also significantly improved compared with Kr OE alone (Figure 5A). These data show that Kr OE causes increased Sh protein, which is sufficient to block synaptic homeostasis. Therefore, overexpression of Kr phenocopies the increased Sh expression that is observed in the *shal* mutant animals, consistent with the conclusion that increased Kr expression is sufficient to increase the expression of Sh protein in motoneurons.

Krüppel is Upregulated in Response to Pharmacological Inhibition of A-type Potassium Currents

We have provided genetic and electro-physiological evidence that increased Kr in motoneurons is sufficient to increase Sh, and that Kr expression is increased in *shal* mutants. Taken together these data support the hypothesis that increased Kr drives upregulation of Sh in *shal* mutants. We next sought to answer two additional questions.

First, is increased Kr seen in *shal* mutants a direct result of the loss of Shal mediated A-type potassium currents? If so, how long must channels be inhibited before Kr expression is increased? We envision two alternative models, based on the fact that Kr is a developmentally regulated gene that is highly expressed in developing motoneurons, but is then turned off and becomes nearly undetectable in motoneurons by the end of larval development. In one model, the absence of *shal* causes Kr expression to be maintained from the embryo through to late larval stages. This model suggests that the homeostatic modulation of ion channel abundance is achieved because motoneurons fail to transition from an early embryonic fate to a fully mature motoneuron fate. This model further predicts that acute changes in *shal* following down-regulation of Kr would be ineffective in initiating a homeostatic change in Sh expression. In a second model, loss of Shal activity at any time during development is sufficient to induce the expression of Kr. In this manner, Kr would function as a type of ‘immediate early gene’ that is directly responsive to change in Shal function (and quite specific to changes in Shal function since loss of other ion channel genes do not induce an increase in Kr expression).

We are able to address these questions by taking advantage of the A-type potassium channel antagonist 4-aminopyridine (4-AP). We fed larvae 4-AP (see methods) for 6, 12, 18, and 24 hours to test whether we could observe an increase in Kr immuno-staining following pharmacological inhibition of A-type potassium currents. Larvae were aged so that they were wandering 3rd instar at the time of dissection. As previously shown, wild-type 3rd instar animals have very few Kr expressing cells in the VNC (Figure 6A). Kr expression remained unchanged following 6 and 12 hours of 4-AP

feeding. In contrast, we observed a slight increase after 18 hours (Figure 6B) and a robust increase by 24 hours (Figure 6C).

This result demonstrates that Kr can be reactivated acutely at a late developmental time point when Kr expression is normally low or eliminated in most neurons. These data also demonstrate that Kr can be activated by acute inhibition of I_A . Although 4-AP will inhibit both Shaker and Shal and may inhibit additional voltage gated potassium channels, our earlier findings demonstrate that Kr is specifically up-regulated in *shal* mutants. Therefore, our data suggest that acute block of the Shal current is sufficient to drive increased Kr expression. These data are consistent with the second model in which Kr expression is directly responsive to changes in Shal function. These data rule out the model that homeostatic control of ion channel abundance is due to the maintenance of an early embryonic neuronal fate.

Finally, we addressed which cells express Kr following inhibition of Shal either genetically or pharmacologically. In order to quantify the number of motoneurons that show increased Kr expression, we used *Ok371-gal4*, *UAS-T2-GFP* animals to label motoneurons. We were surprised to find very little overlap between GFP labeled motoneurons and Kr labeled cells (Figure 6C and Ci). This demonstrates that while Kr is significantly increased in cells throughout the VNC, it is not upregulated in motoneurons following acute block of Shal. Therefore, although increased Kr is sufficient to drive a change in Shaker expression in motoneurons, it does not appear to be responsible for the change in Shaker that is observed in motoneurons. Rather, Kr appears to drive a homeostatic change in Sh expression in a subset of central neurons that does not include

motoneurons, suggesting cell-type specific transcriptional programs that mediate homeostatic regulation of ion channel abundance.

Kr Increase Localizes to Sensory but not Motoneurons

Finding very few motoneurons with increased Kr following 4-AP feeding led us to directly test which cell types had increased Kr seen in *shal* mutants. Due to our inability to visualize motoneurons in *shal* mutants (described above), we employed *shal RNAi* to assess the effect of decreasing Shal activity. Using the motoneuron driver, *Ok371* we found that *shal RNAi* significantly reduces Shal in motoneurons as visualized by the loss of Shal staining in the axon initial segment of motoneurons as they leave the ventral nerve cord compared with wild-type controls (Figure 7). We also observed a significant increase in Kr expression in the central nervous system, although the magnitude of the increase was less than observed in *shal* mutants (136.82 ± 14.53). To increase the effectiveness of Shal knockdown, we drove *shal RNAi* in *shal* heterozygous mutants, which survive to third instar. We additionally drove *UAS-T2-GFP* in order to visualize motoneurons. As in *shal* mutants, we observed significant up-regulation of Kr (Figure 8B and C). However, colocalization between Kr and GFP was not observed, indicating that increased Kr expression does not occur in motoneurons (Figure 8D). Therefore, despite being sufficient to increase Sh in motoneurons, Kr does not mediate the homeostatic ion channel coupling in motoneurons. We hypothesize that there may be cell-type specific transcription factor signaling that controls the homeostatic regulation of ion channel abundance.

Because we also observed *Sh* upregulation in sensory neurons in the peripheral nervous system (PNS) as a result of *Kr* overexpression, we hypothesized that Kr could be upregulated in sensory neurons in *shal* mutants. As in motoneurons, Kr protein is absent from sensory neurons in 3rd instar wild-type animals (Figure 9). However, we observed clear up-regulation of Kr in *shal* mutant sensory neurons (Figure 9). We showed previously that Kr OE in sensory neurons is capable of increasing *sh* (Figure 2). Thus, it appears there are cell-type specific transcriptional programs that achieve homeostatic control of *Sh* expression. Kr may be the key regulator in sensory and other CNS neurons, while the transcription factor responsible for homeostatic control of ion channel abundance in motoneurons remains unknown.

Discussion

Microarray analysis of gene expression in isolated neuronal cell populations identified the developmental connection between *kr* and *sh* expression. Further, overexpression of *kr* in both sensory and motoneurons leads to increased expression of *sh*. From this data we hypothesized that Kr was responsible for the homeostatic increase in Sh seen in *shal* mutants. In support of this hypothesis, we see a dramatic increase in Kr expression, in *shal* mutants. Finally Kr OE phenocopies *shal* mutant physiology, driving increased Sh expression to presynaptic terminals resulting in blocked synaptic homeostasis. These data demonstrate that Kr is sufficient to drive the functional expression of Sh. While not required in motoneurons, our data suggest Kr may be required in sensory neurons and support the model that Kr is required in a cell-type specific manner to increase Sh following loss or inhibition of Shal.

Cell Intrinsic versus Network Compensation

We demonstrate that Kr is increased in sensory neurons and other CNS neurons in *shal* mutants. This suggests that Kr can control this A-type potassium channel homeostasis in some neuronal populations. Most convincingly in support of this hypothesis is our data in sensory neurons. Here we show Kr is upregulated strongly in *shal* mutants, and overexpression of *kr* drives increased *sh*. However, we lack the physiology from sensory neurons to confirm that increased *sh* is functionally expressed to compensate for the loss of Shal.

Another interesting hypothesis is that Kr is acting in the network to increase Sh to turn down excitability, but not always cell intrinsically. Compensatory changes in ion

channel abundance are thought to be cell intrinsic, responding to changes in activity and/or specifically to loss of a particular ion channel within the cell that they are expressed. This has been supported by models of maintaining stable circuit activity, which suggest that cell autonomous sensors working to stabilize activity cell intrinsically are sufficient to govern stability in entire networks (Marder and Prinz, 2002). In addition it has been shown that neurons removed from their synaptic partners can, with time, adjust their complement of ion channels to retarget their own activity pattern (Turrigiano et al., 1995). However, if neurons expressing Shal imperfectly compensate, there will be changes in activity in connecting neurons, which should then result in changes in ion channel abundance in neighboring cells. And although retrograde control of neuronal excitability has not been demonstrated, ours and other labs have demonstrated retrograde control of synaptic efficacy, indicating the existence of intercellular homeostatic signaling (Davis and Bezprozvanny, 2001; Petersen et al., 1997; Plomp et al., 1994; Frank et al., 2006; Burrone et al., 2002). It may be beneficial for the circuit to act in a coordinated way, in this case to turn down activity in cells both up and downstream of Shal expressing cells.

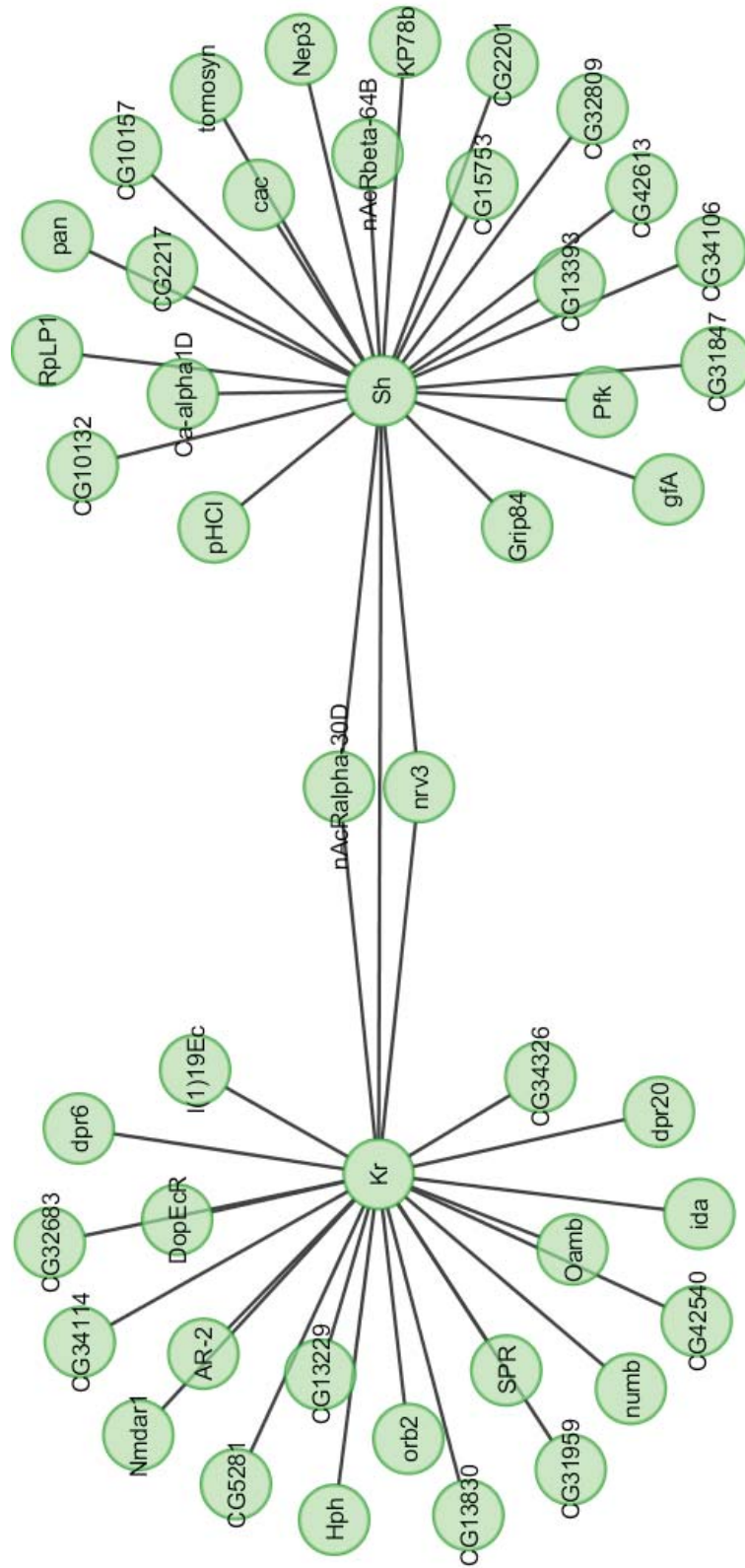
Reutilization of Neuronal Differentiation Transcription Factors in Ion Channel Homeostasis

The demonstration that Kr can be upregulated within 24 hours of A-type potassium channel inhibition is remarkable for several reasons. Kr is a master developmental regulatory transcription factor shown to be involved in early *Drosophila* patterning as well as neuronal specification and differentiation in vertebrates and invertebrates (Abrell

and Jäckle, 2001; Brody and Odenwald, 2000; Isshiki et al., 2001). In addition, Kr-like factor 4 was identified by Yamanaka and colleagues to be one of the transcription factors required for re-differentiation of stem cells (Takahashi and Yamanaka, 2006). It is interesting to speculate that neurons may reuse transcription factors initially required to establish the complement of ion channels expressed in response to long-term block of an ion channel to re-establish proper ion channel balance to restore activity. It will be important to determine if this is a mechanism used by motoneurons as well, and if so, whether we can begin to predict the transcriptional regulators a given cell-type will utilize, perhaps based on their developmental transcription factor profile. It is also important to note that Kr and other early cell-fate regulatory transcription factors of course have numerous gene targets. With this in mind it will also be important to further identify the mechanism underlying which of the many gene targets are actually altered and how this is regulated.

Figure 1. *kr* and *sh* are developmentally linked.

(A) Web depicting all genes developmentally linked to Kr and Sh with genes located in hugs. Based on mutual information theory direct connection of genes predicts developmental regulation. Length of arms has no significanc.



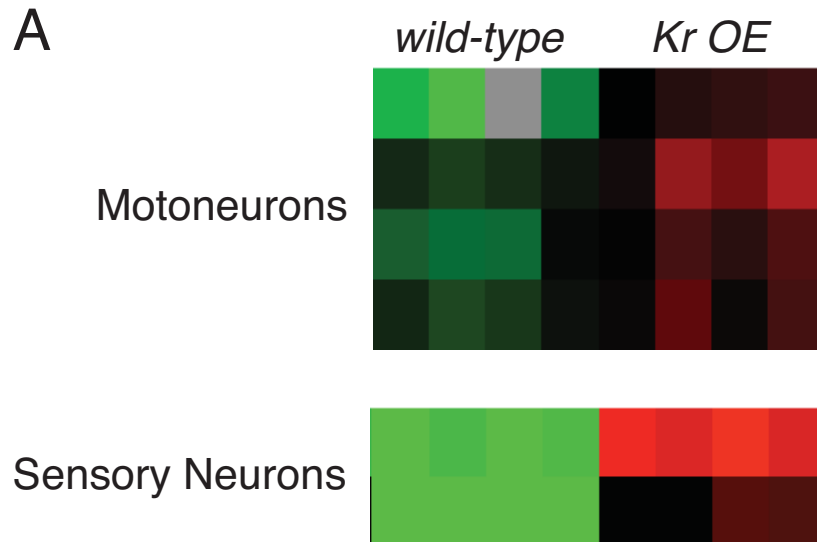


Figure 2.

Overexpression of *kr* drives increase *sh* in sensory and motoneurons.

(A) Top: Heat maps depicting *shaker* expression in isolated motoneuron in *wild-type* (left) versus *Ok371-gal4*; UAS-*Kr* (*Kr OE*). Bottom: Heat maps depicting *shaker* expression in isolated sensory neurons in *wild-type* (left) versus *21-7-gal4*; UAS-*Kr* (*Kr OE*). Green indicates low expression and red indicates high expression. Overexpression of *kr* in either sensory or motoneurons is sufficient to increase *sh* expression in the same cell.

Figure 3. Kr is Aberrantly Expressed in *shal* Mutants

(A) Representative images of Kr protein within the ventral nerve cord and CNS in wt (A) and *shal*⁴⁹⁵ (B). (scale bar = 40 microns). Kr is only expressed in a few cells in wt 3rd instar larvae. Kr is highly expressed in *shal* mutants (C) Quantification of the number of Kr filled cells specifically in the ventral nerve cord normalized to wt. *** indicates $p < 0.001$ (Student's t-test).

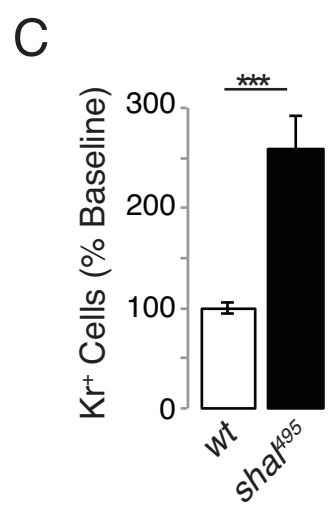
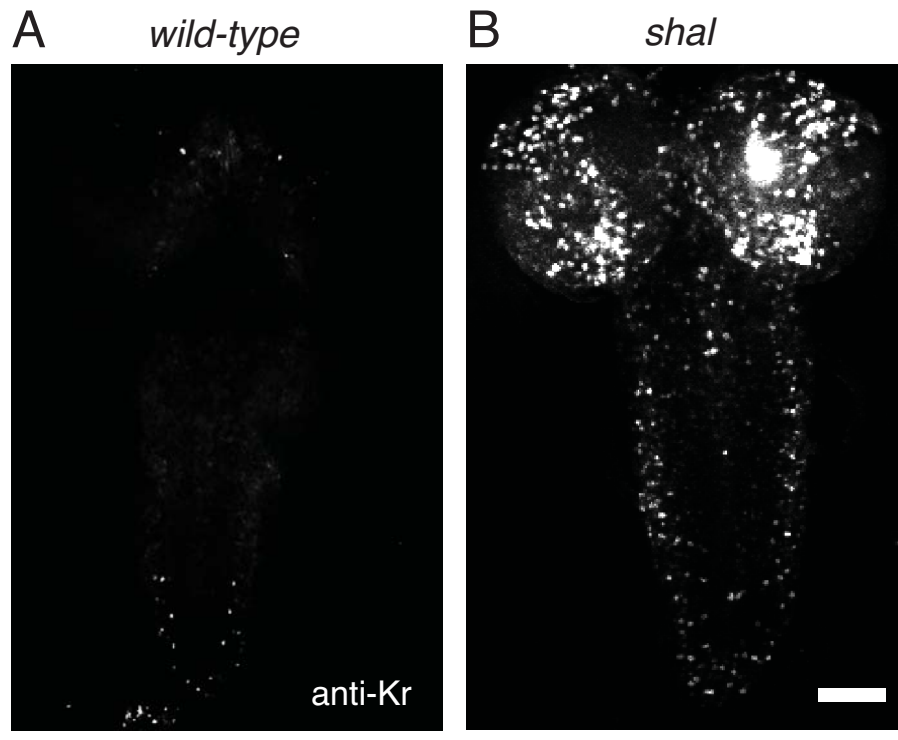


Figure 4. Kr increase is Specific to *shal* Mutants

(A) Quantification of the number of Kr filled cells in the ventral nerve cords of six ion channel mutants normalized to wt. There is a small but significant increase in *para* mutants * indicates $p < 0.05$ (Student's t-test). *shal* mutants show the largest increase in Kr. *** indicates $p < 0.001$ (Student's t-test).

A

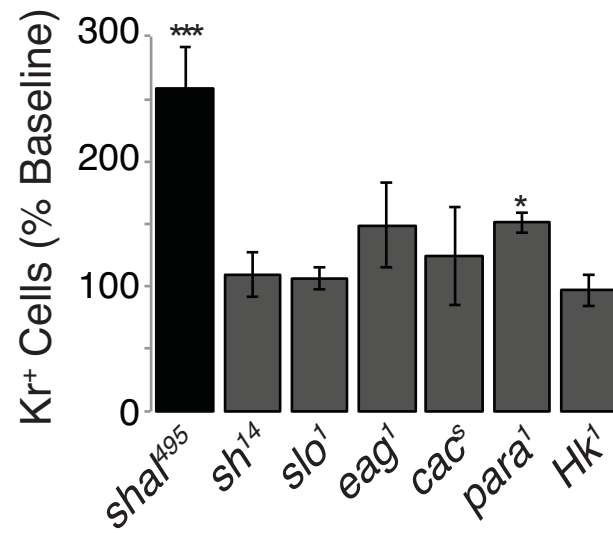
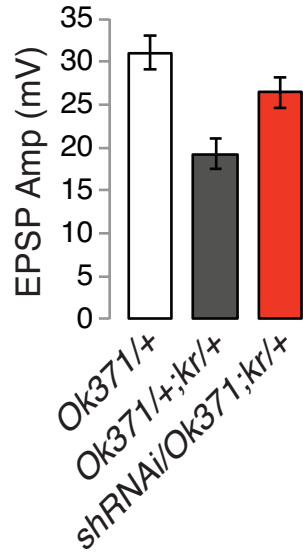


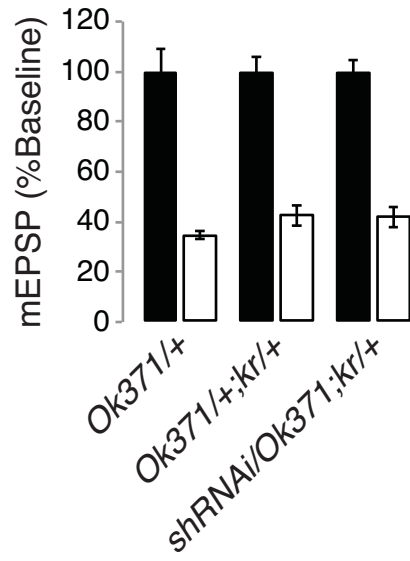
Figure 5. Kr Overexpression Phenocopies *shal* Mutant Physiology

(A) Average EPSP amplitudes are shown for controls, *Ok371-gal4/+*, *Ok371-gal4/+; UAS-Kr/+*, and *Ok371-gal4/Sh RNAi; UAS-Kr/+*. EPSP amplitudes in *Ok371-gal4/+; UAS-Kr/+* is significantly reduced compared to wt. Corresponding reductions in quantal content were observed. (B) Average mEPSP values, normalized to their own baseline for the indicated genotypes, in the absence of PhTx (black bars) and following PhTx incubation (white bars). (C) Average quantal content normalized to baseline as in (B). All statistical comparisons are made within single genotypes. Overexpression of Kr prevents a homeostatic increase in quantal content following PhTx incubation. This can be rescued by co-expression of *shaker RNAi*. *** indicates $p < 0.001$ (Student's t-test).

A



B



C

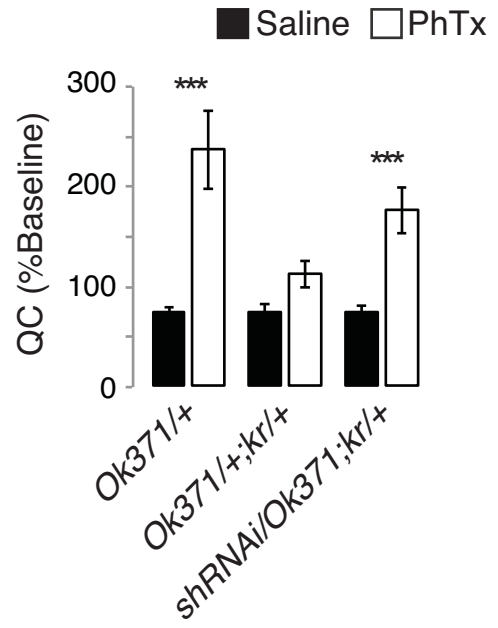


Figure 6. Acute Activation of Kr Following Inhibition of I_A

(A) Representative images of Kr protein (red) within the ventral nerve cord and CNS in *Ok371-gal4, T2 GFP* (A) following 18 hours 4-AP feeding (B) and 24 hours 4-AP feeding (C). Top panels show GFP and Kr overlay. Bottom panels show just Kr (Ci) Higher magnification of the ventral nerve cord following 24 hours 4-AP feeding. Kr is not expressed in GFP labeled motoneurons. (D) Quantification of the number of Kr filled cells specifically in the ventral nerve cord normalized to wt. *** indicates $p < 0.001$ (Student's t-test). Kr expression is significantly increased within 24 hours of 4-AP feeding.

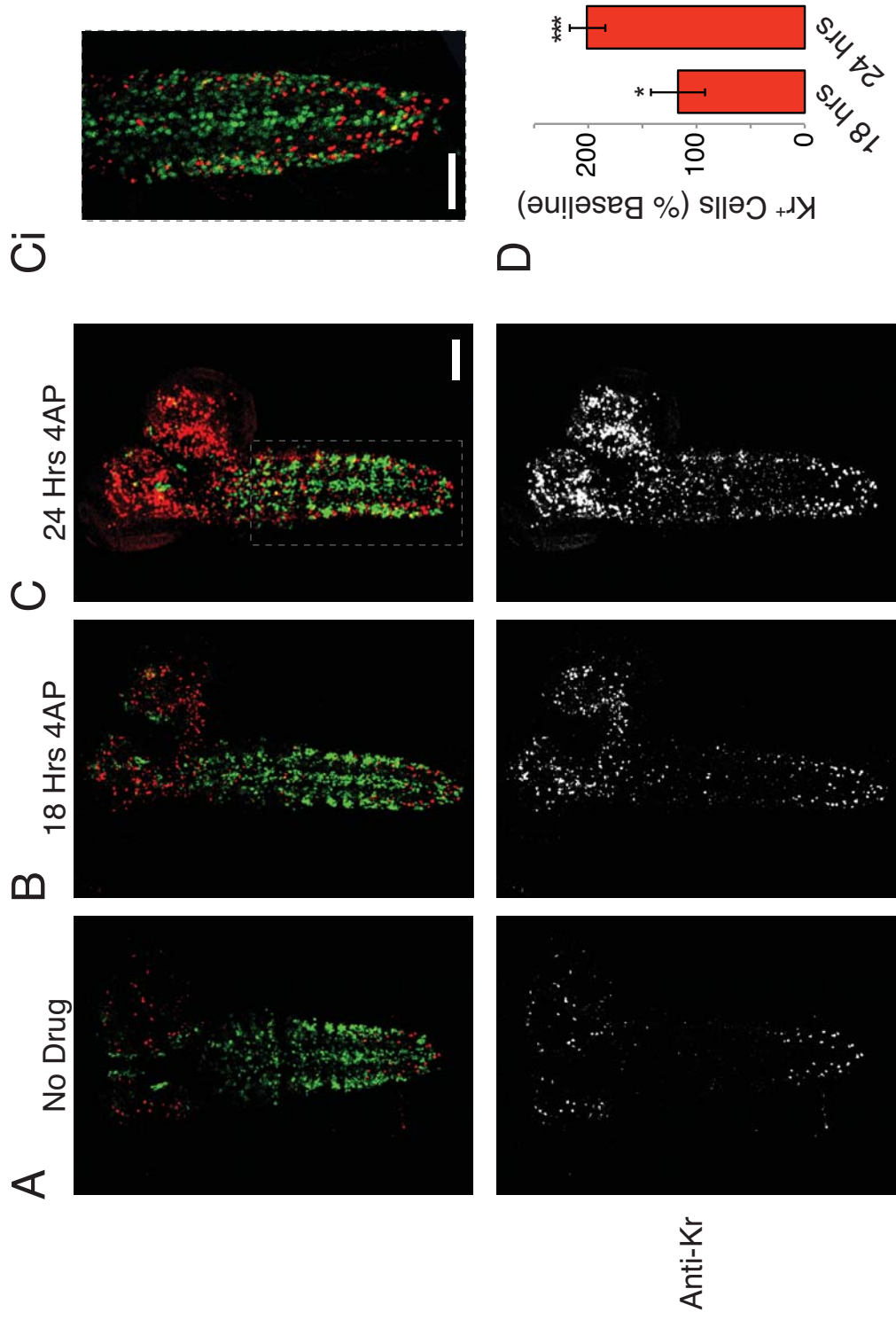


Figure 7. *shal RNAi* Reduces Shal in Motoneurons

(A) Representative images of Shal (green) and Kr (red) protein within the ventral nerve cord and CNS in *wt* (A), *shal⁴⁹⁵* (B), and *Ok371-gal4/shal RNAi* (C) (scale bar = 40 microns). Bottom panels show each color channel in isolation. Shal is highly expressed in the neuropil and axons as they leave the ventral nerve cord. Anti-Shal staining is absent in *shal⁴⁹⁵* mutants. Anti-Shal staining is still present in the neuropil, but is completely absent in the motoneuron axons in animals expressing *shal RNAi* specifically in motoneurons.

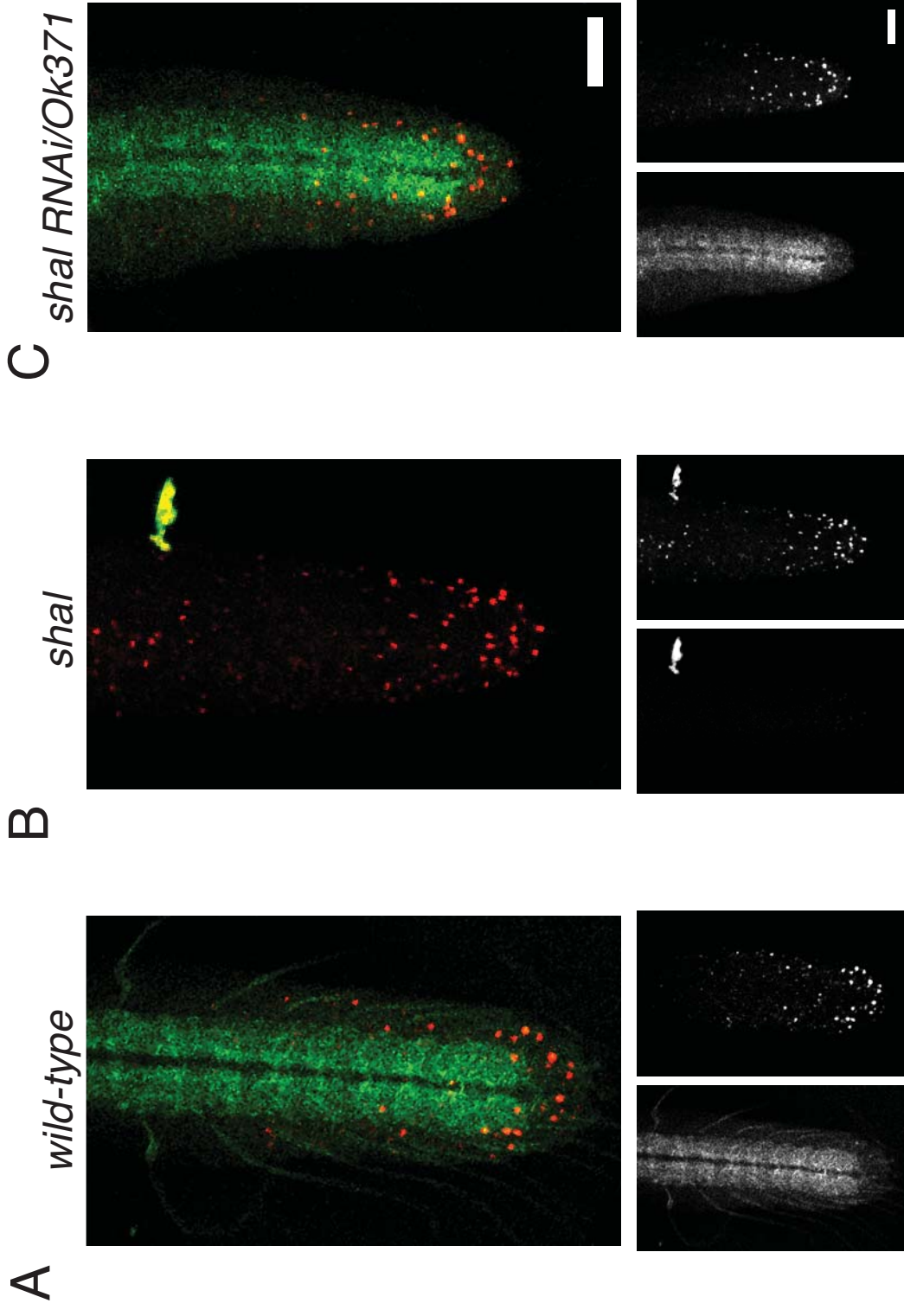
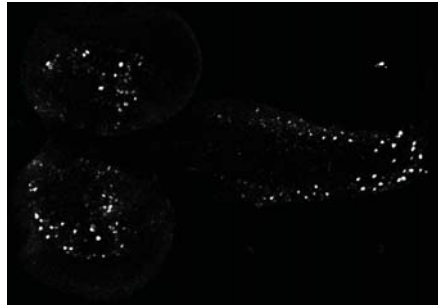
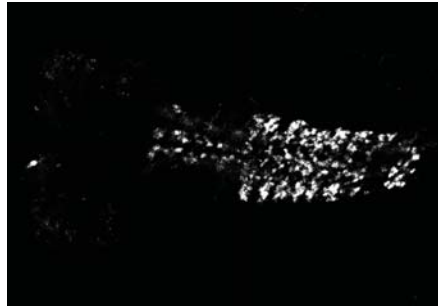
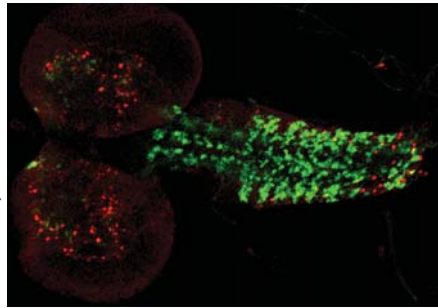


Figure 8. Kr Increase Does Not Localize to Motoneurons

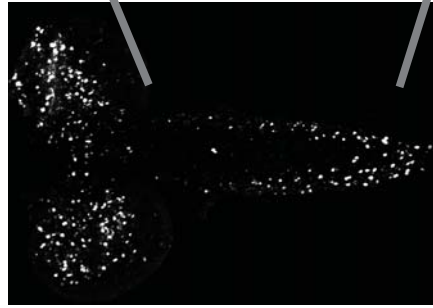
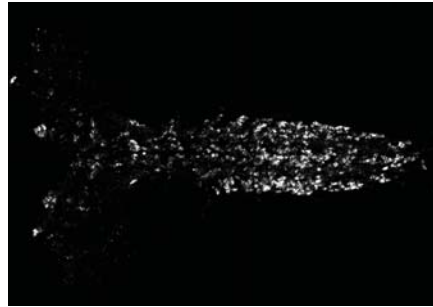
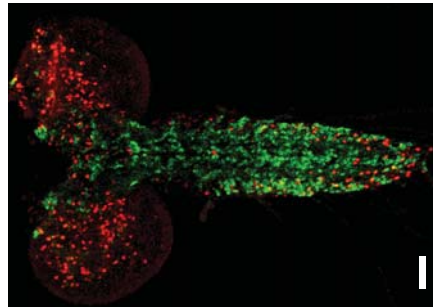
(A) Representative images of Kr protein (red) and GFP within the ventral nerve cord and CNS in *Ok371-gal4, T2 GFP* (A) and *Ok371-gal4/shal RNAi; shal⁴⁹⁵/+* (B). Left panels show overlay, middle panels show GFP and right panels show Kr staining. (C) Quantification of the number of Kr filled cells specifically in the ventral nerve cord normalized to wt. *** indicates $p < 0.001$ (Student's t-test). Kr expression is significantly increased in *Ok371-gal4/shal RNAi; shal⁴⁹⁵/+*. (D) Higher magnification of the ventral nerve cord *Ok371-gal4/shal RNAi; shal⁴⁹⁵/+*. Kr is not expressed in GFP labeled motoneurons.

A *Ok371, T2GFP/+*



B

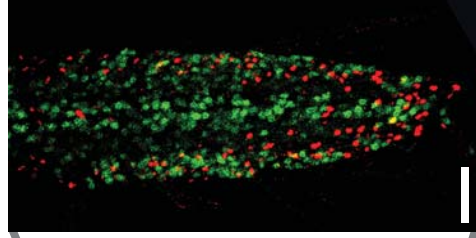
sha1RNAi/Ok371, T2GFP; sha1⁴⁹⁵/+



GFP

Anti-Kr

D



C

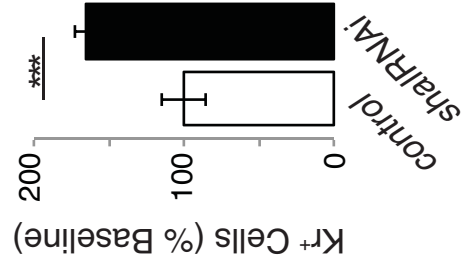
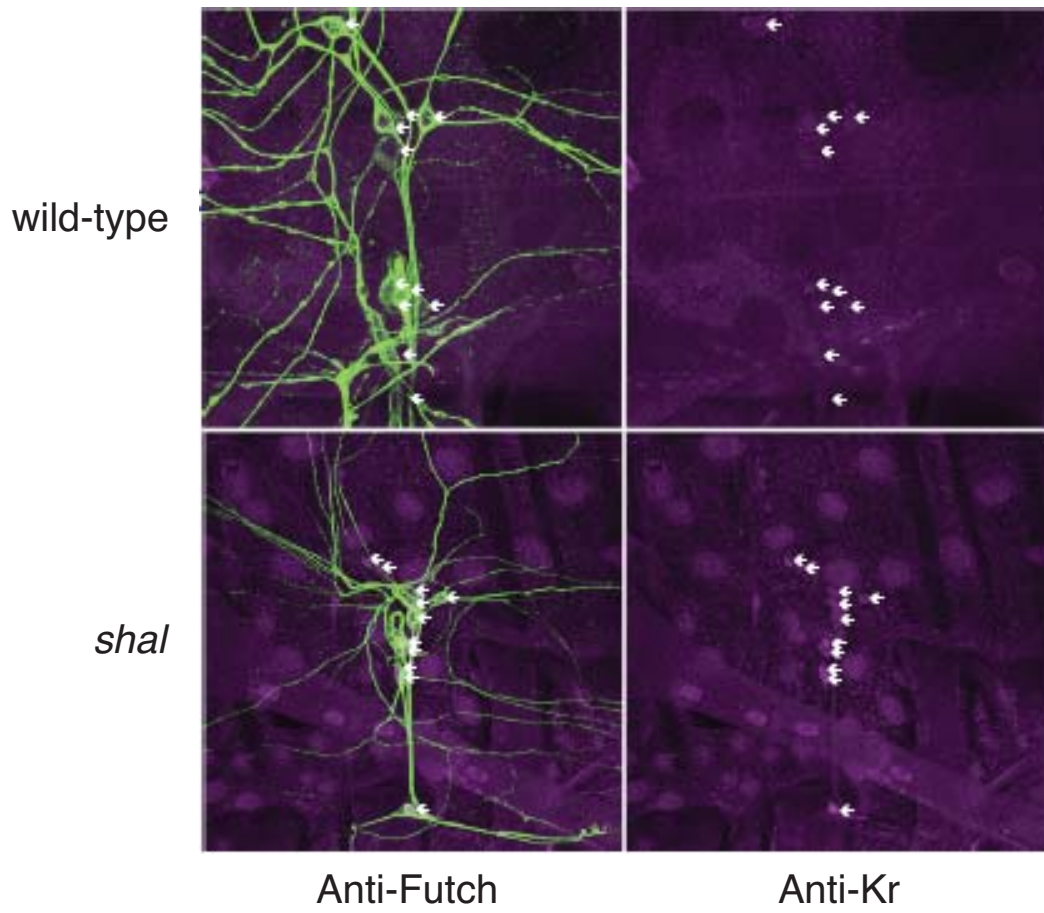


Figure 9. Kr Increase Does Localize to Sensory Neurons

(A) Representative images of Kr protein (purple) and neuron specific Futch protein (green) in PNS sensory neurons in wt (Top panels) and *shal*⁴⁹⁵ (Bottom panels). Left panels show overlay, right panels show Kr staining. Kr is not expressed in wt sensory neurons. Kr is expressed in sensory neurons in *shal*⁴⁹⁵.

A



Chapter 4:

Expression Profiling Isolated Motoneurons: Assessing Compensation in Voltage Gated Ion Channel Mutants

Introduction

The firing properties of a neuron are a result of the complement of ion channels it expresses, and changes in the abundance, type and distribution of these channels lead to altered patterns of activity. Further, while neurons persist a lifetime, ion channel turnover occurs on a timescale of minutes to days. In order to maintain stable intrinsic properties, a neuron must regulate the synthesis, insertion and degradation of the channels that govern its excitability. Homeostatic signaling systems have been proposed to monitor and maintain functional intrinsic membrane properties (Davis and Bezprozvanny, 2001; Frank et al., 2006; Marder and Goaillard, 2006; Marder and Prinz, 2002 and 2003; Perez-Otano and Ehlers, 2005; MacLean et al., 2003; Desai, 2003; Davis, 2006).

There are two mechanisms by which homeostatic regulatory systems have been proposed to maintain intrinsic membrane properties. First, chronic changes in neuronal activity have been demonstrated to cause compensatory changes in ion channel abundance, supporting a model where neuronal activity is homeostatically regulated (Davis, 2006; Marder and Prinz, 2002; Turrigiano and Nelson, 2004; Desai, 2003). Second, in lobster stomatogastric ganglion neurons overexpression of *shal*, which is responsible for the transient I_A potassium current, lead to compensatory increases in the opposing I_H current. The same increase in I_H is seen even when an inactive *Shal* channel is overexpressed, which results in altered neuronal activity. This supports a model where expression of pairs or groups of ion channels is coupled independently of activity (MacLean, 2003; Marder and Prinz, 2003).

Potentially in support of either model above, animals lacking a specific ion channel often maintain normal neuronal activity as a result of compensatory changes in

other ion channels. In these knockout mutants activity is maintained, supporting the first model. However, in many cases compensation comes from altered abundance of only one or two channels suggesting again that there may be specific coupling of pairs of ion channels which govern how a neuron will respond (Chen et al., 2006; MacLean et al., 2003; Marder et al., 1996; Marder and Goaillard, 2006; Nerbonne et al., 2008; Swensen and Bean, 2005; Van Wart and Matthews, 2006).

To determine if a discernable pattern in ion channel compensation exists that would be able to predict the response of a neuron to the loss of any one channel, an unbiased approach to assay all changes in channel expression in an identified neuron is needed. Equally important is the ability to compare between several mutant backgrounds. Well-characterized ion channel mutants exist in *Drosophila* along with the ability to genetically label specific cell-types. Taking advantage of this system, here we perform DNA microarray expression profiling on FACs sorted motoneurons from five different ion channel mutants.

Results

We selected five voltage gated ion channel mutants to begin our study; potassium channels, *shaker*¹⁴ (*sh*), *ether a go-go*¹ (*eag*), and *hyper-kinetic*¹ (*hk*), calcium channel, *cacophony*^s (*cac*), and sodium channel, *paralytic*^{ST76} (*para*). We chose these mutants for two reasons. First, these mutants have all been extensively characterized in *Drosophila* motoneurons and are all severe hypomorphic alleles or complete loss of function mutants to provide a significant homeostatic challenge. Second, we selected mutants that will result in both increased and decreased neuronal excitability to increase the likelihood of being able to distinguish between activity dependent compensatory changes and transcriptional coupling unrelated to activity.

FACs Isolation of Motoneurons

It has been demonstrated that loss of a given ion channel is compensated for in different ways in different cell-types (Chen et al., 2006; Nerbonne et al., 2008; Swensen and Bean, 2005; Van Wart and Matthews, 2006). Therefore, while assaying all neurons will provide insight into common mechanisms of compensation, cell-type specific details will be lost. For this reason we assayed gene expression patterns specifically in dissociated, FACS-sorted GFP-labeled motoneurons. To do this, we expressed the cytosolic UAS-*T2 GFP* with the motoneuron specific driver, *Ok371-gal4* in all of the channel mutants. Demonstration of GFP labeled motoneurons can be seen in figure 1.

Changes in Voltage-Gated Ion Channels

Significant changes in ion channel expression for each mutant assayed are shown in figure 2. In all of our data, significance was determined by SAM analysis with a 1 percent false discovery rate. Several very interesting things emerge from this data set. Interestingly, only three voltage-gated ion channels were found to be significantly altered. It should be noted that many of the known voltage-gated ion channels were below detection level in *wild-type*, most notably, *shal*, which we have shown by quantitative PCR to be increased in *sh* mutants (see discussion). First, *slowpoke (slo)*, the large conductance calcium activated potassium channel is increased in *sh* mutants, revealed by two independent *slo* probes (Fig 2A). Both Slo and Sh are localized at the presynaptic terminal in motoneurons and are both required for repolarization of the terminal. Further it was shown that both *sh* and *slo* mutations alone cause relatively minor delays in repolarization. However, addition of *sh* antagonist 4-aminopyridine (4AP) to *slo* mutants caused significant delays in repolarization (Gho and Ganetzky, 1992). Taken together with our data it suggests Sh and Slo are may be reciprocally coupled to maintain terminal excitability. In addition a previously uncharacterized voltage-gated anion channel, CG17139, is also altered in *sh* mutants (Fig 2A).

Second, *sh* is decreased in *cac* mutants (Fig 2B). *cac* encodes the Ca_v2.1 channel that is exclusively localized in the presynaptic terminal and is required for stimulus-evoked transmitter release at the NMJ (Frank et al., 2006). The *cac^s* mutant is a hypomorphic allele that causes a deficit in basal synaptic transmission. Decreased presynaptic Sh would work to increase calcium influx by extending the terminal repolarization time as mentioned above.

Modulation of Ion Channel Homeostasis

Non-voltage-gated ion channels were the most represented in our data set. These probes are represented across mutants and include: chloride channels, pHCl, CG31116 and CG17139, cation channels, TrpA1, CG34369 and pyx, potassium channels, CG42594, Task6, and the inward rectifying potassium channel, Irk3. Although not expected, this result is perhaps not surprising. Modulation of resting membrane potential will have significant effects on the excitability of the neuron. Understanding how these ion channels function in motoneurons will be of great interest moving forward.

The Nicotinic Acetylcholine Receptor is Surprisingly Decreased in both *cac* and *para*

Excitatory inputs onto *Drosophila* motoneurons are cholinergic. Mutations in both *cac* and *para* will severely decrease excitability and output of motoneurons. It is therefore counterintuitive that the acetylcholine receptor (AcR) subunits are decreased in both these backgrounds. There are, however, multiple AcR subunits in *Drosophila* and it is therefore conceivable this result depicts a reorganization in the receptor subunit complement to perhaps promote a higher conductance complement. Although this has not been well studied in *Drosophila* evidence for receptor subunit composition conferring different conductances has been well demonstrated at the *Drosophila* NMJ and at vertebrate CNS glutamatergic synapses.

Discussion

Activity Dependent versus Transcription Dependent Compensatory Mechanisms

With relatively few channels demonstrated to be significantly different in our data, we still cannot clearly distinguish between these two mechanisms. The numerous channels that appear to regulate ion gradients within the neuron that emerged from our data are suggestive of an additional homeostatic mechanism to control neuronal activity.

Research to this point has focused on active properties of neurons (Davis and Bezprozvanny, 2001; Frank et al., 2006; Marder and Goaillard, 2006; Marder and Prinz, 2002 and 2003; Perez-Otano and Ehlers, 2005; MacLean et al., 2003; Desai, 2003; Davis, 2006). Regulation of the passive properties of a neuron can profoundly alter excitability and leaves numerous compelling questions to pursue. How these channels work in *wild-type* animals let alone whether we will be able to measure changes in resting potential in any of our mutants as a result of these changes are all open questions.

Sh reveals the most changes

We have the most data from Sh mutants. In total we performed 12 independent microarrays (as compared to 4 for all other mutants) comparing *wild-type* and *sh* expression profiles. That we have identified the greatest number of differences in this background is indicative of the fact that many of the voltage-gated ion channels, which were the driving force behind this project, are expressed below detection level even in *wild-type* animals. Concurrent work carried out by our collaborators Charlie Kim and Jay Parrish in the labs of Joe DeRisi and Yuh Nung Jan revealed through expression profiling neurons throughout larval development that most all transcripts encoding genes that are

specific to neuronal function, including neurotransmitters, ion channels, and signaling molecules required for neurotransmission are expressed at high levels early in larval development but are down-regulated by the 1st-2nd instar transition. It has not been determined whether this drop in expression at the transcript level translates to decreasing protein level, but this is unlikely considering the most extensive period of larval growth occurs after the 1st-2nd instar transition. It is therefore possible that by assaying 3rd instar larvae we have missed a lot of the changes in ion channel expression.

In addition to ion channels, our dataset includes the entire expression profile for 3rd instar motoneurons from five different mutant backgrounds. Although this dataset is new, and therefore not fully analyzed to present here, we have obtained a wealth of information to begin to look through to shape future areas of research.

Figure 1. *Ok371, T2 GFP* Labels Motoneurons

(A) Representative images of *Ok371, T2 GFP* (green) labeled motoneurons within the ventral nerve cord and peripheral axons.

A

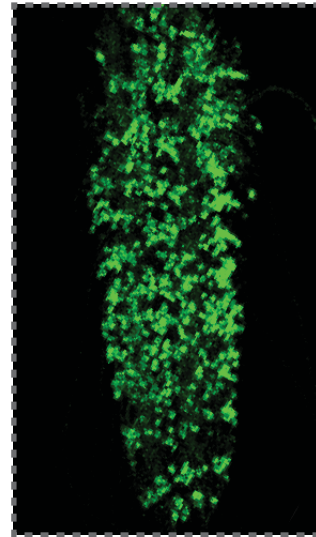
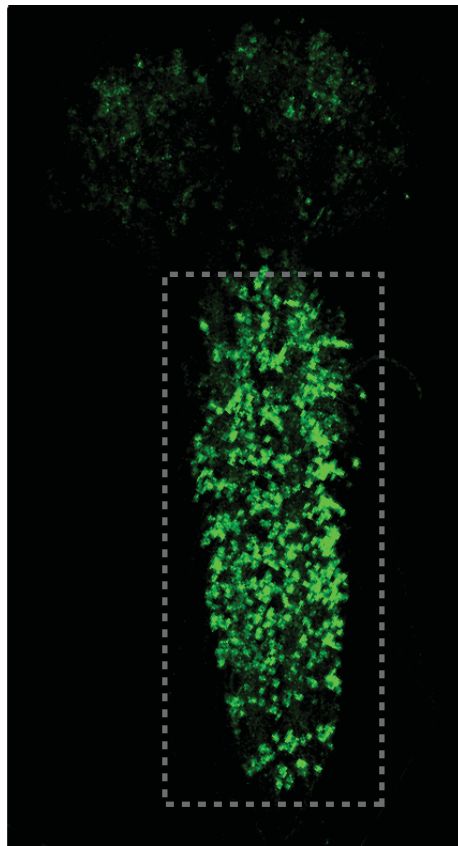
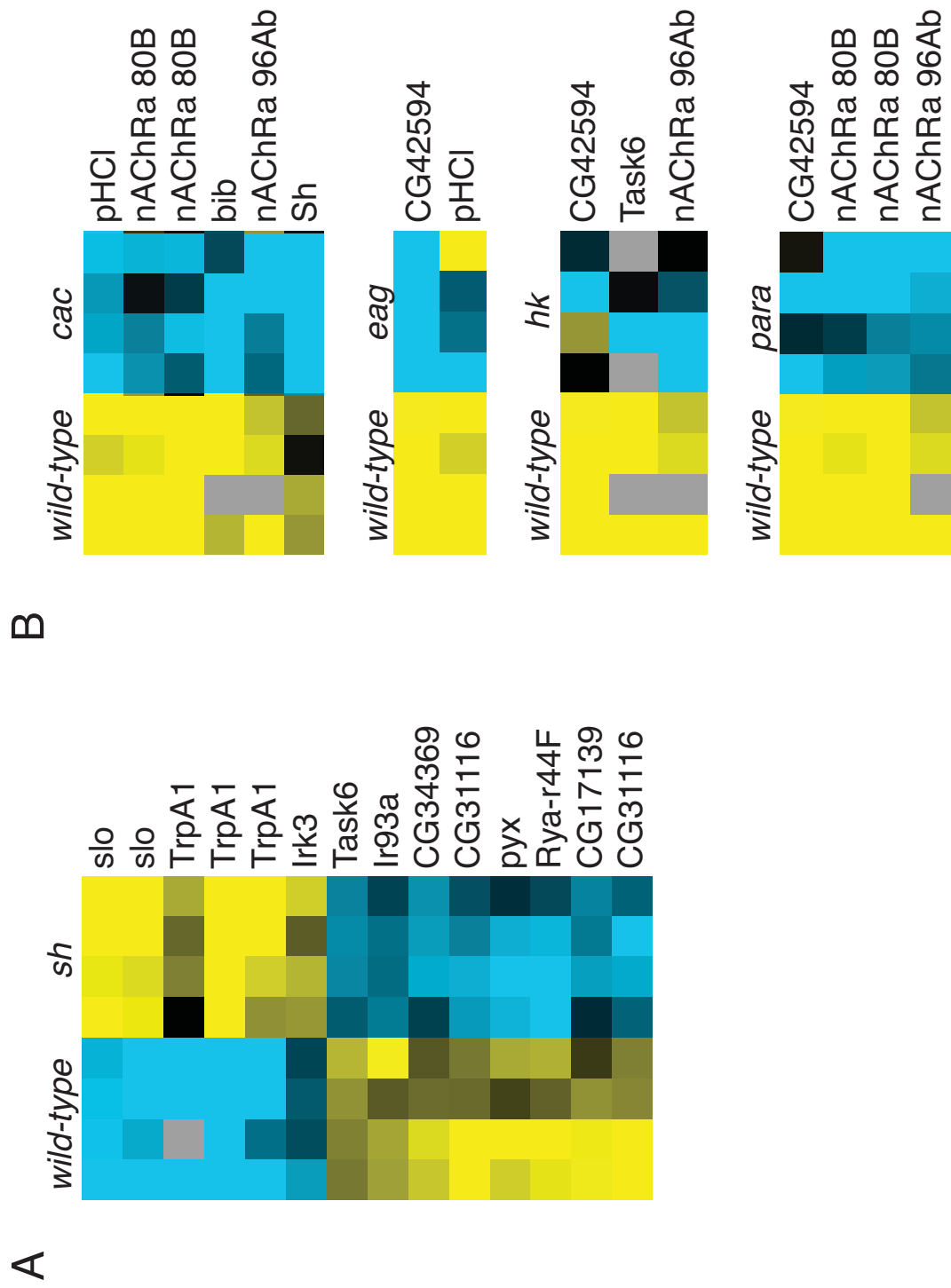


Figure 2. Changes in ion channel expression in ion channel mutants

(A) Heat maps depicting gene expression in wt (left) and *sh* (right) for all ion channels that were significantly altered in *sh* mutants. (B) Heat maps depicting gene expression in wt (left) and indicated mutant (right) for all ion channels that were significantly altered in each mutant. Genes are listed on the right. Repetition indicates multiple probes. Blue is low and yellow is high expression.



Chapter 5:
General Conclusions

The nervous system has an incredible capacity for change. Modification of synaptic strength, cellular excitability and morphology are continuous readouts of the nervous system's ability to respond to new experience. A concurrent and equally important task for the nervous system is to maintain activity within a functional range while still allowing for adaptation. That the nervous system manages to do this is evidence of homeostatic maintenance of neuronal activity. Understanding these homeostatic mechanisms is necessary to understand nervous system function and also will provide insight into a great number of CNS disorders where control of activity is lost.

Work in the previous chapters demonstrates that homeostatic control of both cell intrinsic excitability and synaptic strength function in *Drosophila*. We provide evidence that loss of *shal* induces a compensatory increase in *shaker* expression, and vice versa, suggesting homeostatic maintenance of A-type channel abundance in *Drosophila* motoneurons. Further, compensatory increase in *shaker* occludes synaptic homeostasis. It is unknown whether independent homeostatic signaling systems are somehow coordinated within the nervous system. My work shows that intrinsic excitability is favored over synaptic compensation in this system and argues against coordination.

We then show that loss and acute block of Shal activate the transcription factor *kr*, which is sufficient to drive increased Sh expression. Although Kr is not increased in motoneurons, it is in sensory neurons and is the first demonstration of transcription factor activation leading to compensatory changes in ion channel expression following a homeostatic pressure. We are currently in the process of screening transcription factors in the continued hope of identifying the mechanism of this A-type potassium channel

coupling within motoneurons. It is also an interesting finding that different classes of neurons activate independent transcription factors in response to the same perturbation.

We have only begun to study the molecules involved in the compensatory regulation of ion channels. However, with the relatively (in comparison to vertebrates) few voltage gated ion channels that are expressed within motoneurons, the availability of knockouts, the ability to assay physiology in motoneurons and downstream muscles and finally, the addition of expression profiling, we are well poised to begin this process. In my final chapter we demonstrated that motoneurons are accessible to FACS sorting and microarray analysis. Concurrent work in DeRisi and Jan labs has further demonstrated that most all of the voltage gated ion channels decrease expression through development and by third instar are often undetectable. Therefore, conducting gene expression arrays on 2nd instar may prove far more informative for assessing changes in ion channel abundance and whether, as we predict, there are identifiable rules governing compensatory changes in ion channel abundance.

EXPERIMENTAL PROCEDURES

Chapter 2

Electrophysiology Neuronal recordings:

All experiments were performed on wandering third-instar larvae. Preparations were achieved by gluing both anterior and posterior extremities to sylgard (Silicone Elastomer 2-Part, World Precision Instruments, Inc) coated cover slips and then making a dorsal incision. The fat and guts were removed, care was taken to leave the ventral nerve cord (VNC) intact. The VNC was then glued to the body wall (Glue is Histoacryl, Braun Aesculap). Dissections were made in external saline (in mM, 135 NaCl, 5 KCl, 4 MgCl₂ · 6H₂O, 2 CaCl₂ · 2 H₂O, 5 HEPES, 36 sucrose, pH 7.1). Protease (Protease, Type XIC: Bacterial from *Streptomyces griseus*, Sigma-Aldrich, St. Louis, MO) was focally administered to the ventral nerve cord using a glass pipette pulled to ~10 μm tip diameter. Debris was constantly cleared using the pipette with positive and negative pressure. With adequate exposure to the protease, the outer and inner membranes of the ganglion are disrupted revealing the motor neurons. Motor neurons in the VNC are organized stereotypically with repeating segmental arrays of somata. We focused on the bilaterally symmetric dorsomedial clusters aligned parallel to the midline and containing motor neurons (MN) 1, 6/7, 14, and 30-Ib and MNISN-Is. These neurons form a cross like cluster and are easily isolated due to their dorsal location within the VNC (Choi et al., 2004). To further verify motor neuron identity, several cells were filled during recordings (alexa 488) and imaged post recording. Motor neuron axons project to the body-wall muscle through nerves that exit the VNC in each segment and positively identified the cells as motor neurons. Whole cell recordings were made in K⁺ isolation

saline (external saline with the addition of 1 μ M TTX). Thick-walled borosilicate glass electrodes (GC100TF-10; Harvard Apparatus, Edenbridge, UK) were pulled and fire polished to a resistance of 5-10 M Ω . Internal solution contained (in mM: 140 KCH₃SO₃, 2 MgCl₂ · 6H₂O, 2 EGTA, 5 KCl, 20 HEPES, pH 7.4). Recordings were obtained with an axopatch 200B amplifier (Axon Instruments, Union City, CA, USA). Cells were held at -60mV. To isolate the I_A, two separate electrophysiological protocols were run. The first used a hyperpolarized conditioning pulse (-90mV), which removed inactivation from I_A, and was followed by depolarizing command pulses (-60 to +20mV), which activated both I_A and I_K. The second protocol was then run starting with a more depolarized (-40mV) conditioning pulse, which completely inactivated I_A, and was then followed by the same command pulses, activating only I_K. Currents recorded under these two protocols were then electronically subtracted offline using Clampfit 9.0 (Axon Instruments) to give the isolated I_A.

Muscle recordings:

All neuronal recordings were performed on central neurons from wandering third-instar larvae (see Supplemental Methods for additional detail). For muscle recordings, quantal content was calculated for each individual recording by calculating the average EPSP/average mEPSP (Albin and Davis, 2004; Davis et al., 1998; Paradis et al., 2001). EPSPs, mEPSPs, and quantal contents calculated for each recording were then averaged across animals for a given genotype. As a control, all calculated quantal content values were corrected for non-linear summation (Davis and Dickman, 2009). In no case does this correction alter the statistical significance of our comparisons or conclusions.

Therefore, the majority of our data are presented as non-corrected values with the exception of data presented in Figure 3, which compares quantal contents across a range of extracellular calcium concentration.

Anatomical Analysis

Third-instar larval preparations were fixed in Bouins, washed and incubated overnight at 4°C in primary antibody: anti-shal (1:500; rabbit; a kind gift from Dr. Ronald Harris-Warrick). Ventral Nerve Cord image stacks were captured using a Zeiss Axioskop 2 microscope and the Zeiss LSM 510 Meta Laser Scanning System. Staining quantification was done using Image J software. Shal fluorescence intensity along the axons was calculated within a $10\mu\text{m}^2$ box. This box was then moved along the length of the axon in $10\mu\text{m}$ increments. The box was oriented in the HRP channel to properly visualize the axons and then switched to the shal channel for intensity calculations. Four axons from four animals were used for each genotype. Anatomical visualization of the NMJ to quantify bouton numbers was achieved by staining the NMJ with anti-nc82 (gift from Erich Buchner) and anti-Dlg (Pielage et al., 2008). Bouton numbers were quantified as described previously (Albin and Davis, 2004).

Statistical Analyses

All comparisons were analyzed using both Student's t-test and either a one-way or two-way ANOVA including Bonferroni post-test. In all cases, the conclusions and statistical significance remained the same for both types of analysis. Figure legends indicate which test is depicted in graphical form.

CNS Quantitative RT-PCR

Primer-probes specific for real-time PCR detection of Shal, Shaker, Ribosomal protein L32 (RpL32) were designed and developed by Applied Biosystems. The CNS was removed from 25 third-instar larvae per sample (3-6 samples/genotype). Total RNA was isolated from each sample using the standard Trizol protocol. A DNase digestion was then done to remove all potential DNA contamination (RQ1 RNase-free DNase Promega). RT was performed (Taqman reverse transcription reagents, Applied Bioscience) using random hexamers and 1 μ g total RNA. A no RT control was performed for each sample. Purified cDNA was used as a template in 30 μ l PCR reaction (TaqMan Universal PCR Master Mix, no AmpErase UNG, Applied Biosystems). This 30 μ l reaction was divided into three 10 μ l triplicates. In addition, one 10 μ l no RT reaction was used for each sample. The ABI Prism 7900 was used for all PCRs. Cycle threshold (C_T) was determined by automated threshold analysis using SDS2.3 software according to the manufacturer's instructions (Applied Biosystems, Foster City, CA). Comparative Shal and Shaker levels (between wt and mutant animals) were determined using the $\Delta\Delta C_T$ method (Applied Biosystems User Bulletin No. 2). To determine if the two amplification reactions have the same PCR efficiency, ΔC_T (C_T of experimental gene - C_T of reference gene) values are determined across the serial dilutions and plotted against the log of the cDNA dilution. A slope close to zero indicates equivalent amplification efficiency. This was done and both Shal and Shaker have approximately equal amplification efficiencies compared with the endogenous control, RpL32. Briefly, the $\Delta\Delta C_T$ method is as follows: ΔC_T values are determined as explained above. Next, experimental animal (mutants) ΔC_T

values were subtracted from control animal (wt) ΔC_T values to give the $\Delta\Delta C_T$. Finally using the equation $2^{(-\Delta\Delta C_T)} \times 100$ the percent expression of each gene in experimental compared to control animals was calculated. Each control animal sample was compared to each wild type sample (Applied Biosystems User Bulletin No. 2). In four *shal*⁴⁹⁵ samples, Shal levels were below detection levels. To generate averages these samples were counted as 0.

Fly stocks and Genetics

In all experiments, the *w*¹¹¹⁸ strain was used as the wild-type control and animals were raised at 22°C unless otherwise noted. *shaker* RNAi (*shakerRNAi*) was obtained from Vienna Stock Center (VDRC stock 23671 and 23673). *shakerRNAi; shal*⁴⁹⁵ were crossed to *c155-gal4;;shal*⁴⁹⁵ and raised at 30°C in parallel with controls. *EKO-222* (a kind gift from Dr. Haig Keshishian) flies were crossed to *Ok6-gal4* and raised at 25°C in parallel with controls. All other mutant fly lines were obtained from the Bloomington Drosophila stock center (Bloomington, IN) or the Exelixis Drosophila disruption lines (Harvard University, MA).

Chapter 3 and 4

Cell dissociation and sorting

Ventral Nerve Cord (VNC) cell suspensions of dissected tissue were generated using mechanical and enzymatic dissociation. VNCs were dissected out of 3rd instar larvae in PBS. Approximately 50 brains were used per sample. Collagenase A (1mg/mL) was

added to the VNCs to a final volume of 500 μ L. Dissociation was obtained by three repetitions of the following: mixing 5 min at 1000 RPM in 37°C ependorf thermomixer and triturating by pipetting 10x through a 1000 μ L pipet tip. Following dissociation, samples were filtered through a 70 μ m filter and sorted on a FACS Aria II (Becton, Dickinson and Company). Neuronal populations exhibited unique forward scatter (FSC) and side scatter (SSC) properties, which increased gating specificity. GFP⁺ non-autofluorescent events were sorted into Trizol and samples were immediately frozen on dry ice.

RNA isolation, amplification, and hybridization

Sorted cells were sorted into Trizol, and processed for RNA as per the manufacturer recommendation, including DNase treatment. RNA samples went through one round of linear amplification using the Aminoallyl MessageAmp II kit (Ambion). Dye-coupled aRNA was fragmented and hybridized to custom-designed microarrays (Designed by Charlie Kim).

Microarray design

Charlie Kim designed two 60-mer oligonucleotide probes for each of the 20,726 coding sequences in the annotated fly genome (release 5.2) using ArrayOligoSelector (Bozdech et al., 2003), resulting in 35,272 successful probe designs, 16,717 additional probes against alternatively spliced transcripts, and 546 probes targeting non-coding RNA (244 snoRNA, 108 tRNA, 24 snRNA, 74 rRNA, 3 miRNA, 93 other). The final probe set was filtered to remove redundant probes, overlapping probes, and those with cross

hybridization potential (based on a -21.6 kcal/mol threshold, which was chosen to fit the number of probes allowed in the Agilent 4 x 44k design specification). This resulted in 33,792 probes to CDS, 8744 probes to alternatively spliced transcripts, and 546 RNA probes. In total, 43,803 probes were included in the design.

Feature extraction, normalization, and filtering

Microarrays were scanned on an Axon 4000B scanner and feature information extracted in GenePix 6 (Molecular Devices). GPR files were uploaded into Acuity (Molecular Devices) and ratio normalized. Data was retrieved using quality filters for reference channel intensity, background intensity, pixel saturation, pixel variance, feature diameter, % pixel intensity over background, and feature circularity. “Ratio of Medians” data was further filtered for 70% present data, Cy5 net median intensity > 350 across a minimum of 3 arrays, Cy3 net median intensity > 150 across a minimum of 20 arrays. Expression ratios were log₂ transformed, median centered across arrays, and median centered across genes before analysis.

DroID microarray correlation meta-analysis

A table containing pairwise gene expression correlations measured from 844 microarray datasets spanning 49 studies available in the NCBI Gene Expression Omnibus was downloaded from the *Drosophila* Interactions Database (DroID, version 5). All possible pairwise gene expression correlations were calculated across populations and time points in our dataset. A correlation of correlations was calculated between pairwise gene correlations from DroID and the pairwise gene correlations from this study. A

background distribution was generated by randomly associating the pairwise gene correlations in DroID with the microarray pairwise gene correlations, calculating a correlation of correlations, and iterating this process 50,000 times. Normality was confirmed using the Kolmogorov-Smirnov goodness of fit test, and a z -score and associated p -value were calculated for the observed correlation of correlations value with regard to the random distribution.

DroID interactions correlation meta-analysis

Tables of known gene interactions were downloaded from DroID (Yu et al., 2008), including the Finley, Curagen, and Hybrigenics yeast two hybrid datasets; worm, yeast, and human interlog datasets; a manually curated dataset of known physical interactions; and a manually curated dataset of known genetic interactions. For each of these categories, an average pairwise gene correlation was calculated from the pairwise gene correlations for the whole dataset and compared to a background distribution generated as above. The same correlation calculates were conducted using pairwise gene correlations calculated from population-specific data and compared to whole animal data generated in this study.

Fly stocks and Genetics

In all experiments, the w^{1118} strain or *Ok371-gal4*, *UAS-T2 GFP* (for FACs sorting) were used as the wild-type control and animals were raised at 22°C unless otherwise noted. For sorting *Ok371-gal4*, *UAS-T2 GFP* was placed in background of all mutants. All mutant fly lines were obtained from the Bloomington Drosophila stock center (Bloomington, IN).

REFERENCES

- Albin, S.D., and Davis, G.W. (2004). Coordinating structural and functional synapse development: postsynaptic p21-activated kinase independently specifies glutamate receptor abundance and postsynaptic morphology. *J Neurosci* *24*, 6871-6879.
- Andrasfalvy, B., Makara, J., Johnston, D., and Magee, J. (2008). Altered synaptic and non-synaptic properties of CA1 pyramidal neurons in Kv4. 2 knockout mice. *The Journal of Physiology* *586*, 3881-3892.
- Aoto, J., Nam, C., Poon, M., Ting, P., and Chen, L. (2008). Synaptic Signaling by All-Trans Retinoic Acid in Homeostatic Synaptic Plasticity. *Neuron* *60*, 308-320.
- Baines, R. (2005). Neuronal homeostasis through translational control. *Molecular neurobiology* *32*, 113-121.
- Baines, R., and Bate, M. (1998). Electrophysiological development of central neurons in the *Drosophila* embryo. *Journal of Neuroscience* *18(12)*, 4673-4683.
- Baines, R., Uhler, J., and Thompson, A., Sweeney, ST, and Bate, M. (2001). Altered electrical properties in *Drosophila* neurons developing without synaptic transmission. *Journal of Neuroscience* *21(5)*, 1523-1531.
- Baines, R.A., Uhler, J.P., Thompson, A., Sweeney, S.T., and Bate, M. (2001). Altered electrical properties in *Drosophila* neurons developing without synaptic transmission. *J Neurosci* *21*, 1523-1531.
- Baker, K., and Salkoff, L. (1990). The *Drosophila* Shaker gene codes for a distinctive K current in a subset of neurons. *Neuron* *2*, 129-140.
- Baro, D.J., Coniglio, L.M., Cole, C.L., Rodriguez, H., Lubell, J., Kim, M., and Harris-Warrick, R. (1996). Lobster shal: comparison with *Drosophila* shal and native potassium currents in identified neurons. *Journal of Neuroscience* *16(5)*, 1689-1701.
- Baro, D.J., and Harris-Warrick, R.M. (1998). Differential expression and targeting of K⁺ channel genes in the lobster pyloric central pattern generator. *Ann N Y Acad Sci* *860*, 281-295.
- Baro, D.J., Ayali, A., French, L., Scholz, N.L., Labenia, J., Lanning, C., Graubard, K., and Harris-Warrick, R. (2000). Molecular Underpinnings of Motor Pattern Generation: Differential Targeting of Shal and Shaker in the Pyloric Motor System. *Journal of Neuroscience* *20(17)* 6619-6630.
- Beck, H., and Yaari, Y. (2008). Plasticity of intrinsic neuronal properties in CNS disorders. *Nat Rev Neurosci* *9*, 357-369.
- Becker, A., Poolos, N., Beck, H., and Johnston, D. (2004). Acquired dendritic channelopathy in

temporal lobe epilepsy. *Science* 303, 532-535.

Bergquist, S., Dickman, D.K., and Davis, G.W. (2010). A hierarchy of cell intrinsic and target-derived homeostatic signaling. *Neuron* 66, 220-234.

Bernard, C., and Johnston, D. (2003). Distance-Dependent Modifiable Threshold for Action Potential Back-Propagation in Hippocampal Dendrites. *Journal of neurophysiology* 90, 1807-1816.

Bernard, C., Marsden, D., and Wheal, H. (2001). Changes in neuronal excitability and synaptic function in a chronic model of temporal lobe epilepsy. *Neuroscience* 103, 17-26.

Birnbaum, S., Varga, A., Yuan, L., and Anderson, A., Sweatt, D. and Schrader, L. (2004). Structure and function of Kv4-family transient potassium channels. *Physiological reviews* 84, 803-833.

Borodinsky, L., Root, C., Cronin, J., and Sann, S., Gu, X. and Spitzer, N.C. (2004). Activity-dependent homeostatic specification of transmitter expression in embryonic neurons. *Nature* 429, 523-530.

Brager, D., and Johnston, D. (2007). Plasticity of Intrinsic Excitability during Long-Term Depression Is Mediated through mGluR-Dependent Changes in I_h in Hippocampal CA1 Pyramidal Neurons. *Journal of Neuroscience* 27(51), 13926-13937.

Burrone, J., O'Byrne, M., and Murthy, V.N. (2002). Multiple forms of synaptic plasticity triggered by selective suppression of activity in individual neurons. *Nature* 420, 414-418.

Castro, P., Cooper, E., Lowenstein, D., and Baraban, S. (2001). Channels in the Methylazoxymethanol Model of Cortical Malformations and Epilepsy *Journal of Neuroscience* 21(17), 6626-6634.

Chen, X., Yuan, L., Zhao, C., and Birnbaum, S., Frick, A., Jung, W., Schwarz, T.L., Sweatt, J.D., Johnston, D. (2006). Deletion of Kv4.2 Gene Eliminates Dendritic A-Type K^+ Current and Enhances Induction of Long-Term Potentiation in Hippocampal CA1 Pyramidal Neurons. *Journal of Neuroscience* 26(47), 12143-12151.

Choi, J., Park, D., and Griffith, L. (2004). Electrophysiological and Morphological Characterization of Identified Motor Neurons in the *Drosophila* Third Instar Larva Central Nervous System. *Journal of neurophysiology* 91, 2353-2365.

Cooper, E., Milroy, A., Jan, Y., and Jan, L. and Lowenstein, D.H. (1998). Presynaptic Localization of Kv1.4-Containing A-Type Potassium Channels Near Excitatory Synapses in the Hippocampus *Journal of Neuroscience* 18(3), 955-974.

Cossart, R., Dinocourt, C., Hirsch, J., and Merchán-Pérez, A., De Felipe, J., Ben-Ari, Y.,

- Esclapez, M. and Bernard, C. (2001). Dendritic but not somatic GABAergic inhibition is decreased in experimental epilepsy. *Nat Neurosci* 4(1), 52-62.
- David, Y., Cacheaux, L.P., Ivens, S., Lapilover, E., Heinemann, U., Kaufer, D., and Friedman, A. (2009). Astrocytic Dysfunction in Epileptogenesis: Consequence of Altered Potassium and Glutamate Homeostasis? *Journal of Neuroscience* 29, 10588-10599.
- Davis, G. (2006). Homeostatic Control of Neural Activity: From Phenomenology to Molecular Design. *Annu Rev Neurosci* 29, 307-323.
- Davis, G., DiAntonio, A., Petersen, S., and Goodman, C. (1998). Postsynaptic PKA Controls Quantal Size and Reveals a Retrograde Signal that Regulates Presynaptic Transmitter Release in *Drosophila*. *Neuron* 20, 305-315.
- Davis, G., and Goodman, C. (1998). Genetic analysis of synaptic development and plasticity: homeostatic regulation of synaptic efficacy. *Current Opinion in Neurobiology* 8, 149-156.
- Desai, N.S. (2003). Homeostatic plasticity in the CNS: synaptic and intrinsic forms. *J Physiol Paris* 97, 391-402.
- Desai, N.S., Rutherford, L.C., and Turrigiano, G.G. (1999). Plasticity in the intrinsic excitability of cortical pyramidal neurons. *Nat Neurosci* 2, 515-520.
- di Sanguinetto, S., Dasen, J., and Arber, S. (2008). Transcriptional mechanisms controlling motor neuron diversity and connectivity. *Current Opinion in Neurobiology* 18, 36-43.
- Diao, F., Waro, G., and Tsunoda, S. (2009). Fast inactivation of Shal (Kv4) K⁺ channels is regulated by the novel interactor SKIP3 in *Drosophila* neurons. *Molecular and Cellular Neuroscience* 42, 33-44.
- Dixit, R., Vijayraghavan, K., and Bate, M. (2008). Hox genes and the regulation of movement in *Drosophila*. *Developmental Neurobiology* 68, 309-316.
- Eisen, M.B., Spellman, P.T., Brown, P.O., and Botstein, D. (1998). Cluster analysis and display of genome-wide expression patterns. *Proc Natl Acad Sci USA* 95, 14863-14868.
- El-Hassar, L., Milh, M., Wendling, F., and Ferrand, N. (2007). Cell domain-dependent changes in the glutamatergic and GABAergic drives during epileptogenesis in the rat CA1 region *The Journal of Physiology* 578(1), 193-211.
- Frank, C., Pielage, J., and Davis, G. (2009). Structural Homeostasis: Compensatory Adjustments of Dendritic Arbor Geometry in Response to Variations of Synaptic Input. *Neuron* 61, 556-569.
- Frank, C.A., Kennedy, M.J., Goold, C.P., Marek, K.W., and Davis, G.W. (2006). Mechanisms underlying the rapid induction and sustained expression of synaptic homeostasis. *Neuron* 52, 663-677.

- French, L., Lanning, C., Matly, M., and Harris-Warrick, R. (2004). Cellular localization of Shab and Shaw potassium channels in the lobster stomatogastric ganglion. *Neuroscience* 123, 919-930.
- Frohlich, F., Bazhenov, M., and Sejnowski, T. (2008). Pathological effect of homeostatic synaptic scaling on network dynamics in diseases of the cortex. *Journal of Neuroscience* 28(7), 1709-1720.
- Ganetzky, B., and Wu, C. (1982). *Drosophila* mutants with opposing effects on nerve excitability: genetic and spatial interactions in Repetitive Firing. *Journal of neurophysiology* 47(3), 501-514.
- Gardoni, F., Mauceri, D., Marcello, E., Sala, C., and DiLuca, M. and Jeromin, A. (2007). SAP97 directs the localization of Kv4. 2 to spines in hippocampal neurons: regulation by CaMKII. *Journal of Biological Chemistry* 282(39), 28691-28699.
- Gho, M., and Ganetzky, B. (1992). Analysis of repolarization of presynaptic motor terminals in *drosophila* larvae using potassium- channel-blocking drugs and mutations *Journal of Experimental Biology* 170, 93-111.
- Glykys, J., and Mody, I. (2006). Hippocampal Network Hyperactivity After Selective Reduction of Tonic Inhibition in GABAA Receptor alpha5 Subunit-Deficient Mice. *Journal of neurophysiology* 95, 2796-2807.
- Goaillard, J.-M., Taylor, A.L., Schulz, D.J., and Marder, E. (2009). Functional consequences of animal-to-animal variation in circuit parameters. *Nat Neurosci* 12, 1424-1430.
- Goldberg, E., Watanabe, S., and Chang, S., Joho, R.H., Huang, Z.J., Leonard, C.S. and Rudy, B. (2005). Specific Functions of Synaptically Localized Potassium Channels in Synaptic Transmission at the Neocortical GABAergic Fast-Spiking Cell Synapse. *Journal of Neuroscience* 25(21), 5230-5235.
- Goold, C., and Davis, G. (2007). The BMP Ligand Gbb Gates the Expression of Synaptic Homeostasis Independent of Synaptic Growth Control. *Neuron* 56, 109-123.
- Groth, R., and Tsien, R. (2008). A Role for Retinoic Acid in Homeostatic Plasticity. *Neuron* 60, 192-194.
- Guan, Z., Saraswati, S., Adolfsen, B., and Littleton, J.T. (2005). Genome-wide transcriptional changes associated with enhanced activity in the *Drosophila* nervous system. *Neuron* 48, 91-107.
- Harris-Warrick, R. (2000). Ion channels and receptors: molecular targets for behavioral evolution. *Journal of Comparative Physiology A* 186, 605-616.
- Hatt, H., Guckenheimer, J., and Harris-Warrick, R. (2003). Overexpression of a Hyperpolarization-Activated Cation Current (I_h) Channel Gene Modifies the Firing Activity

of Identified Motor Neurons in a Small Neural Network. *Journal of Neuroscience* 23(27), 9059-9067.

Hernandez-Pineda, R., Chow, A., and Amarillo, Y., Moreno, H., Saganich, M., Vega-Saenz, E., Hernandez-Cruz, A. and Rudy, B. (1999). Kv3.1–Kv3.2 Channels Underlie a High-Voltage–Activating Component of the Delayed Rectifier K⁺ Current in Projecting Neurons From the Globus Pallidus. *Journal of neurophysiology* 82, 1512-1528.

Hoffman, D. (2008). Firing first: compensatory changes in K⁺ channel knockout mice preserve excitability but not synaptic scaling. *The Journal of Physiology* 586, 3731-3732.

Hoffman, D., and Johnston, D. (1998). Downregulation of Transient K Channels in Dendrites of Hippocampal CA1 Pyramidal Neurons by Activation of PKA and PKC *Journal of Neuroscience* 18(10), 3521-3528.

Ibata, K., Sun, Q., and Turrigiano, G.G. (2008). Rapid synaptic scaling induced by changes in postsynaptic firing. *Neuron* 57, 819-826.

Isshiki, T., Pearson, B., Holbrook, S., and Doe, C.Q. (2001). *Drosophila* neuroblasts sequentially express transcription factors which specify the temporal identity of their neuronal progeny. *Cell* 106, 511-521.

Itri, J., Michel, S., Vansteensel, M., and Meijer, J., Colwell, C.S. (2005). Fast delayed rectifier potassium current is required for circadian neural activity. *Nat Neurosci* 8(5), 650-656.

Jan, L., and Jan, Y. (1997). Voltage-gated and inwardly rectifying potassium channels. *The Journal of Physiology* 505(2) 267-282.

Jan, L.Y., and Jan, Y.N. (1994). Potassium channels and their evolving gates. *Nature* 371, 119-122.

Jan, Y., Jan, L., and Dennis, M. (1977). Two mutations of synaptic transmission in *Drosophila*. *Proceedings of the Royal Society of London Series B* 198, 87-108.

Jung, S., Kim, J., and Hoffman, D. (2008). Rapid, Bidirectional Remodeling of Synaptic NMDA Receptor Subunit Composition by A-type K⁺ Channel Activity in Hippocampal CA1 Pyramidal Neurons *Neuron* 60, 657-671.

Jung, S., Kim, J., and Hoffman, D. (2008). Rapid, Bidirectional Remodeling of Synaptic NMDA Receptor Subunit Composition by A-type K⁺ Channel Activity in Hippocampal CA1 Pyramidal Neurons. *Neuron* 60, 657-671.

Kalivas, P.W. (2009). The glutamate homeostasis hypothesis of addiction. *Nat Rev Neurosci* 10, 561-572.

Kaneko, M., Stellwagen, D., and Malenka, R.C. and Stryker, M.P. (2008). Tumor Necrosis

Factor-a Mediates One Component of Competitive, Experience-Dependent Plasticity in Developing Visual Cortex Neuron *58*, 673-680.

Kim, J., Jung, S., Clemens, A., and Petralia, R.S. and Hoffman, D.A. (2007). Regulation of Dendritic Excitability by Activity-Dependent Trafficking of the A-Type K⁺ Channel Subunit Kv4.2 in Hippocampal Neurons. *Neuron* *54*, 933-947.

Landgraf, M., and Thor, S. (2006). Development of Drosophila motoneurons: specification and morphology. *Semin Cell Dev Biol* *17*, 3-11.

Levitani, E.S., and Takimoto, K. (1998). Dynamic regulation of K⁺ channel gene expression in differentiated cells. *Journal of neurobiology* *37*, 60-68.

Lichtinghagen, R., Stocker, M., and Wittka, R., Boheim, G., Stuhmer, W., Ferrus, A. and Pongs, O. (1990). Molecular basis of altered excitability in Shaker mutants of *Drosophila melanogaster*. *The EMBO Journal* *9*(13), 4399-4407.

Liss, B., Franz, O., Sewing, S., Bruns, R., and Neuhoff, H. and Roeper, J. (2001). Tuning pacemaker frequency of individual dopaminergic neurons by Kv4. 3L and KChip3. 1 transcription. *The EMBO Journal* *20*(20), 5715-5724.

Littleton, J., and Ganetzky, B. (2000). Ion Channels and Synaptic Organization Analysis of the *Drosophila* Genome. *Neuron* *26*, 35-43.

Lott, S.E., Kreitman, M., Palsson, A., Alekseeva, E., and Ludwig, M.Z. (2007). Canalization of segmentation and its evolution in *Drosophila*. *Proc Natl Acad Sci USA* *104*, 10926-10931.

MacLean, J., An, W., Lanning, C., and Harris-Warrick, R. (2003). KChIP1 and Frequentin Modify shal-Evoked Potassium Currents in Pyloric Neurons in the Lobster Stomatogastric Ganglion *Journal of neurophysiology* *89*, 1902-1909.

MacLean, J., Zhang, Y., Johnson, B., and Harris-Warrick, R. (2003). Activity-independent homeostasis in rhythmically active neurons. *Neuron* *37*, 109-120.

Manu, Surkova, S., Spirov, A.V., Gursky, V.V., Janssens, H., Kim, A.-R., Radulescu, O., Vanario-Alonso, C.E., Sharp, D.H., Samsonova, M., Reinitz, J. (2009). Canalization of gene expression in the *Drosophila* blastoderm by gap gene cross regulation. *PLoS Biology* *7*(3), 591-603.

Marder, E., Abbott, L., Turrigiano, G., and Liu, Z. (1996). Memory from the dynamics of intrinsic membrane currents. *Proceedings of the National Academy of Sciences* *93*(24), 13481-13486.

Marder, E., and Bucher, D. (2007). Understanding circuit dynamics using the stomatogastric nervous system of lobsters and crabs. *Annu Rev Physiol* *69*, 291-316.

- Marder, E., and Goaillard, J.-M. (2006). Variability, compensation and homeostasis in neuron and network function. *Nat Rev Neurosci* 7, 563-574.
- Marder, E., and Prinz, A. (2002). Modeling stability in neuron and network function: the role of activity in homeostasis. *Bioessays* 24(12), 1145-1154.
- Marder, E., and Prinz, A. (2003). Current compensation in neuronal homeostasis. *Neuron* 37(1), 2-4.
- Marie, B., Pym, E., Bergquist, S., and Davis, G.W. (2010). Synaptic homeostasis is consolidated by the cell fate gene gooseberry, a *Drosophila* pax3/7 homolog. *J Neurosci* 30, 8071-8082.
- Martinez-Padron, M., and Ferrus, A. (1997). Presynaptic Recordings from *Drosophila*: Correlation of Macroscopic and Single-Channel K⁺ Currents *Journal of Neuroscience* 17(10), 3412-3424.
- Matyash, A., Singh, N., Hanes, S.D., Urlaub, H., and Jäckle, H. (2009). SAP18 promotes Krüppel-dependent transcriptional repression by enhancer-specific histone deacetylation. *The Journal Of Biological Chemistry* 284, 3012-3020.
- McDonald, J.A., Fujioka, M., Odden, J.P., Jaynes, J.B., and Doe, C.Q. (2003). Specification of motoneuron fate in *Drosophila*: integration of positive and negative transcription factor inputs by a minimal eve enhancer. *Journal of neurobiology* 57, 193-203.
- Mody, I. (2005). Aspects of the homeostatic plasticity of GABA_A receptor-mediated inhibition. *The Journal of Physiology* 526(1), 37-46.
- Montana, E.S., and Littleton, J.T. (2006). Expression profiling of a hypercontraction-induced myopathy in *Drosophila* suggests a compensatory cytoskeletal remodeling response. *The Journal of Biological Chemistry* 281, 8100-8109.
- Moody, W.J., And Bosma, M.M. (2005). Ion Channel Development, Spontaneous Activity, and Activity-Dependent Development in Nerve and Muscle Cells. *Physiol Rev* 85, 883-941.
- Muraro, N.I., Weston, A.J., Gerber, A.P., Luschnig, S., Moffat, K.G., and Baines, R.A. (2008). Pumilio Binds para mRNA and Requires Nanos and Brat to Regulate Sodium Current in *Drosophila* Motoneurons. *Journal of Neuroscience* 28, 2099-2109.
- Murthy, V.N., Schikorski, T., Stevens, C.F., and Zhu, Y. (2001). Inactivity produces increases in neurotransmitter release and synapse size. *Neuron* 32, 673-682.
- Nerbonne, J., Gerber, B., and Norris, A. (2008). Electrical remodelling maintains firing properties in cortical pyramidal neurons lacking KCND2-encoded A-type K⁺ currents. *The Journal of Physiology* 586(6), 1565-1579.
- Okaty, B.W., Sugino, K., and Nelson, S.B. (2011). A Quantitative Comparison of Cell-Type-Specific Microarray Gene Expression Profiling Methods in the Mouse Brain. *PLoS ONE* 6(1), 1-

10.

Paradis, S., Sweeney, S., and Davis, G. (2001). Homeostatic control of presynaptic release is triggered by postsynaptic Membrane Depolarization. *Neuron* 30, 737-749.

Parrish, J. Z., Emoto, K., Kim, M. D., and Jan, Y. N. (2007). Mechanisms that regulate establishment, maintenance, and remodeling of dendritic fields. *Annu. Rev. Neurosci* 30, 399-423.

Park, K., Mohapatra, D., Misonou, H., and Trimmer, J. (2006). Graded regulation of the Kv2. 1 potassium channel by variable phosphorylation. *Science* 313, 976-979.

Peng, I.-F., and Wu, C.-F. (2007). *Drosophila* cacophony Channels: A Major Mediator of Neuronal Ca²⁺ Currents and a Trigger for K⁺ Channel Homeostatic Regulation. *Journal of Neuroscience* 27, 1072-1081.

Pereanu, W., Spindler, S., Im, E., Buu, N., and Hartenstein, V. (2007). The emergence of patterned movement during late embryogenesis of *Drosophila*. *Developmental Neurobiology* 67, 1669-1685.

Petersen, S., Fetter, R., Noordermeer, J., and Goodman, C. and DiAntonio, A. (1997). Genetic Analysis of Glutamate Receptors in *Drosophila* Reveals a Retrograde Signal Regulating Presynaptic Transmitter Release. *Neuron* 19, 1237-1248.

Pielage, J., Cheng, L., Fetter, R., and Carlton, P., Sedat, J., Davis, G.W. (2008). A Presynaptic Giant Ankyrin Stabilizes the NMJ through Regulation of Presynaptic Microtubules and Transsynaptic Cell Adhesion. *Neuron* 58, 195-209.

Prinz, A., Bucher, D., and Marder, E. (2004). Similar network activity from disparate circuit parameters. *Nat Neurosci* 7(12), 1345-1352.

Pym, E., Southall, T., Mee, C., Brand, A. and Baines, R.A. (2006). The homoeobox transcription factor *Even-skipped* regulates acquisition of electrical properties in *Drosophila* neurons. *Neural Development* 1(3), 1-15.

Raab-Graham, K., Haddick, P., Jan, Y., and Jan, L. (2006). Activity- and mTOR-dependent suppression of Kv1. 1 channel mRNA translation in dendrites. *Science* 314, 144-148.

Rudy, B., and McBain, C. (2001). Kv3 channels: voltage-gated K⁺ channels designed for high-frequency repetitive firing. *Trends in Neurosciences* 24(9), 517-526.

Rutherford, L.C., Nelson, S.B., and Turrigiano, G.G. (1998). BDNF has opposite effects on the quantal amplitude of pyramidal neuron and interneuron excitatory synapses. *Neuron* 21, 521-530.

Schulz, D., Goillard, J., and Marder, E. (2006). Variable channel expression in identified single and electrically coupled neurons in different animals. *Nat Neurosci* 9(3) 356-362.

- Schulz, D., Goillard, J., and Marder, E. (2007). Quantitative expression profiling of identified neurons reveals cell-specific constraints on highly variable levels of gene expression. *Proceedings of the National Academy of Sciences* *104*(32), 13187-13191.
- Sheng, M., Liao, Y., Jan, Y., and Jan, L. (1993). Presynaptic A-current based on heteromultimeric K⁺ channels detected in vivo. *Nature* *365*, 72-75.
- Shirasaki, R., and Pfaff, S. (2002). Transcriptional Codes And The Control Of Neuronal Identity. *Annu Rev Neurosci* *25*, 251-281.
- Solc, C., and Aldrich, R. (1988). Voltage-gated potassium channels in larval CNS neurons of *Drosophila*. *Journal of Neuroscience* *8*(7), 2556-2570.
- Spitzer, N., and Ribera, A. (1998). Development of electrical excitability in embryonic neurons: mechanisms and roles. *Developmental Neurobiology* *37*, 190-197.
- Spitzer, N.C., Kingston, P.A., Manning, T.J., and Conklin, M.W. (2002). Outside and in: development of neuronal excitability. *Current Opinion in Neurobiology* *12*, 315-323.
- Stellwagen, D., and Malenka, R. (2006). Synaptic scaling mediated by glial TNF- α . *Nature* *44*, 1054-1059.
- Sweeney, S.T., Broadie, K., Keane, J., Niemann, H., and O'Kane, C.J. (1995). Targeted expression of tetanus toxin light chain in *Drosophila* specifically eliminates synaptic transmission and causes behavioral defects. *Neuron* *14*, 341-351.
- Swensen, A.M. and Bean, B.P. (2005). Robustness of Burst Firing in Dissociated Purkinje Neurons with Acute or Long-Term Reductions in Sodium Conductance. *Journal of Neuroscience* *25*, 3509-3520.
- Tanouye, M., Ferrus, A., and Fujita, S. (1981). Abnormal action potentials associated with the Shaker complex locus of *Drosophila*. *Proceedings of the National Academy of Sciences* *78*(10), 6548-6552.
- Thaler, J.P., Lee, S.-K., Jurata, L.W., Gill, G.N., and Pfaff, S.L. (2002). LIM factor Lhx3 contributes to the specification of motor neuron and interneuron identity through cell-type-specific protein-protein interactions. *Cell* *110*, 237-249.
- Toledo-Rodriguez, M., Blumenfeld, B., Wu, C., Luo, J., Attali, B., Goodman, P., and Markram, H. (2004). Correlation maps allow neuronal electrical properties to be predicted from single-cell gene Expression Profiles in Rat Neocortex. *Cerebral Cortex* *14*(12), 1312-1327.
- Tripodi, M., Evers, J., Mauss, A., Bate, M., and Landgraf, M. (2008). Structural Homeostasis: Compensatory Adjustments of Dendritic Arbor Geometry in Response to Variations of Synaptic Input. *PLoS Biology* *6*(10), 2172-2187.

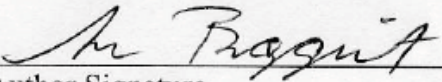
- Tsunoda, S., and Salkoff, L. (1995). Genetic analysis of drosophila neurons: Shal, Shaw, and Shab encode most embryonic potassium currents. *Journal of Neuroscience* 15(3), 1741-1754.
- Turrigiano, G. (2007). Homeostatic signaling: the positive side of negative feedback. *Curr Opin Neurobiol* 17, 318-324.
- Turrigiano, G., LeMasson, G., and Marder, E. (1995). Selective Regulation of Current Densities Underlies Spontaneous Changes in the Activity of Cultured Neurons *Journal of Neuroscience* 15(5), 3640-3652.
- Turrigiano, G.G. (2008). The self-tuning neuron: synaptic scaling of excitatory synapses. *Cell* 135, 422-435.
- Turrigiano, G.G., and Nelson, S.B. (2004). Homeostatic plasticity in the developing nervous system. *Nat Rev Neurosci* 5, 97-107.
- Tusher, V.G., Tibshirani, R., and Chu, G. (2001). Significance analysis of microarrays applied to the ionizing radiation response. *Proc Natl Acad Sci USA* 98, 5116-5121.
- Ueda, A., and Wu, C. (2006). Distinct frequency-dependent regulation of nerve terminal excitability and synaptic transmission by I_A and I_K potassium channels revealed by drosophila Shaker and Shab mutations. *Journal of Neuroscience* 26(23), 6238-6248.
- Van Wart, A., and Matthews, G. (2006). Impaired firing and cell-specific compensation in neurons lacking nav1.6 sodium channels. *Journal of Neuroscience* 26(27), 7172-7180.
- White, B.H., Osterwalder, T.P., Yoon, K.S., Joiner, W.J., Whim, M., Kaczmarek, L., and Keshishian, H. (2001). Targeted Attenuation of Electrical Activity in Drosophila Using a Genetically Modified K^+ Channel. *Neuron* 31, 699-711.
- Wu, C., Ganetzky, B., Haugland, F., and Liu, A. (1983). Potassium currents in Drosophila: different components affected by mutations of two genes. *Science* 220, 1076-1078.
- Yao, W., and Wu, C. (1999). Auxiliary Hyperkinetic Beta Subunit of K^+ Channels: Regulation of Firing Properties and K^+ Currents in Drosophila Neurons. *Journal of neurophysiology* 81, 2472-2484.
- Zhang, Y., Mori, M., Burgess, D., and Noebels, J. (2002). Mutations in High-Voltage-Activated Calcium Channel Genes Stimulate Low-Voltage-Activated Currents in Mouse Thalamic Relay Neurons. *Journal of Neuroscience* 22(15), 6362-6371.

Publishing Agreement

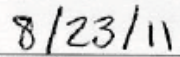
It is the policy of the University to encourage the distribution of all theses, dissertations, and manuscripts. Copies of all UCSF theses, dissertations, and manuscripts will be routed to the library via the Graduate Division. The library will make all theses, dissertations, and manuscripts accessible to the public and will preserve these to the best of their abilities, in perpetuity.

Please sign the following statement:

I hereby grant permission to the Graduate Division of the University of California, San Francisco to release copies of my thesis, dissertation, or manuscript to the Campus Library to provide access and preservation, in whole or in part, in perpetuity.



Author Signature



Date